NATIONAL ADVISORY COMMITTEE FOR AERONAUTICS

WARTIME REPORT

ORIGINALLY ISSUED

June 1944 as
Advance Restricted Report 4F15

GENERAL TANK TESTS ON THE HYDRODYNAMIC CHARACTERISTICS OF FOUR FLYING-BOAT HULL MODELS OF DIFFERING LENGTH-BEAM RATIO

By Kenneth S. M. Davidson and F. W. S. Locke, Jr.
Stevens Institute of Technology

NACA

WASHINGTON

NATIONAL ADVISORY COMMITTEE FOR AERONAUTICS

ADVANCE RESTRICTED REPORT

GENERAL TANK TESTS ON THE HYDRODYNAMIC CHARACTERISTICS OF FOUR FLYING-BOAT HULL MODELS OF DIFFERING LENGTH-BEAM RATIO

By Kenneth S. M. Davidson and F. W. S. Locke, Jr.

SUMMARY

The main purpose of this report is to present the results of "general" tests on the hydrodynamic characteristics of four related flying-boat hull models of differing length-beam ratio.

Evidence available before the work was started indicated that length-beam ratio had important effects on resistance and suggested that it might have important effects on most of the hydrodynamic characteristics. The present investigation accordingly included consideration of five different characteristics, in an effort to gain perspective and to determine which characteristic were governing. The following were studied:

(a) Resistance

(b) Porpoising

(c) Main forebody spray blister

(d) Bow spray in rough water (windshield wetting)

(e) Yawing stability near hump speeds

The tests were made by methods described in previous reports of the Stevens Experimental Towing Tank, and covered ranges of load and speed which an earlier analysis of past practice had indicated to be of interest from a practical point of view; values of C_{Δ_o} and C_{V_G} were

progressively increased as the length-beam ratio was increased. The results are presented in terms of the usual NACA nondimensional coefficients, which facilitates their application in analyses or comparisons of different sorts.

Two comparisons are presented to show the significance of length-beam ratio under a given relationship of load to speed, one (fig. 2) for models having the same plan form area and the other (fig. 3) for models having the same beam. These comparisons, for reasonably high beam loadings on the basis of current practice (C_{Δ_0} = 1.00 for L/b = 6.19), indicate a general improvement in the hydrodynamic characteristics with increase of length-beam ratio, if not carried too far.

INTRODUCTION

The ratio of length to beam is obviously a major consideration of proportioning in the design of any type of hull.

The flying-boat hull is a special type of hull, which ordinarily has been viewed as primarily a planing hull, and only secondarily as a displacement hull. In a planing hull, the emphasis has usually been placed on beam (and dead rise); within reason, the length of a planing hull is relatively unimportant while the hull is planing. The length becomes of major importance only at low speeds, before planing has been established, where it can affect the performance materially; it also controls the static flotation. Thus, broadly speaking, the choice of the length and the choice of the beam of a flying-boat hull are governed by different considerations. But, once both have been chosen for a particular case, the result is a fixed hull of given length and given beam, and it is necessary to view this result in over-all fashion, considering both planing and displacement speeds; it is proper, also, to investigate the over-all effects of altering the ratio between length and beam.

It may often be desired to evaluate the effects of altering length on a fixed beam, or of altering beam on a fixed length. In both cases the length-beam ratio will be changed. But it will be clear that if the same change of length-beam ratio is made in both ways, the resulting

Fig. 1

Constant beam

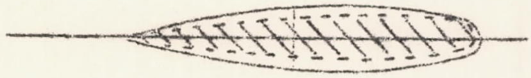

Constant length

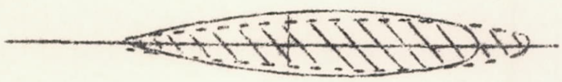

Constant plan form area

Note:

Comparisons on the basis of Constant Plan Form Area are believed to eliminate most nearly the effects of differences of size. A comparison of this type, for typical conditions of load and speed, is shown for the models here considered, on Fig. 2.

An additional comparison is included on Fig. 3 to bring out differences resulting from a failure to eliminate size as a factor. This comparison, for the same models and loading conditions, is on the basis of Constant Beam; a comparison on the basis of Constant Length would have served the same purpose.

Figure 1.- Changes of length-beam ratio.

hulls are certainly of different size, whatever reasonable definition of size is adopted. (See fig. 1 on p. 3.)

Changes of size, under the same conditions of load and speed, are well known to affect the hydrodynamic characteristics. Hence the true influence of length-beam ratio as such will not be brought out if changes of size cannot be eliminated. This is not an entirely straightforward matter, since size can be defined in various ways. However, the definition recently used by Bell (reference 1) is an entirely reasonable one, and certainly better than most others. According to this definition, two hulls of differing length-beam ratio are said to have the same size when they have the same plan form area, $L \times b$.

If the foregoing definition of size is adopted, the problem of determining the true influence of length-beam ratio, apart from the influence of size, is reduced to that of comparing the hydrodynamic characteristics of hulls of differing length-beam ratio which have the same $L \times b$ product, under the same conditions of load and speed. When this is done, the load per unit plan form area remains fixed; the values of C_{Δ_0} increase, however, with increasing values of L/b, the relationship being

$$C_{\Delta_0} \text{ proportional to } (L/b)^{3/2} \tag{1}$$

A recent analysis (reference 2) has indicated that an average of actual practice in the past, including both flying-boat hulls and seaplane floats in a wide variety of sizes and designs, is tolerably well represented by the relationship

$$L/b = 6.05\, C_{\Delta_0}{}^{1/3}$$

which can be written

$$C_{\Delta_0} \text{ proportional to } (L/b)^{3} \tag{2}$$

in which form it is directly comparable with equation (1) and shows that, in fact, the beam loading has been allowed to increase with increasing values of L/b at a rate considerably faster (third power) than that corresponding to constant load on a given plan form area (three-halves power). Equation (2) may perhaps rest upon somewhat too

broad a range of types and designs for present purposes. There is nevertheless the clear implication that the hydrodynamic characteristics must have been found to be inherently improved by increase of length-beam ratio; otherwise, it is difficult to see how the higher loading could have been acceptable. This implication was emphasized in laying out the test schedules for the present investigation.

The major purpose of the present investigation was to provide comprehensive hydrodynamic data for related models of differing length-beam ratio, as a basis for analyses or comparisons of whatever type desired. An auxiliary purpose was to study the question brought out in the foregoing discussion; namely, the rate at which the loading per unit plan form area may successfully be increased as the length-beam ratio is increased. For the first purpose, the experimental data are presented in general form, in terms of the usual NACA nondimensional coefficients. As a start toward the second purpose, two representative comparisons are presented of selected models, to show the influence of length-beam ratio under fixed loading conditions.

Previous experimental investigations of the effects of altering length-beam ratio have been reported in:

U.S.E.M.B. Report No. 51 and reference 3 and 4 (1922, 1934, and 1937, respectively), which are concerned primarily with resistance characteristics

Reference 5, June 1943, which considers resistance and porpoising

Reference 1, October 1943, which considers resistance and spray

Reference 6, December 1943, which considers the spray at the bow at low taxying speeds in waves (windshield wetting)

Reference 7, November 1943, which considers spray

The present investigation was conducted at the Stevens Institute of Technology. Except for the work on bow-spray characteristics, it was conducted under the sponsorship of, and with financial assistance from, the National Advisory

Committee for Aeronautics. The bow-spray work in rough water was carried out for the Bureau of Aeronautics, Navy Department, but a summary of the results has subsequently been published by the NACA. (See reference 6.)

SCOPE OF THE EXPERIMENTAL INVESTIGATION

Four models were used:

L/b	5.07	6.19	7.32	8.45
Model No.	339-22	339-1	339-23	339-46

The parent for the series was Stevens Model No. 339-1, which had the lines of the XPB2M-1. The other three models were derived systematically from the parent; the relative length-beam ratios are

0.82 1.00 1.18 1.36

The first three models were previously used for resistance and porpoising studies reported in reference 5; all four models were used in the studies of bow spray in rough water reported in reference 6.

The following characteristics were investigated:

(a) Resistance, over the entire speed range to get-away

(b) Porpoising and trimming moment, at planing speeds

(c) Main forebody spray blister, at speeds up to and including the hump

(d) Bow spray, in rough water at taxying speeds

(e) Yawing stability, at speeds up to and including the hump

In each instance, the tests were made by "general" methods and in accordance with the usual procedures at the Stevens Experimental Towing Tank, as described in previous reports.

Ranges of loading coefficient and get-away speed coefficient for the several models were selected from the analyses of past practice discussed in reference 2. These appeared to be the best information available at the start of the investigation, and it was considered necessary to restrict the breadth of the testing in some fashion, in the interests of economy of time. The pertinent charts from reference 2 are reproduced here on figure 10, from which it is seen that the ranges of load coefficient varied in general accordance with equation (2) on page 4. The approximate test ranges selected are indicated on these charts; the actual ranges used are listed below.

L/b		5.07	6.19	7.32	8.45
Ranges of C_{Δ_0}	High	0.80	1.40	2.00	3.20
	Low	.40	.60	1.00	1.60
Ranges of C_{V_G}	High*	10.0	12.0	13.6	16.0
	Low	5.4	6.2	7.4	8.6

It will be seen that the ranges for each successive model overlap those of the preceding model.

The bow-spray tests were run at one speed, $C_V = 1.05$, with three sizes of waves, having lengths of 6, 4, and 2 beams, all with a length-height ratio of 20. For each model at each wave size, the runs were made at loadings from $C_\Delta = 0.60$ up to the load coefficient at which the model swamped and sank.

MODELS

The hull of the XPB2M-1 was selected for the parent model of the series, primarily because of the large background of experience with this form, and with various

---

*These values are nominal. Limitations of the testing facilities prevented reaching the maximum values of C_{V_G} desired. They were therefore simulated by appropriate changes of load in combination with the maximum value of C_{V_G} attainable.

types of systematic modifications of it, already available at the Stevens Experimental Towing Tank. (See references 5, 6, 8 and 9.)

The models were built to the same beam, and the same body plans were used for all four models; these are given on figure 5, at full size for the models.

The length was altered, thereby altering the length-beam ratio, by applying a constant multiplier to the station spacing of the parent model. The forebody sections were shifted in or out along lines parallel to a tangent to the forebody keel at the main step, and the afterbody sections were shifted along the afterbody keel. This procedure kept the step height and the afterbody angle fixed for the series, thereby eliminating two variables known from previous work (reference 5) to have major influences on the hydrodynamic performance in their own right, and obviously extraneous to an investigation of length-beam ratio.

No attempt was made to eliminate changes in variables resulting directly from expanding or contracting the lengths of the forebody and afterbody. In this connection it is worth noting that the parent form has a slightly warped forebody bottom in the vicinity of the main step. The amount of the warping was automatically altered in direct proportion to the changes of length, and since forebody bottom warping is known to have an independent effect of its own, the changes which occurred in this instance, though small, may have had some effect on the results.

The distance from the main step to the rear gun turret was held constant, thus allowing considerable changes of length in the region between the sternpost and the turret. The character of this region was preserved as far as was practicable, and the height of the turret was adjusted slightly as seemed desirable to insure clean lines.

Profile drawings of the four models, at reduced scale, are given on figure 6; pertinent particulars and specifications are on page 26.

For the studies of bow spray in rough water, the forward part of each forebody was a complete representation of the hull; that is, the nose and windshield were

reproduced. The windshield was located the same distance aft of the forepoint and the same distance above the tangent to the forebody keel at the step in all cases. Sketches of the profiles are included on figures 7 and 8; further details will be found in reference 6.

APPARATUS AND PROCEDURE

The various pieces of test equipment used for the experiments herein reported have been described in previous reports of the Stevens Experimental Towing Tank with the exception of the apparatus for general porpoising experiments.

The reported resistances include the air drag of the model; the air drag of the apparatus with no model in place has been subtracted.

The equipment for measuring the forebody spray blister is described in reference 8.

The equipment used to photograph the bow spray in rough water is described in reference 6.

The apparatus for determining yawing stability is described in reference 9.

The apparatus for general porpoising tests is an adaptation of the apparatus used for specific porpoising tests, and described in reference 5, with the hydrofoil system removed. Changes of load are accomplished by means of weights so arranged that there is no alteration to the mass in vertical oscillation when the model is loaded or unloaded, or during porpoising. A photograph of this apparatus is on figure 9.

The detailed procedures used in the various experiments are described in the same references in which the pieces of test equipment are described. No new procedures were developed for the work herein reported.

The center of gravity was located the same distance ahead of the step and the same distance above the keel in all four models. The location chosen was based on the findings of reference 10, to provide suitable moment-trim relationships in the planing range. The values used were:

Center of Gravity Location

[35 percent of beam forward of main step
90 percent of beam above forebody keel]

For the general porpoising tests, fixed values of the mass in vertical oscillation and the longitudinal radius of gyration were established. The first of these was based upon the relationship for gross load used to determine the test ranges of loading for the various models.

$$L/b = 6.05\, C_{\Delta_0}^{\ 1/3} \quad \text{(see p. 4 and fig. 10)}$$

transformed to

$$m = \rho_w \left(\frac{L}{6.05}\right)^3 \tag{3}$$

where m is the total mass in vertical oscillation. The second was based upon the relationship

$$k = 0.225\, L \tag{4}$$

where k is the radius of gyration. Both these relations are discussed in reference 10.

The tail damping was limited to 0.25, one of the three values of the dimensionless criterion $M_q \Big/ \frac{\rho}{2} V b^4$ discussed in reference 10. The use of a single value for all four models means that, in effect, the tail area and the length (its distance from the c.g.) were considered to remain fixed when the hull length was altered with beam constant.

The over-all accuracy of the results can best be judged by the scatter of the test points on the various charts. It is believed that individual measurements were made to within the following limits:

Resistance (at displacement speeds), pound	±0.03
(at planing speeds), pound	±0.05
Trim (during resistance tests), deg	±0.1
(during porpoising tests), deg	±0.3
Yaw angle, deg	±0.2

Trimming moment, inch-pound	± 0.2
Yawing moment (except in regions of discontinuity), inch-pound	± 0.1
Spray dimensions, inch	$\pm 1/2$

PRESENTATION OF TEST RESULTS

The results of the tests are presented in terms of the usual NACA "C" coefficients:

Load coefficient	$C_\Delta = \Delta/wb^3$
Speed coefficient	$C_V = V/\sqrt{gb}$
Resistance coefficient	$C_R = R/wb^3$
Trimming moment coefficient	$C_M = M/wb^4$
Yawing moment coefficient	$C_{M_\psi} = M_\psi/wb^4$
Draft coefficient	$C_d = d/b$
Length/beam ratio	L/b

where

Δ load on water, pounds

w specific weight of water, pounds per cubic foot (62.3 for Stevens)

b beam at main step, feet

V speed, feet per second

g acceleration of gravity, feet per second per second

R resistance, pounds

M trimming moment, pound-feet

M_ψ yawing moment, pound-feet

d draft of keel at main step, feet

L length of hull from forepoint to sternpost, feet

Moment data are referred to the center of gravity, and water trimming moments which tend to raise the bow are considered positive. Water yawing moments which tend to rotate the bow toward the starboard (right) are considered positive. Yaw angles to starboard are considered positive.

Trim (τ) is the angle between the tangent to the forebody keel at the main step and the horizontal.

Yaw (ψ) is the angle between the center line of the hull and the course, measured in a plane parallel to the still-water surface.

Resistance

The resistance tests were in two groups: free-to-trim at displacement speeds, and fixed trim at planing speeds.

Figures 11 to 14 show free-to-trim resistances and trim angles over the range of displacement speeds. There is one chart for each model, giving C_R and τ against C_V, with C_Δ as parameter.

Figures 15 to 31 show fixed-trim resistances and moment characteristics at planing speeds. There is a group of charts for each model, each chart relating to a different value of C_V, and showing C_R against τ with C_Δ and C_M as parameters. The method of plotting is that developed by Dawson. (See reference 11.) Trim limits of stability, taken from the charts listed in the following paragraph, also are shown.

Porpoising

Figures 32 to 35 show trim limits of stability for the planing range, in the condensed form of plotting discussed in reference 10. There is one chart for each model, giving trim limits against $\sqrt{C_\Delta}/C_V$. Contours of constant C_M also are shown. The trim limits are consistent with those on the resistance charts for the planing range, listed in the preceding paragraphs.

Main Forebody Spray Blister

Figures 36 to 39 show measurements of the location of the peak of the main forebody spray blister, in the form of plotting discussed in reference 8. The position of the blister peak is given with respect to the model, as a function of C_Δ and C_V. There is one chart for each model.

Bow Spray in Rough Water at Low Speed

Figure 40 shows photographs of the worst spray condition at the bow during the course of a cycle of wave encounter, as selected from a series of exposures taken at the rate of 60 per second and covering several cycles. This chart, for the largest of the three wave sizes covered in the tests, shows the spray in the free-to-trim condition for three values of C_Δ, and at the one value of C_V selected as representative of the worst condition.

The series of photographs on figure 40 is only part of a larger series, reported in reference 6, in which the loading was progressively increased from $C_\Delta = 0.60$, until the spray conditions became so bad that the model swamped. The highest loadings at which each model stayed afloat are given in the following table:

L/b	5.07	6.19	7.32	8.45
C_Δ	1.40	2.20	3.00	3.60

Directional Stability

Figures 41 to 44 show diagrams of yawing moment C_{M_ψ} against yaw angle ψ, grouped to bring out the functional relation of the yawing characteristics, with C_Δ and C_V, in the free-to-trim condition at displacement speeds, where yawing is usually of most importance. This form of presentation is discussed in reference 9. There is one chart for each model.

The term "hooking" is used on these charts to describe the condition in which the unstable slope of the yawing moment curve is so steep at small yaw angles as to constitute, in effect, a discontinuity. Very rapid yawing, or hooking, may occur in the flying boat, and the unstable moments are so high that even unbalanced power may be insufficient to counteract them unless very rapidly applied at the first sign of yawing.

COMPARISONS BETWEEN MODELS

Use of the usual NACA "C" coefficients to present the test results conforms with common practice in reporting tests on flying-boat hull models and permits direct comparisons with the results of tests on other variables.

It should be noted that, because the characteristic linear dimension in the NACA coefficients is the beam, the use of these coefficients means that, in effect, hulls of differing length-beam ratio are compared on the basis of equal beam and differing length. The charts of test results enumerated in the preceding section can therefore be used as they stand to evaluate the effects of altering length on given beam.

The effects of altering beam on given length can be evaluated by entering the charts of test results with the following relative values, where the parent model (L/b = 6.19) is considered as the basic starting point.

Length Constant

L/b	5.07 (percent)	6.19 (percent)	7.32 (percent)	8.45 (percent)
Beam, b	122	100	84.6	73.3
C_Δ (for constant Δ)	55	100	165	254
C_R (for constant R)	55	100	165	254
C_V (for constant V)	90.5	100	109	117

Similarly, the effects of altering length-beam ratio with constant plan form area can be evaluated by entering the charts with

Length-Beam Product Constant

L/b	5.07 (percent)	6.19 (percent)	7.32 (percent)	8.45 (percent)
L x b	100	100	100	100
L	90.5	100	109	117
b	111	100	92	85.5
C_Δ (for constant Δ)	74.2	100	128	160
C_R (for constant R)	74.2	100	128	160
C_V (for constant V)	95.2	100	104	108

As is pointed out in the Introduction, comparisons on the basis of constant plan form area are believed to eliminate most nearly the effects of differences of size and, therefore, to provide the best indication of the influence of length-beam ratio alone. Accordingly, a comparison of this type has been worked out from the charts of test results and is presented on figure 2.

A second comparison, but on the basis of constant beam with varying length, is included on figure 3 in order to bring out differences resulting from a failure to eliminate size changes. The introduction of a third comparison, on the basis of constant length with varying beam, was considered, but decided against on the ground that it would merely illustrate another way of introducing size changes, and therefore not add materially to the discussion at this point.

Each of the two comparisons shows the hydrodynamic characteristics of particular models, having the four length-beam ratios considered in the investigation, compared under fixed conditions of load and speed. The same load-speed relationship is used for both comparisons, and the parent model (L/b = 6.19) is identical in size in both cases. The data are given at model size, and various

particulars for the several models are listed on the sheets. Data are given, or referred to, for each of the five characteristics covered by the investigation.

With reference to either of the comparisons (fig. 2 or fig. 3) it may be said that, to a first approximation, increasing the length-beam ratio -

(a) Helps the hump resistance and trim, but shifts the hump to higher speed.

(b) Helps the high-speed resistance.

(c) Injures the stable range of trim angles.

(d) Lowers the height of the main spray blister.

(e) Reduces the bow spray at taxying speeds in rough water.

(f) Injures the yawing stability slightly, though not materially altering the speed ranges for the various types of yawing stability.

The first two of these conclusions are the same as were reached by Bell, Garrison, and Zeck, in reference 1.

At first glance, the differences between the two comparisons may not appear very striking. This is perhaps fundamentally because, from an abstract physical point of view, the over-all range of change of the length-beam ratio was not very great. From a practical point of view, however, the range of change was considerable, and the differences between the comparisons are important. Thus, when the length-beam ratio is increased, it is seen that in the second comparison (beam constant) as compared with the first (plan form area constant) -

(a) The improvement in hump resistance is greater.

(b) The improvement in high-speed resistance is less.

(c) The injury to the stable range of trim angles is less.

(d) The lowering of the main spray blister is greater.

(e) The reduction of bow spray is materially greater.

(f) The injury to the yawing stability is a little less.

A more detailed study of the comparisons seems to indicate with some clarity that, for the loading conditions represented, a length-beam ratio of 5.07 is too small, and a length-beam ratio of 8.45 is too large. This statement is based upon the appearance of abnormal trends in the principal characteristics, resistance, trim limits of stability, and main-spray-blister height. Specifically,

With L/b = 5.07, the resistances and the main spray blister increase abnormally.

With L/b = 8.45, the stable range of trim angles diminishes abnormally.

The other two characteristics, bow spray and yawing stability, while probably of secondary importance, nevertheless do not offer contradictory evidence in this connection.

Suppose, now, that the parent hull were increased in length-beam ratio, from its actual value of 6.19, to 7.32 or thereabouts.

(1) If the plan form area were held constant (beam diminished) -

(a) The hump and high-speed resistances would be decreased.

(b) The lower limit of stability would be raised.

(c) The spray blister height would be largely unaffected.

(2) If the plan form area were increased (beam constant) -

(a) The hump resistance would be a little lower than before, and the high-speed resistance a little higher.

(b) The lower limit of stability would not be raised as much as before.

(c) The spray blister height would be lowered.

DISCUSSION

In appraising the results of a study of the present type, the manner in which the changes of the variable under consideration are effected in the models has an important bearing. The aim must be to avoid changes of other variables, as far as this is practicable. In the present instance, it is believed that by avoiding changes of step height and afterbody angle, the largest of the extraneous variables which might otherwise have seriously interfered with an adequate evaluation of the influence of length-beam ratio have been eliminated. On the other hand, changes resulting solely from the alterations of proportion, and therefore the direct consequence of the choice of parent form, have been preserved as legitimate; they are believed to have been treated fairly in the method adopted for altering the length.

Length-beam ratio is a variable which differs from most other variables characterizing hull form (such as dead-rise angle, afterbody angle, etc.) in that, unless special precautions are taken, its effects are likely to be confused with the effects of changes of size. The precautions taken herein, of introducing a comparison of hulls of differing length-beam ratio on a basis of constant plan form area, is believed adequate to avoid confusion on this point.

The two comparisons of specific hulls actually carried through on figures 2 and 3 give an over-all picture of the influence of length-beam ratio, with and without a change of hull size (as arbitrarily defined), for loading conditions approximating those of current practice. These comparisons are indicative, but they make no pretense of covering all the ramifications which alterations of length-beam ratio may involve, or of being conclusive in themselves. In particular, they do not delineate clearly the rate at which the loading may be increased with increase of length-beam ratio, or the maximum loadings possible. They are thought to provide a suitable pattern, however, for a more extended series of comparisons aimed at clarifying these matters more fully.

The data on page 13, from the tests for bow spray in rough water, afford direct evidence regarding maximum possible loadings. It is seen in the following table that the values of C_Δ just prior to swamping are well expressed by the equation

$$C_{\Delta_{max}} = K\ (L/b)^2 \tag{5}$$

where K has a mean value of 0.0546

L/b	5.07	6.19	7.32	8.45
$C_{\Delta_{max}}$	1.40	2.20	3.00	3.60
$K = \dfrac{C_{\Delta_{max}}}{(L/b)^2}$	.0545	.0574	.0560	.0504

The preceding equation has the same form as the equation adopted by Parkinson in reference 7 in discussing spray, except that it uses the total length L instead of the forebody length L_f. Since the ratio of L_f/L for the present series of models is 0.556, the equation

$$C_{\Delta_{max}} = 0.0546\ (L/b)^2 \tag{6}$$

becomes

$$C_{\Delta_{max}} = 0.1760\ (L_f/b)^2 \tag{7}$$

when $(L_f/b)^2$ is substituted for $(L/b)^2$. The 0.1760 constant for maximum possible loading is some 2.5 times as large as the constant of 0.0675, recommended in reference 7 for "satisfactory" spray characteristics in normal service. Apart from all questions of the exact value adopted for either constant, however, the fact seems clear that the beam loading can be increased as the square of the length-beam ratio, whichever condition is under consideration.

In further comparative studies along the lines of figures 2 and 3, it is believed practical to consider

only what have been referred to in this report as the "principal" characteristics: resistance, porpoising, and the main spray blister. The problem is, essentially, to find the influence of length-beam ratio, size, and loading, on these characteristics. Previous experience has indicated that undesirable bow spray or yawing characteristics can usually be corrected independently, by relatively small local changes which do not appreciably alter the principal characteristics.

Practically all the necessary data for further comparative studies are available in the charts of test results on figures 11 to 39. The only reservation is that since the test ranges for the several models were laid out in accordance with equation (2) on page 4, as previously explained, the values of C_Δ for low-speed tests at the larger values of length-beam ratio may sometimes be found to be on the high side.*

It has been pointed out that desirable values of the length-beam ratio, as indicated by the present investigation, appear to lie between the two extreme values tested. The lowest value tested, 5.07, fails largely through its excessive resistance and forebody spray; the highest value, 8.45, fails because of its abnormally narrow range of stable trim angles, the cause of which is not very clear, but may perhaps be laid in part to the test procedure. As noted on page 9, a constant mass was used for each model in the general porpoising tests, this mass being proportional to the cube of the length-beam ratio in conformity with the test ranges of C_{Δ_0}. Thus, with the radius of gyration proportional to the length, the moment of inertia increased as the fifth power of the length-beam ratio. Since, in the light of the test results in general, a rate of increase of loading in proportion to the cube of the length-beam ratio now appears to be higher than is practicable, the rate of increase of mass and moment of inertia actually used probably was excessive. The effect of the moment of inertia on the stability limits previously has been found to be small (references 5 and 10.) but the changes of moment of inertia involved in the present instance are much greater than were previously considered, and may have had more effect.

Should further study indicate distinct advantages

*The charts in the appendix help to overcome this difficulty.

for the largest length-beam ratio (8.45) from points of view other than porpoising, it is possible that additional porpoising tests, made with lower mass and moment of inertia, might show an improvement in its porpoising characteristics. Further consideration might well be given, at the same time, to the value of the pitch-damping rate, which, in the present tests, was held the same for all four models. Reference 10 may be reviewed in connection with the mass, moment of inertia, and pitch-damping rate.

It is important to keep clearly in mind that the present investigation refers to altering the length-beam ratio in a very specific way - namely, by expanding the forebody and afterbody lengths in the same ratio and without changing step height or afterbody angle. Since the functions of the forebody and the afterbody differ in important respects, their respective lengths have certain more or less independent effects on performance. Thus, when the two lengths are altered in direct proportion to each other, the resulting performance is bound to reflect the combined influences of both alterations. For example, referring to the comparison on figure 3, it is thought that the progressively lower hump resistance obtained when the length-beam ratio is increased, is largely attributable to the longer afterbody rather than to the longer forebody. Similarly, the failure of the greatest length-beam ratio to continue the downward trend in planing range resistances probably is attributable to greater wetting of the longer afterbody. On the other hand, the strength of the present study is that it permits a visualization of the over-all consequences of the simple, specific change to which it refers.

CONCLUDING REMARKS

The test results herein presented provide the necessary material for studies of various types aimed at clarifying the significance of length-beam ratio from a hydrodynamic point of view.

On the basis of the family of models investigated, and the loading conditions used in the comparisons on figures 2 and 3, the following conclusions are indicated:

(1) If the plan form area and the loading conditions are held constant, increasing the length-beam ratio -

(a) Helps the hump resistance and trim, but shifts the hump to higher speed.

(b) Helps the high-speed resistances.

(c) Injures the stable range of trim angles.

(d) Lowers the height of the main spray blister.

(e) Reduces the bow spray at taxying speeds in rough water.

(f) Injures the yawing stability slightly, though not materially altering the speed ranges for the various types of yawing stability.

(2) If the beam and the loading conditions are held constant, then, compared with the foregoing case -

(a) The improvement in hump resistance is greater.

(b) The improvement in high-speed resistances is less.

(c) The injury to the stable range of trim angles is less.

(d) The lowering of the main spray blister is greater.

(e) The reduction of bow spray is materially greater.

(f) The injury to the yawing stability is much the same.

(3) It seems clear enough that the beam loading cannot be increased as rapidly as in proportion to the cube of the length-beam ratio (equation (2) on p. 4) without important sacrifices in respect to one or more of the principal hydrodynamic characteristics: resistance, porpoising, or main spray. A rate proportional to the square of the length-beam ratio, as discussed on page 19, appears to be more nearly the maximum possible.

Experimental Towing Tank,
Stevens Institute of Technology,
Hoboken, N. J., April 24, 1944.

APPENDIX

METHOD FOR PRESENTING THE PRINCIPAL CHARACTERISTICS OF INDIVIDUAL MODELS IN CONDENSED FORM

The purpose of the appendix is to present a condensed form of report on the principal characteristics of individual models.

Each of figures 45, 46, 47, and 48 shows the test results for resistance, porpoising, and main-spray-blister height, for one model:

The main spray characteristics are shown at the top in the same form as on figures 36 to 39.

The free-to-trim resistances and trims for the lower half of the take-off speed range (in what has been called the displacement range) are shown in the middle of the sheet in the collapsed form of plotting discussed in reference 12.

The stability limits and moment characteristics for the planing range are shown at the bottom in the same form as on figures 32 to 35. Contours of resistance at planing speeds are superimposed as discussed in reference 12.

These condensed reports are believed to have a great advantage in that they condense onto one sheet all the pertinent information on the principal hydrodynamic characteristics of a given hull form. It is hoped that they may be used in something like the same fashion as an airfoil polar diagram and that, when they become available for a larger number of hull forms, they will provide the designer with a simple tool for comparing hull lines. They represent a coordination of developments toward this end which have been in progress at the Stevens Experimental Towing Tank for several years; they constitute the next step following the work in reference 12. Some fairing is necessarily done in their preparation.

In connection with the present investigation, the charts may be used to advantage in extrapolating for loads outside of the test ranges.

REFERENCES

1. Bell, Joe W., Garrison, Charlie C., and Zeck, Howard: Effect of Length-Beam Ratio on Resistance and Spray of Three Models of Flying-Boat Hulls. NACA ARR No. 3J23, 1943.

2. Locke, Fred W. S., Jr.: A Correlation of the Dimensions, Proportions, and Loadings of Existing Seaplane Floats and Flying-Boat Hulls. NACA ARR, March 1943.

3. Shoemaker, James M., and Parkinson, John B.: Tank Tests of a Family of Flying-Boat Hulls. NACA TN No. 491, 1934.

4. Sottorf, W.: The Design of Floats. NACA TM No. 860, 1938.

5. Davidson, Kenneth S. M., and Locke, F. W. S., Jr.: Some Systematic Model Experiments on the Porpoising Characteristics of Flying-Boat Hulls. NACA ARR No. 3F12, 1943.

6. Locke, F. W. S., Jr.: Some Systematic Model Experiments of the Bow-Spray Characteristics of Flying-Boat Hulls Operating at Low Speeds in Waves. NACA ARR No. 3L04, 1943.

7. Parkinson, John B.: Design Criterions for the Dimensions of the Forebody of a Long-Range Flying Boat. NACA ARR No. 3K08, 1943.

8. Locke, F. W. S., Jr., and Bott, Helen L.: A Method for Making Quantitative Studies of the Main Spray Characteristics of Flying-Boat Hull Models. NACA ARR No. 3K11, 1943.

9. Locke, F. W. S., Jr.: Some Yawing Tests of a 1/30-Scale Model of the Hull of the XPB2M-1 Flying Boat. NACA ARR No. 3G06, 1943.

10. Locke, F. W. S., Jr.: General Porpoising Tests of Flying-Boat-Hull Models. NACA ARR No. 3I17, 1943.

11. Dawson, John R.: A General Tank Test of a Model of the Hull of the P3M-1 Flying Boat including a Special Working Chart for the Determination of Hull Performance. NACA TN No. 681, 1938.

12. Locke, F. W. S., Jr.: General Resistance Tests on Flying-Boat Hull Models. NACA ARR No. 4B19, 1944.

TABLE I

PARTICULARS OF MODELS

L/b	5.07	6.19	7.32	8.45
Stevens Model No.	339-22	339-1	339-23	339-46
Beam at main step, in.	5.40	5.40	5.40	5.40
Hull length, forepoint to sternpost, in.	27.37	33.45	39.53	45.61
Forebody length, in.	15.22	18.60	21.98	25.36
Afterbody length, in.	12.15	14.85	17.55	20.25
Step height, in.	0.27	0.27	0.27	0.27
Afterbody angle, deg	7.0	7.0	7.0	7.0
Dead rise at keel at main step, deg	20.0	20.0	20.0	20.0
Forebody length/beam	2.82	3.44	4.07	4.70
Afterbody length/beam	2.25	2.75	3.25	3.75
Step height, percent b	5.0	5.0	5.0	5.0
Sternpost angle, deg	8.25	8.00	7.75	7.50
Forebody warping, deg/b	2.1	1.7	1.4	1.2

For the general propoising tests, mean values of the mass in vertical oscillation and of the moment of inertia were established and used throughout. These were based on equations (3) and (4), respectively, on page10, and are shown below:

Δ_0, lb	3.35	6.10	10.05	15.50
C_{Δ_0}	0.59	1.07	1.77	2.72
I_p, lb-in.^{2}	160	356	811	1658

All trim angles measured relative to the tangent to the forebody keel at main step.

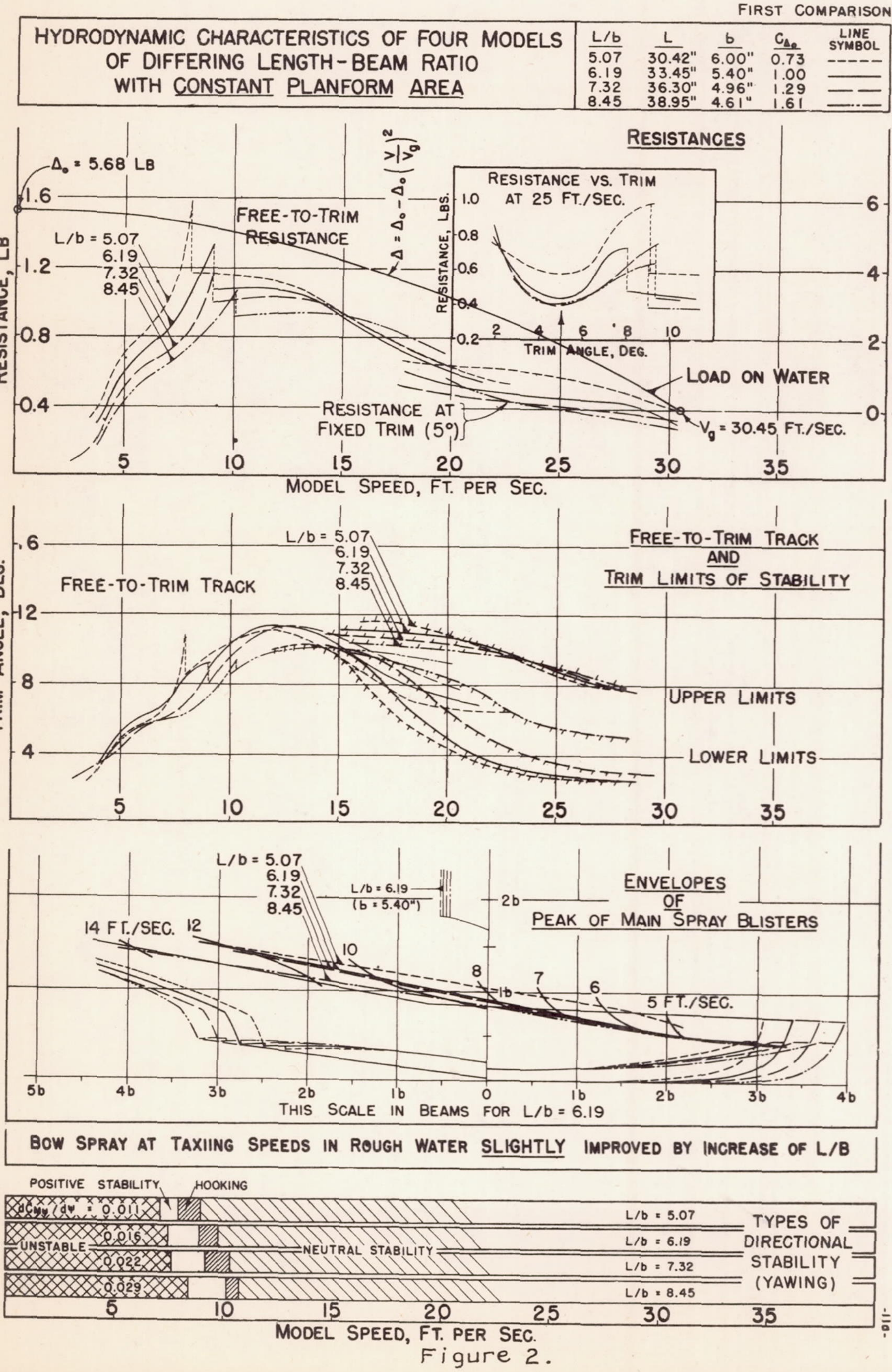
FIRST COMPARISON
HYDRODYNAMIC CHARACTERISTICS OF FOUR MODELS OF DIFFERING LENGTH-BEAM RATIO WITH CONSTANT PLANFORM AREA
L/b L b C$_{\Delta_0}$ LINE SYMBOL
5.07 30.42" 6.00" 0.73
6.19 33.45" 5.40" 1.00
7.32 36.30" 4.96" 1.29
8.45 38.95" 4.61" 1.61
RESISTANCES
Δ_0 = 5.68 LB
FREE-TO-TRIM RESISTANCE
$\Delta = \Delta_0 - \Delta_0 \left(\frac{V}{V_g}\right)^2$
RESISTANCE VS. TRIM AT 25 FT./SEC.
RESISTANCE, LBS.
TRIM ANGLE, DEG.
LOAD ON WATER
RESISTANCE AT FIXED TRIM (5°)
V_g = 30.45 FT./SEC.
RESISTANCE, LB
LOAD ON WATER, LB
MODEL SPEED, FT. PER SEC.
L/b = 5.07 6.19 7.32 8.45
FREE-TO-TRIM TRACK
FREE-TO-TRIM TRACK AND TRIM LIMITS OF STABILITY
UPPER LIMITS
LOWER LIMITS
TRIM ANGLE, DEG.
ENVELOPES OF PEAK OF MAIN SPRAY BLISTERS
L/b = 6.19 (b = 5.40")
14 FT./SEC.
5 FT./SEC.
THIS SCALE IN BEAMS FOR L/b = 6.19
BOW SPRAY AT TAXIING SPEEDS IN ROUGH WATER SLIGHTLY IMPROVED BY INCREASE OF L/B
POSITIVE STABILITY
HOOKING
$dC_{N\psi}/d\psi$ = 0.011
0.016
0.022
0.029
UNSTABLE
NEUTRAL STABILITY
L/b = 5.07
L/b = 6.19
L/b = 7.32
L/b = 8.45
TYPES OF DIRECTIONAL STABILITY (YAWING)
MODEL SPEED, FT. PER SEC.
R 247 -11a-

Figure 2.

SECOND COMPARISON

HYDRODYNAMIC CHARACTERISTICS OF FOUR MODELS OF DIFFERING LENGTH-BEAM RATIO WITH CONSTANT BEAM	L/b	L	b	C_{Δ_0}	LINE SYMBOL
	5.07	27.37"	5.40"	1.00	-----
	6.19	33.45"	5.40"	1.00	———
	7.32	39.53"	5.40"	1.00	— —
	8.45	45.61"	5.40"	1.00	—··—

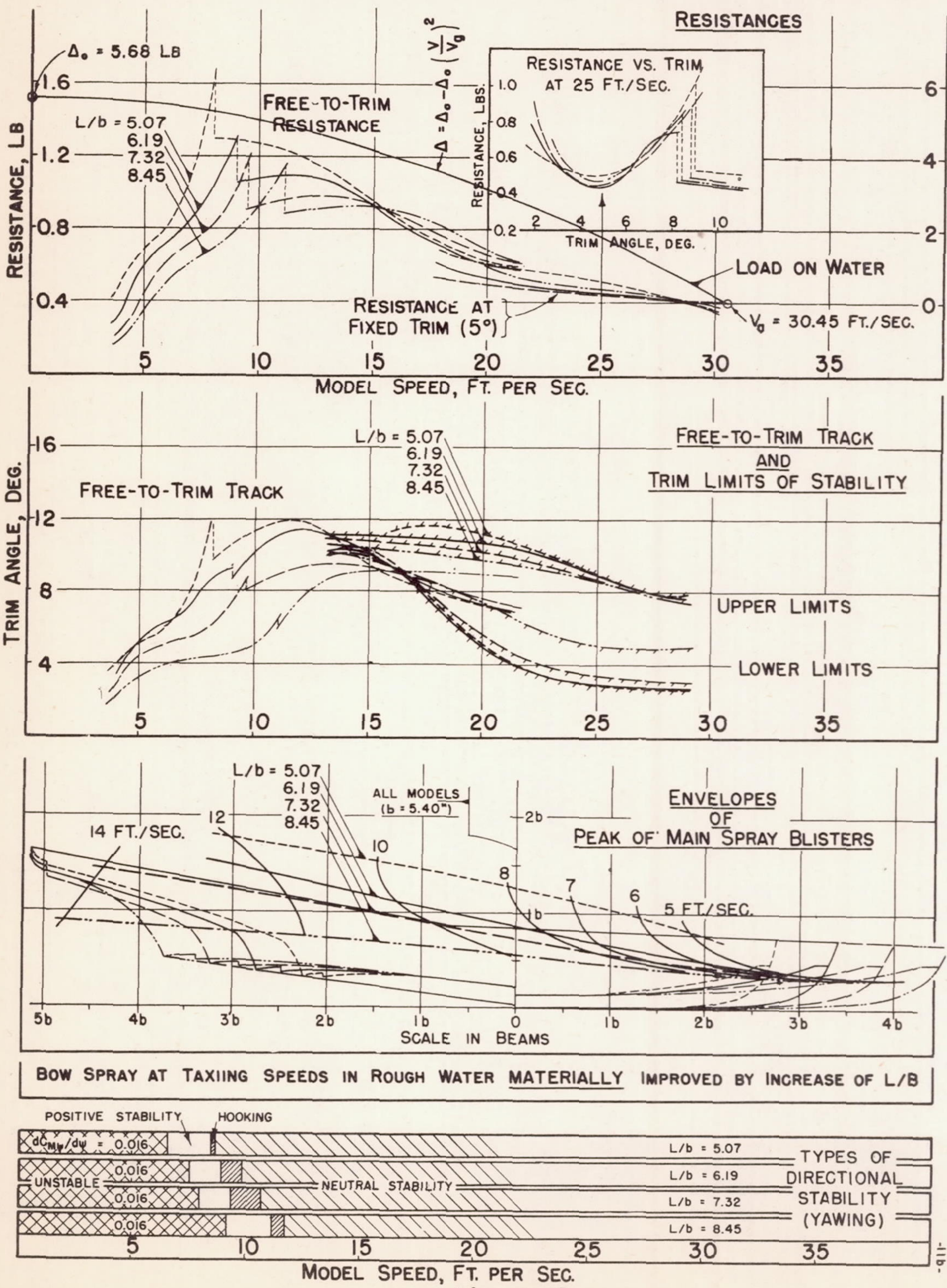

Figure 3.

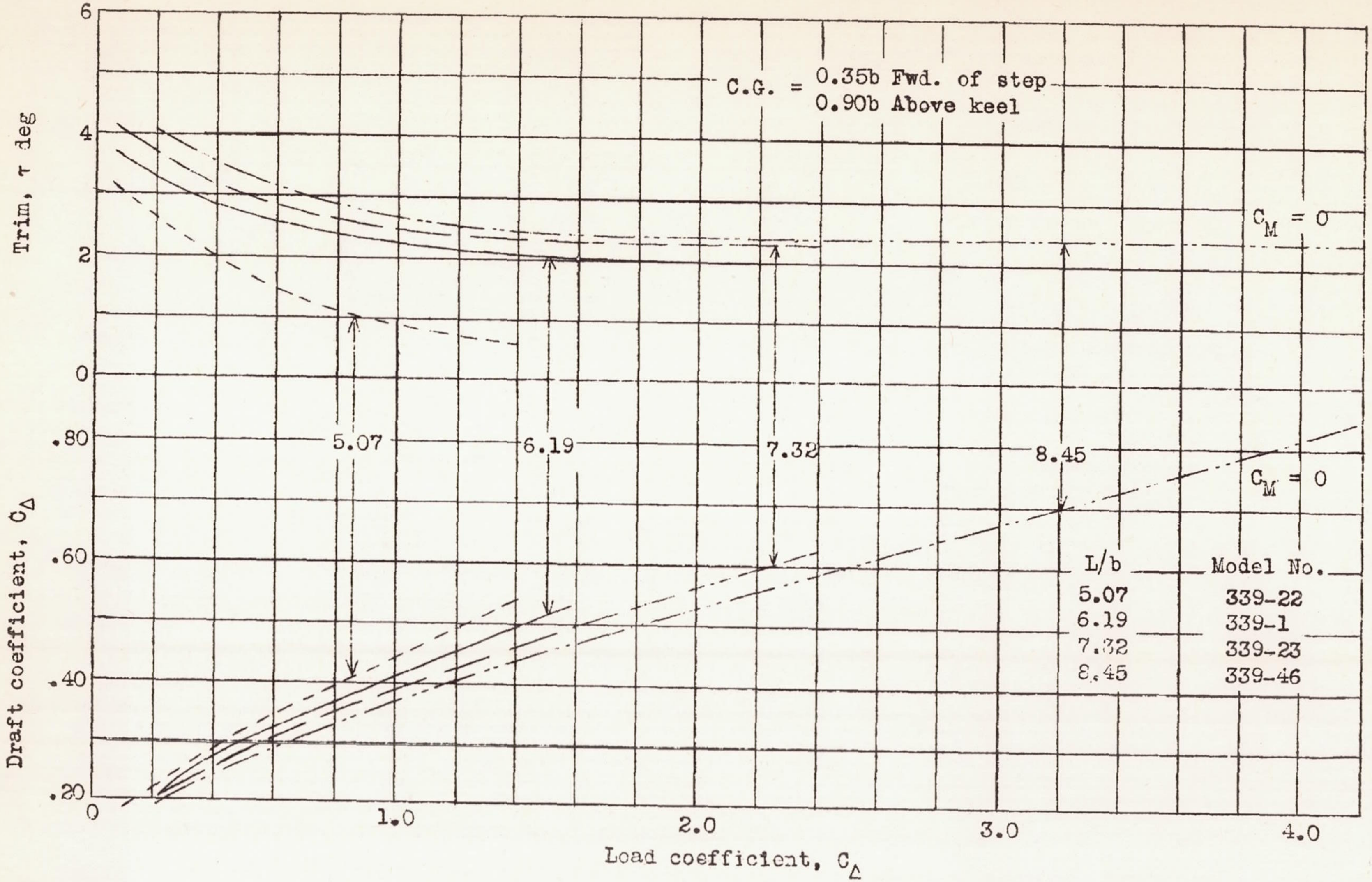

Figure 4.- Static properties of the four models

BODY PLAN OF PARENT

XPB2M-1

STEVENS MODEL NO. 339-1

L/b = 6.19

STATION NOS. ARE INCHES AFT OF F.P. FOR THIS L/b. STATIONS REMAIN THE SAME FOR OTHER L/b RATIOS, THEIR SPACING BEING CHANGED BY A CONSTANT MULTIPLIER.

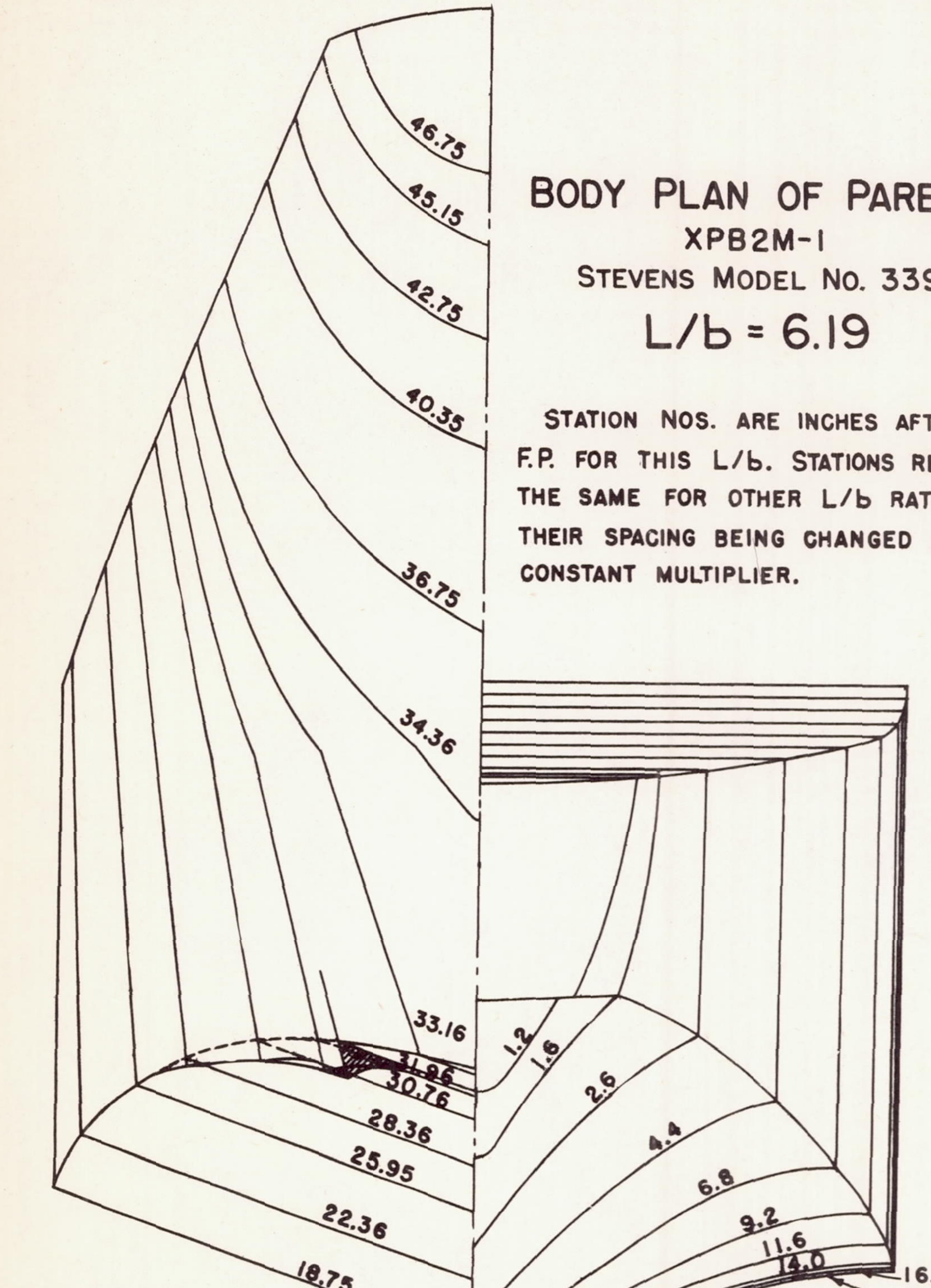

Figure 5.

SCALE: FULL SIZE FOR MODEL

PROFILE VIEWS OF MODELS IN L/b SERIES

THE PARENT IS THE XPB2M-1

SCALE = 1/6 FULL SIZE FOR MODEL

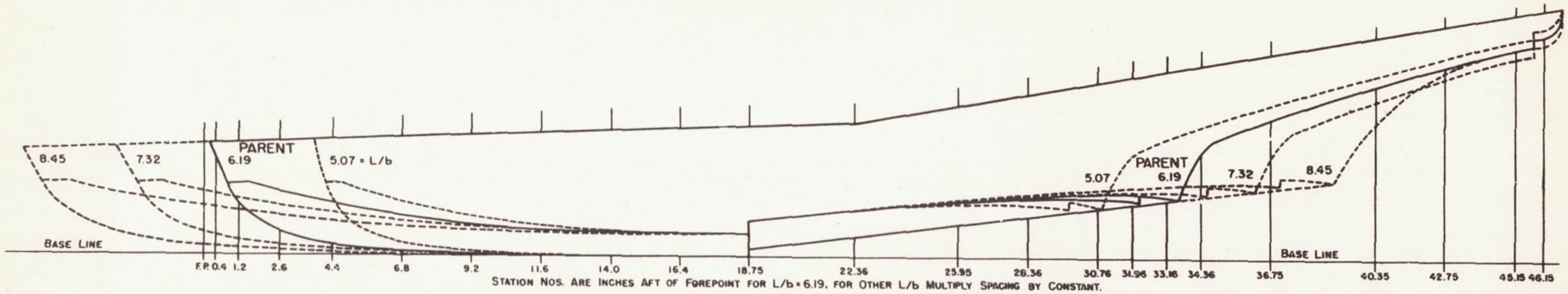

AFTERBODY ANGLE, ANGLE BETWEEN FOREBODY AND AFTERBODY KEELS, 7°.

STERNPOST ANGLE, ANGLE BETWEEN TANGENT TO FOREBODY KEEL AT MAIN STEP AND A LINE JOINING TIP OF MAIN STEP WITH TIP OF STERNPOST, 8° FOR L/b = 6.19, SLIGHTLY DIFFERENT IN OTHER MODELS.

Figure 6.

FULL NOSE PROFILE FOR ROUGH WATER TESTS
(See Page 8)

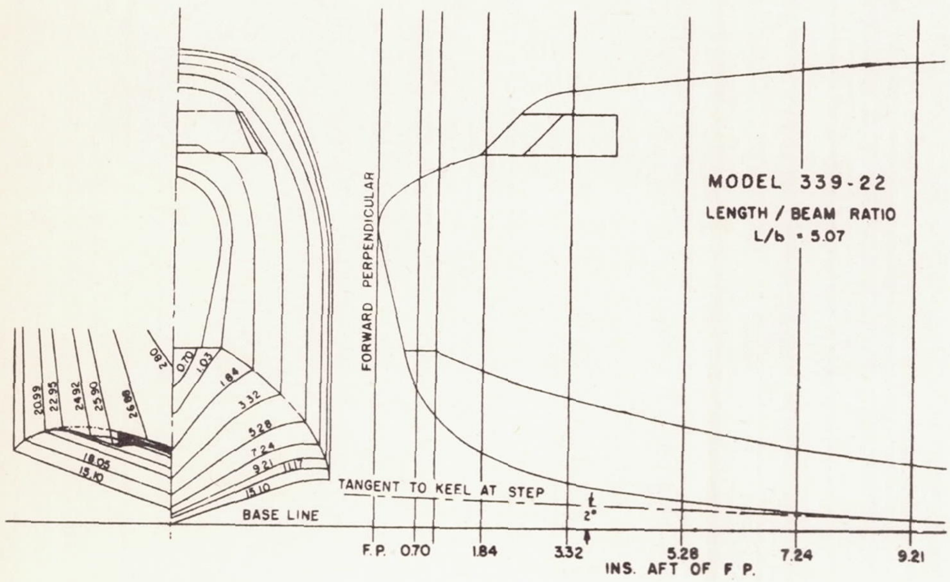

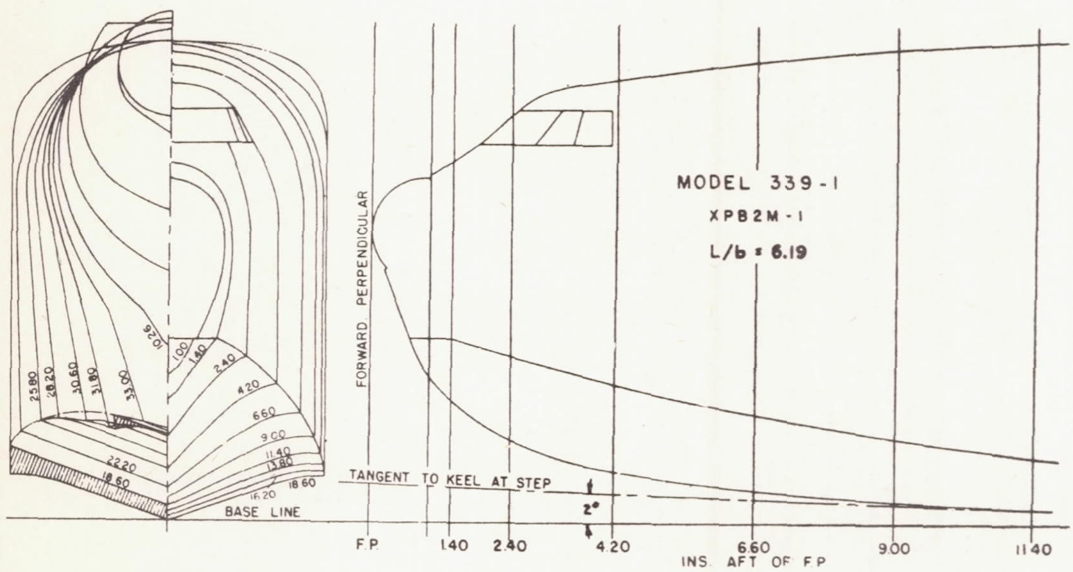

Figure 7.

FULL NOSE PROFILE FOR ROUGH WATER TESTS
(See Page 8)

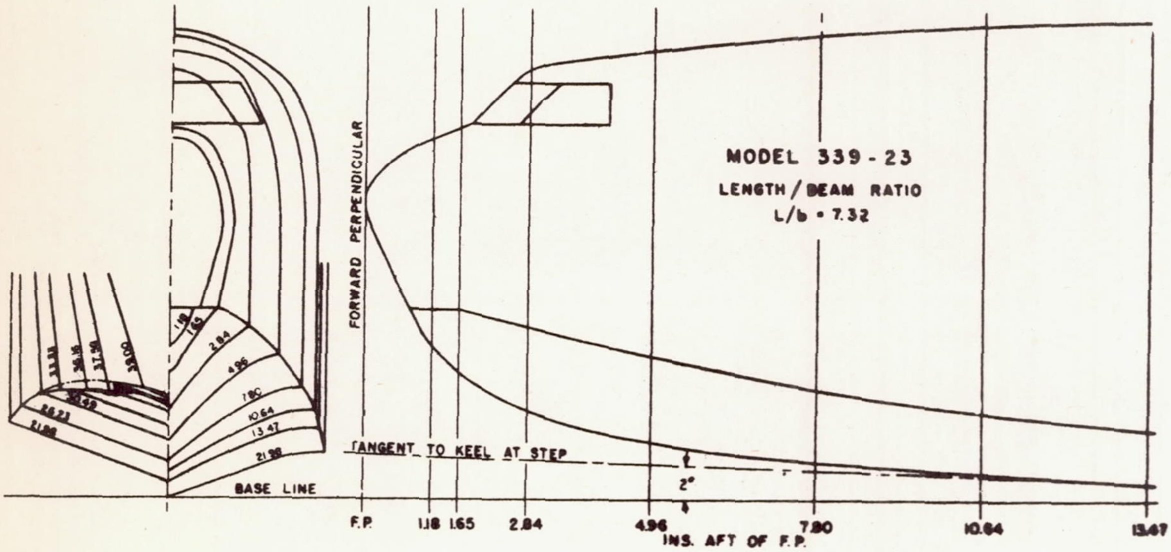

THE LINES OF THE PARENT, MODEL NO. 339-1, ON BOTTOM OF PAGE 20

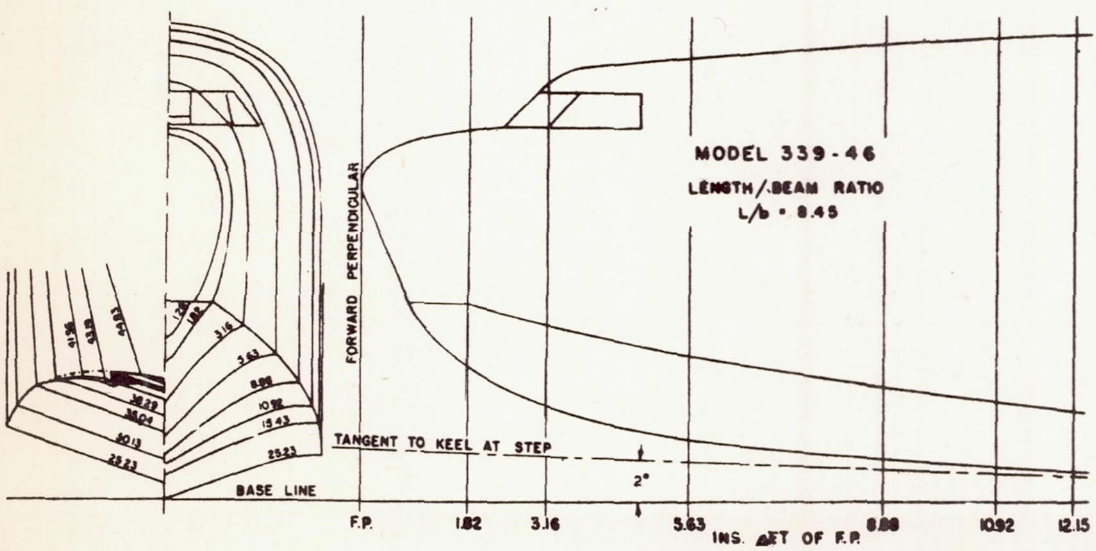

Figure 8.

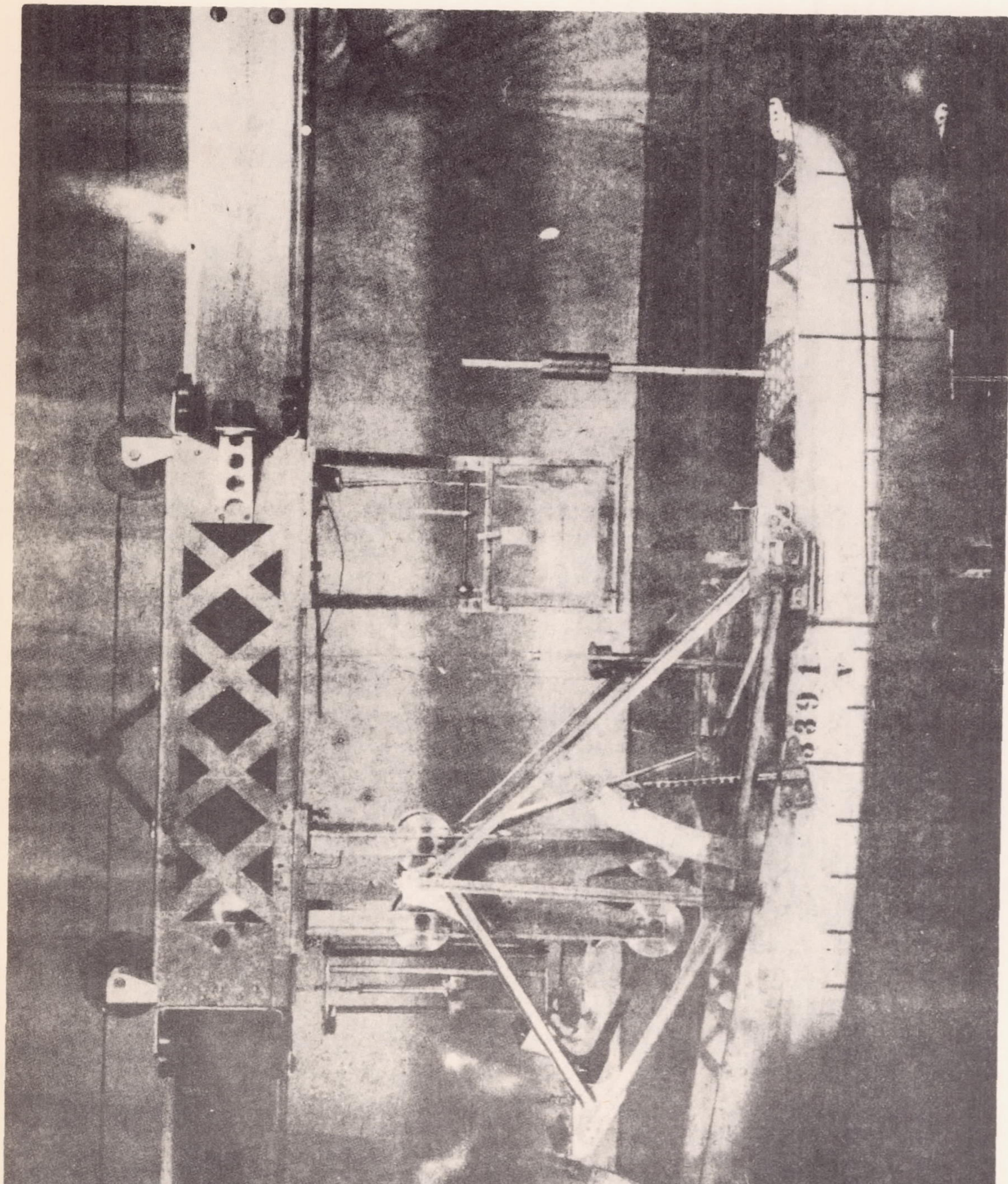

Figure 9.- APPARATUS FOR GENERAL PORPOISING TESTS

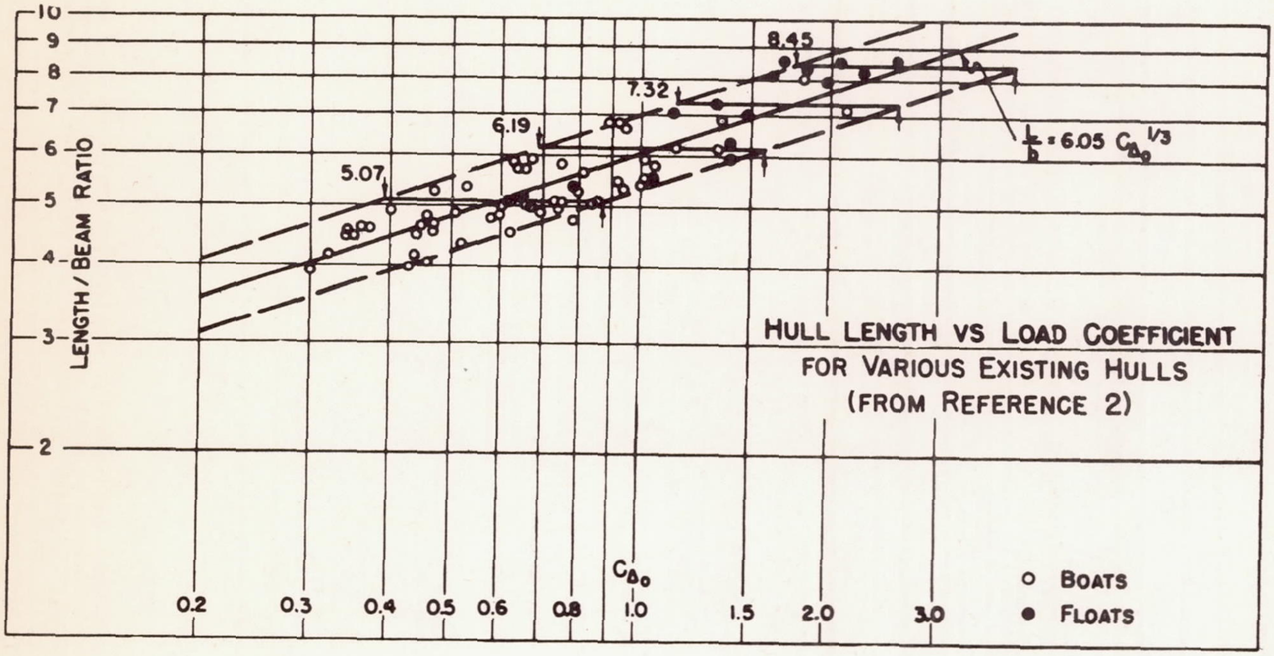

CHARTS TO DETERMINE RANGE OF C_{Δ_0} AND C_{V_G} USED FOR THE MODELS OF DIFFERENT LENGTH/BEAM RATIOS

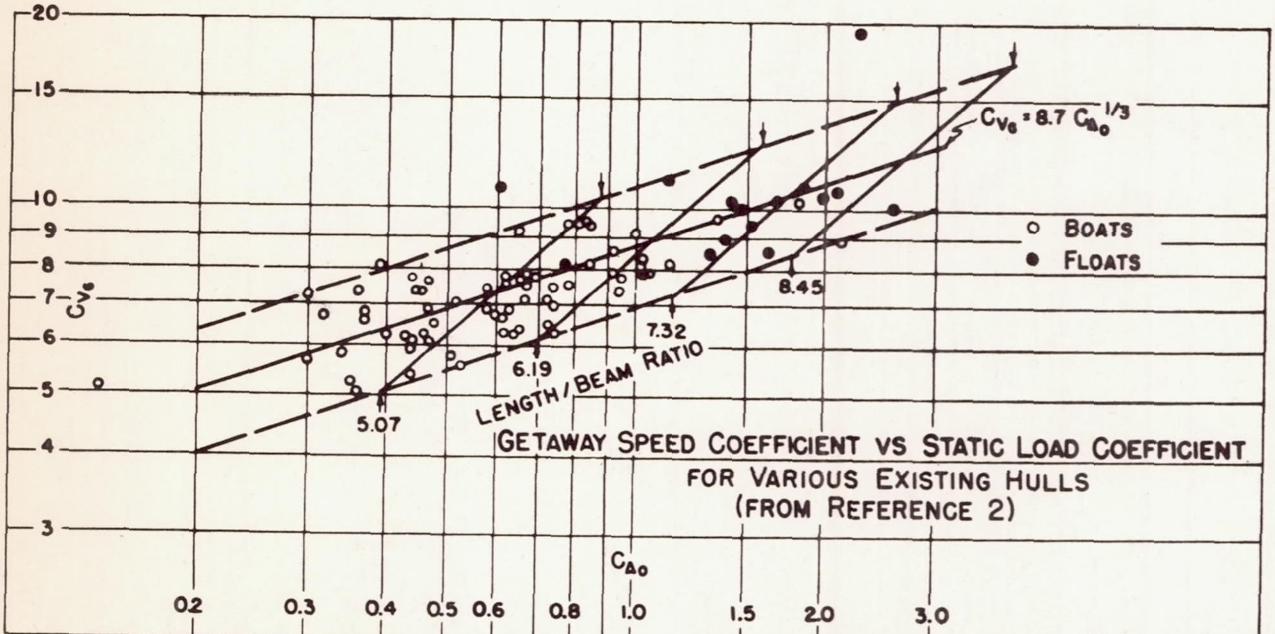

Figure 10.

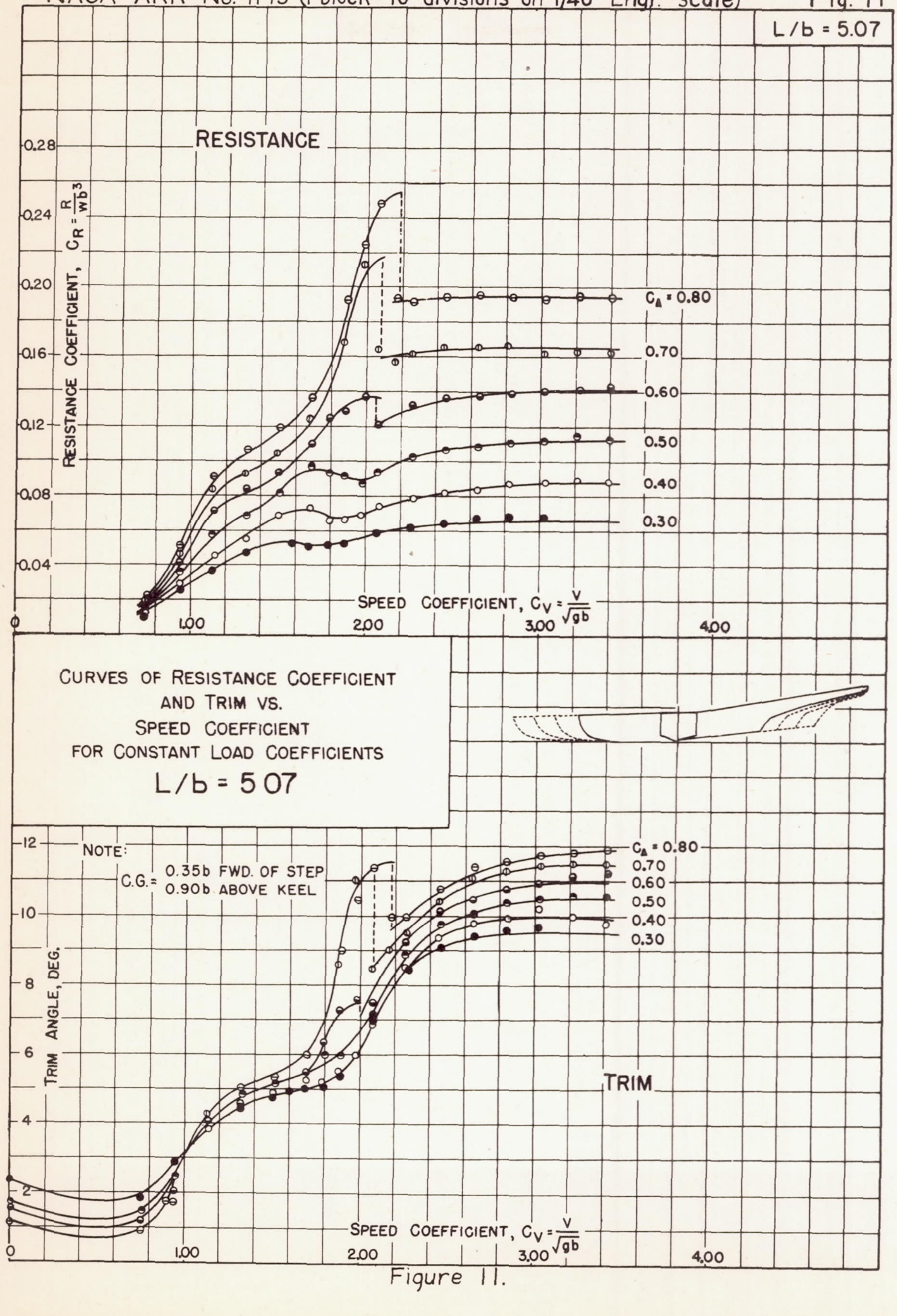
L/b = 5.07
RESISTANCE
RESISTANCE COEFFICIENT, $C_R = \frac{R}{wb^3}$
0.28
0.24
0.20
0.16
0.12
0.08
0.04
0
C_Δ = 0.80
0.70
0.60
0.50
0.40
0.30
SPEED COEFFICIENT, $C_V = \frac{V}{\sqrt{gb}}$
1.00
2.00
3.00
4.00
CURVES OF RESISTANCE COEFFICIENT
AND TRIM VS.
SPEED COEFFICIENT
FOR CONSTANT LOAD COEFFICIENTS
L/b = 5.07
NOTE:
C.G. = 0.35b FWD. OF STEP
0.90b ABOVE KEEL
TRIM ANGLE, DEG.
12
10
8
6
4
2
0
C_Δ = 0.80
0.70
0.60
0.50
0.40
0.30
TRIM
SPEED COEFFICIENT, $C_V = \frac{V}{\sqrt{gb}}$
1.00
2.00
3.00
4.00

Figure 11.

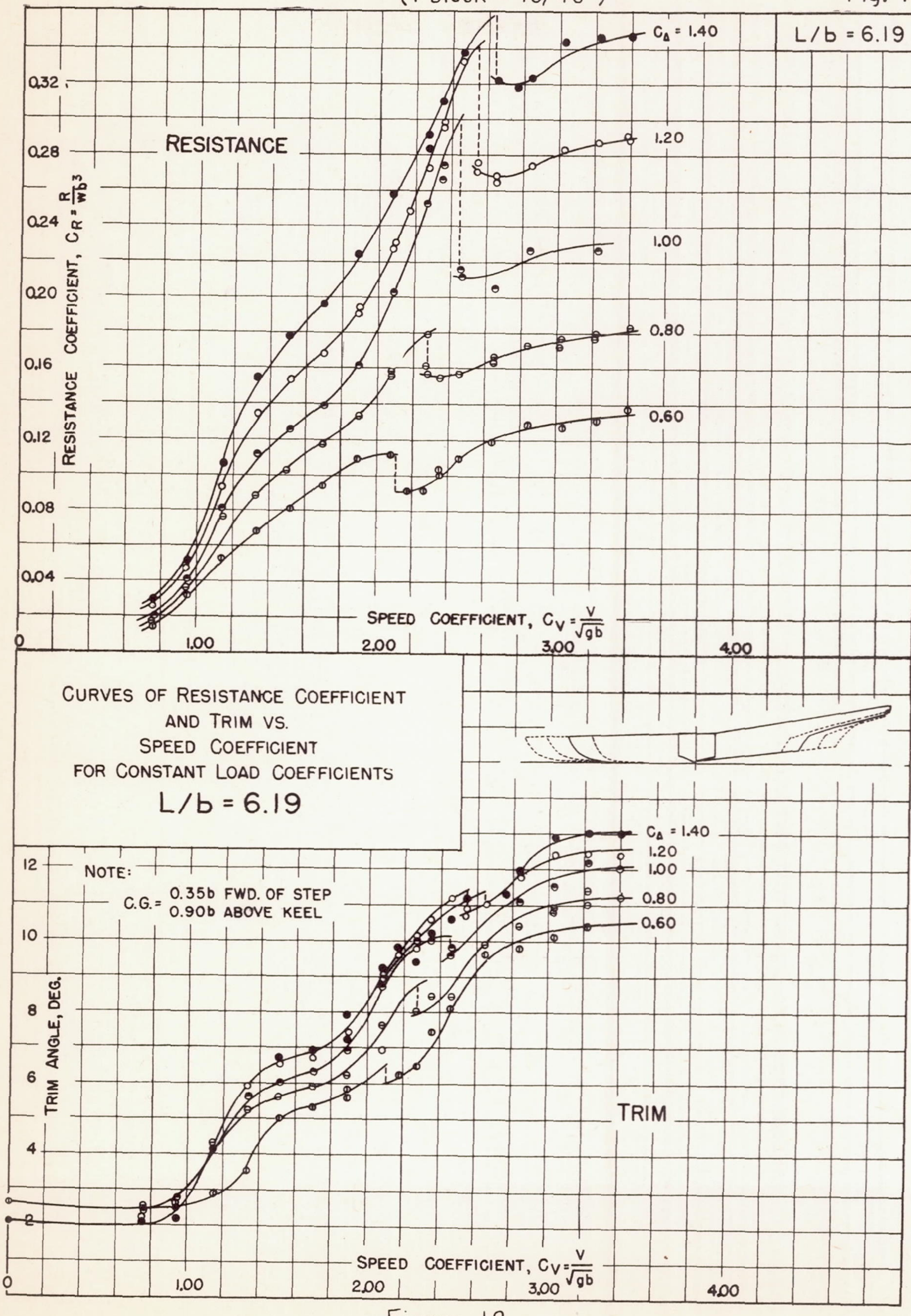
L/b = 6.19
RESISTANCE
RESISTANCE COEFFICIENT, $C_R = \frac{R}{wb^3}$
C_Δ = 1.40
1.20
1.00
0.80
0.60
SPEED COEFFICIENT, $C_V = \frac{V}{\sqrt{gb}}$
CURVES OF RESISTANCE COEFFICIENT
AND TRIM VS.
SPEED COEFFICIENT
FOR CONSTANT LOAD COEFFICIENTS
L/b = 6.19
NOTE:
C.G. = 0.35b FWD. OF STEP
0.90b ABOVE KEEL
TRIM ANGLE, DEG.
TRIM

Figure 12.

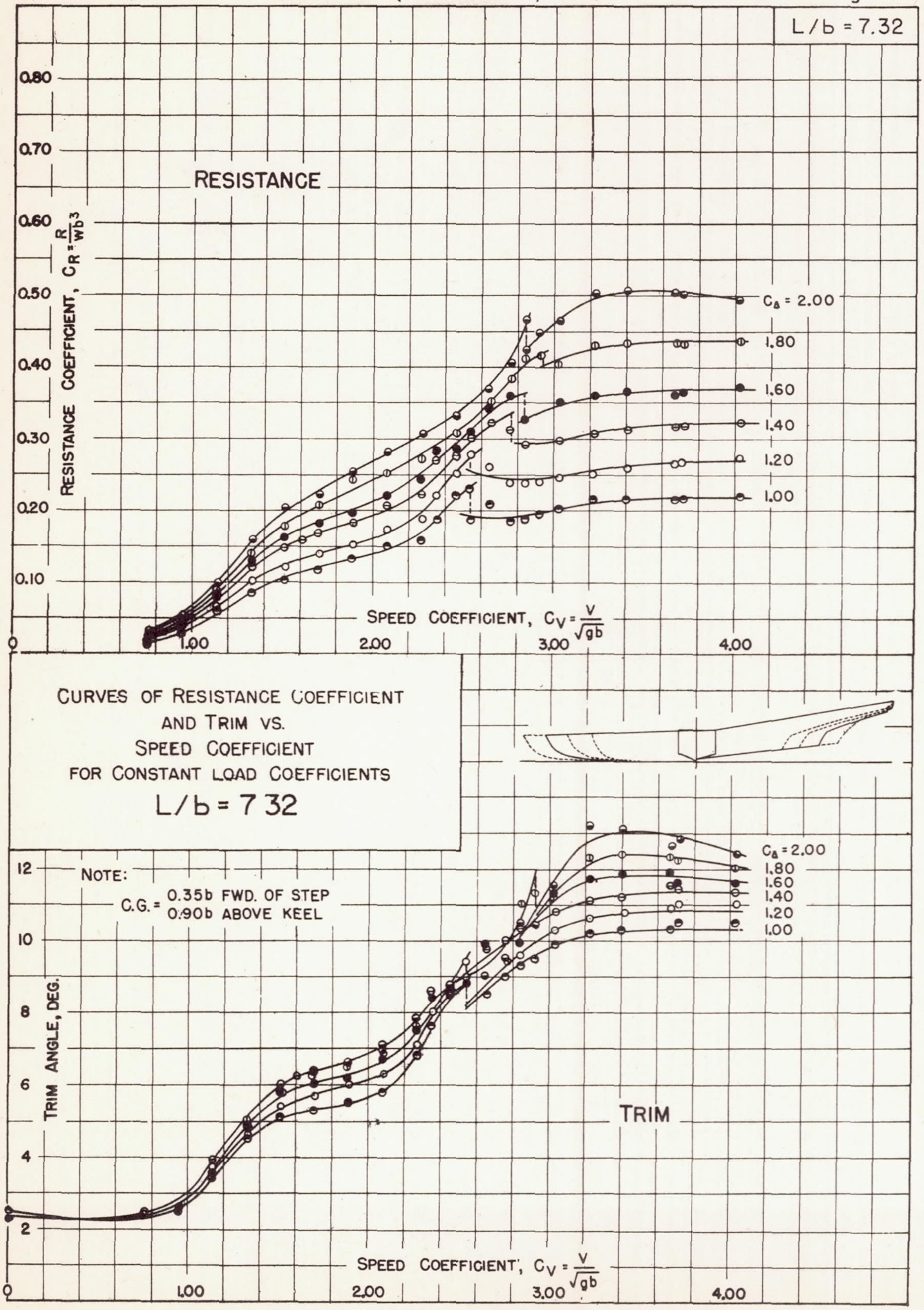

Figure 13.

W-105

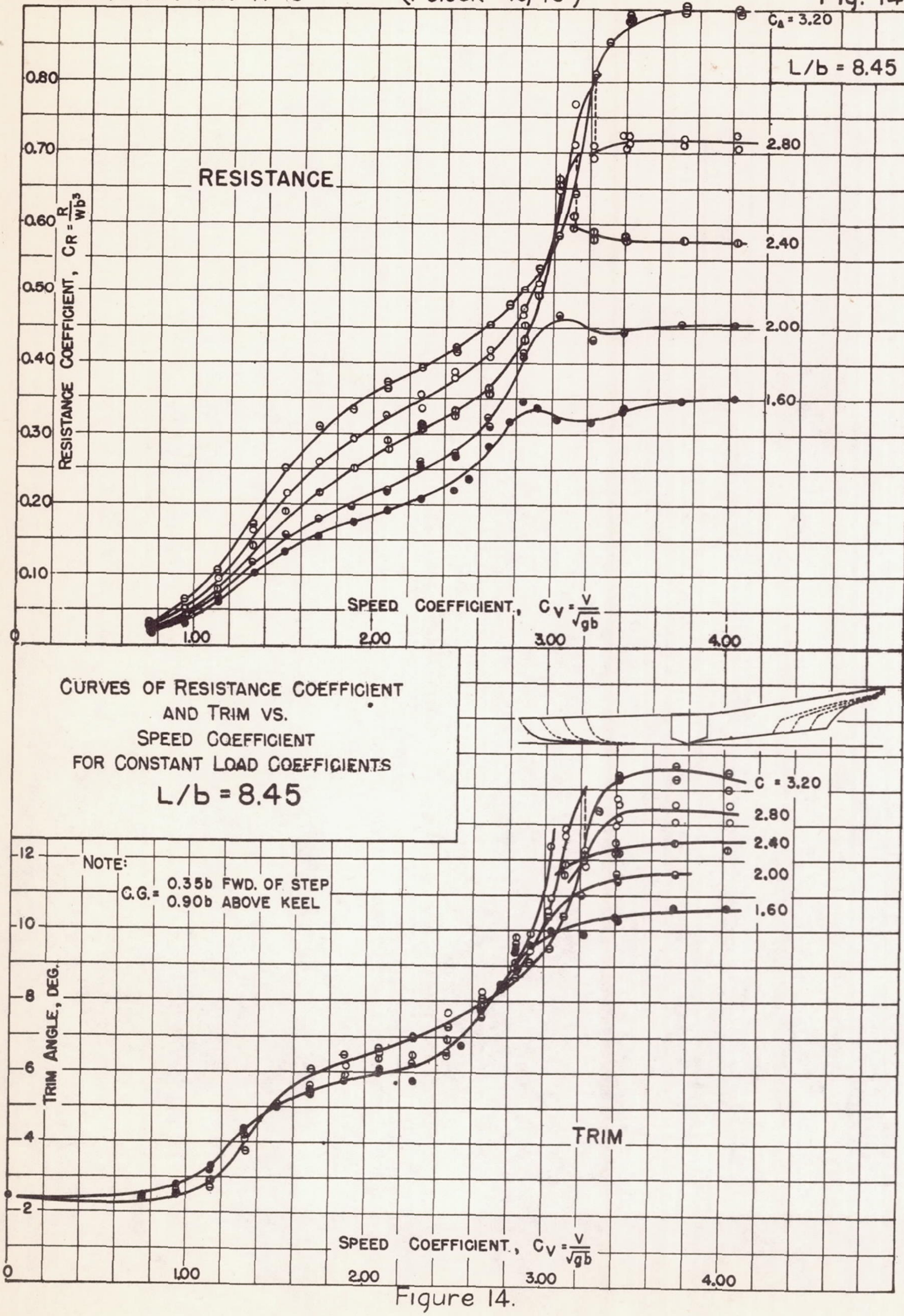

RESISTANCE
L/b = 8.45
C_Δ = 3.20
2.80
2.40
2.00
1.60
RESISTANCE COEFFICIENT, $C_R = \frac{R}{wb^3}$
0.80
0.70
0.60
0.50
0.40
0.30
0.20
0.10
0
SPEED COEFFICIENT, $C_V = \frac{V}{\sqrt{gb}}$
1.00
2.00
3.00
4.00
CURVES OF RESISTANCE COEFFICIENT
AND TRIM VS.
SPEED COEFFICIENT
FOR CONSTANT LOAD COEFFICIENTS
L/b = 8.45
NOTE:
C.G. = 0.35b FWD. OF STEP
0.90b ABOVE KEEL
C = 3.20
2.80
2.40
2.00
1.60
TRIM ANGLE, DEG.
12
10
8
6
4
2
TRIM
SPEED COEFFICIENT, $C_V = \frac{V}{\sqrt{gb}}$
0
1.00
2.00
3.00
4.00

Figure 14.

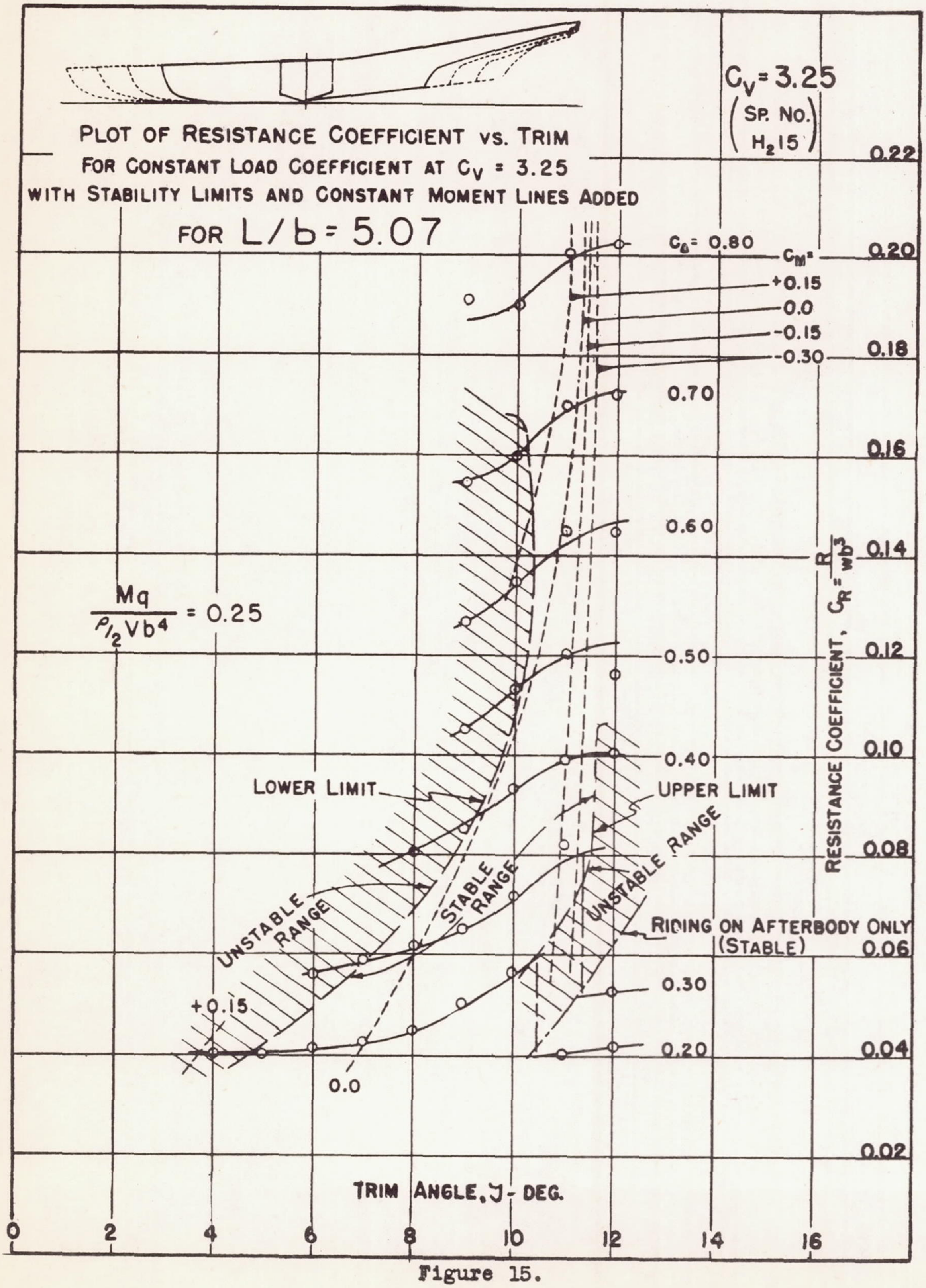

PLOT OF RESISTANCE COEFFICIENT vs. TRIM
FOR CONSTANT LOAD COEFFICIENT AT C_V = 3.25
WITH STABILITY LIMITS AND CONSTANT MOMENT LINES ADDED
FOR L/b = 5.07
C_V = 3.25 (SP. NO. $H_2$15)
$\frac{Mq}{\rho/_2 V b^4}$ = 0.25
C_Δ = 0.80
C_M =
+0.15
0.0
-0.15
-0.30
0.70
0.60
0.50
0.40
0.30
0.20
LOWER LIMIT
UPPER LIMIT
UNSTABLE RANGE
STABLE RANGE
UNSTABLE RANGE
RIDING ON AFTERBODY ONLY (STABLE)
+0.15
0.0
RESISTANCE COEFFICIENT, $C_R = \frac{R}{wb^3}$
0.22
0.20
0.18
0.16
0.14
0.12
0.10
0.08
0.06
0.04
0.02
TRIM ANGLE, τ - DEG.
0
2
4
6
8
10
12
14
16

Figure 15.

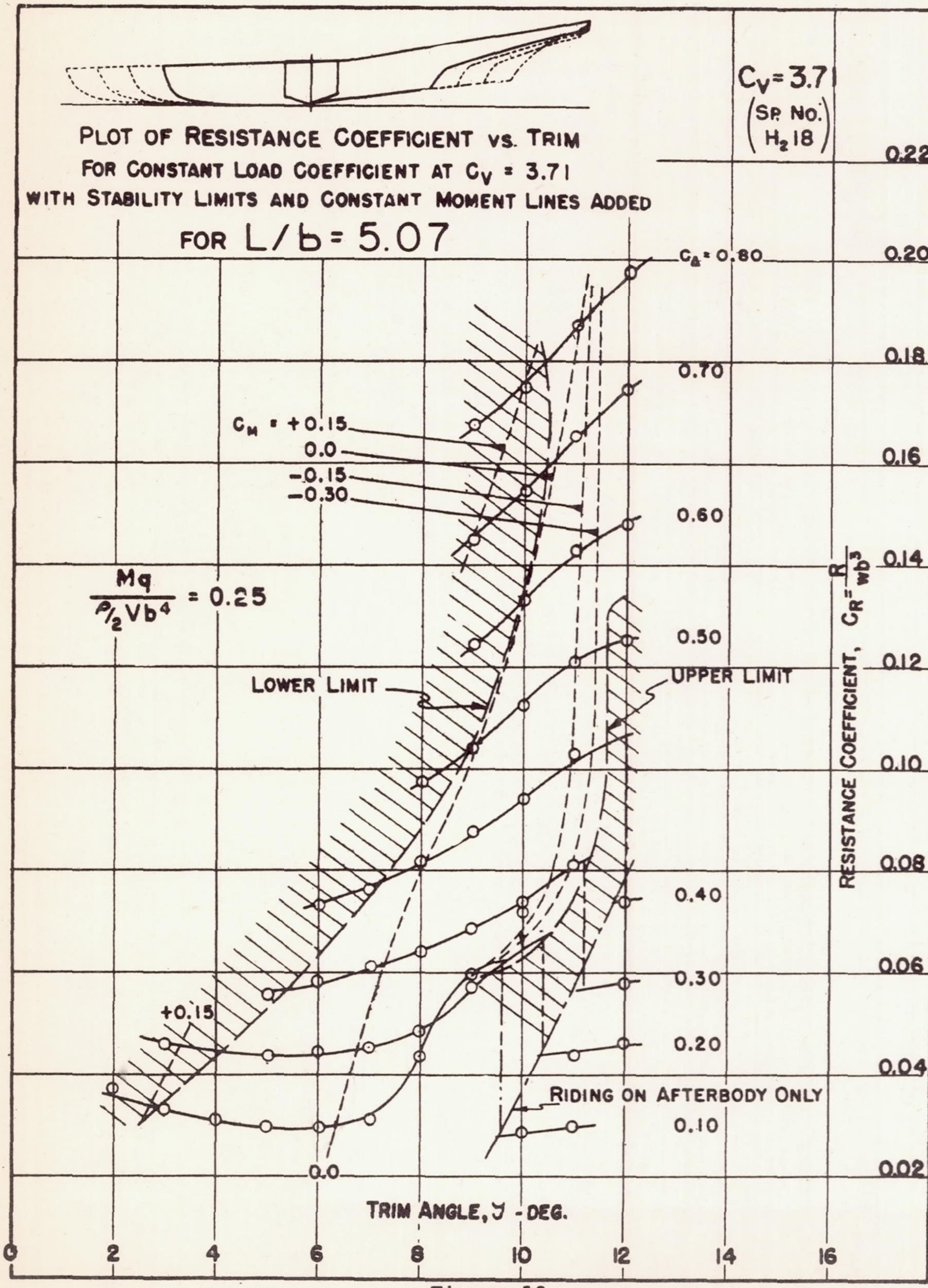
PLOT OF RESISTANCE COEFFICIENT vs. TRIM
FOR CONSTANT LOAD COEFFICIENT AT C_V = 3.71
WITH STABILITY LIMITS AND CONSTANT MOMENT LINES ADDED
FOR L/b = 5.07
C_V = 3.71
(SP. NO. $H_2$18)
$\frac{Mq}{\rho/_2 V b^4}$ = 0.25
C_Δ = 0.80
0.70
0.60
0.50
0.40
0.30
0.20
0.10
C_M = +0.15
0.0
-0.15
-0.30
+0.15
0.0
LOWER LIMIT
UPPER LIMIT
RIDING ON AFTERBODY ONLY
TRIM ANGLE, τ - DEG.
0
2
4
6
8
10
12
14
16
RESISTANCE COEFFICIENT, $C_R = \frac{R}{wb^3}$
0.02
0.04
0.06
0.08
0.10
0.12
0.14
0.16
0.18
0.20
0.22

Figure 16.

W-105

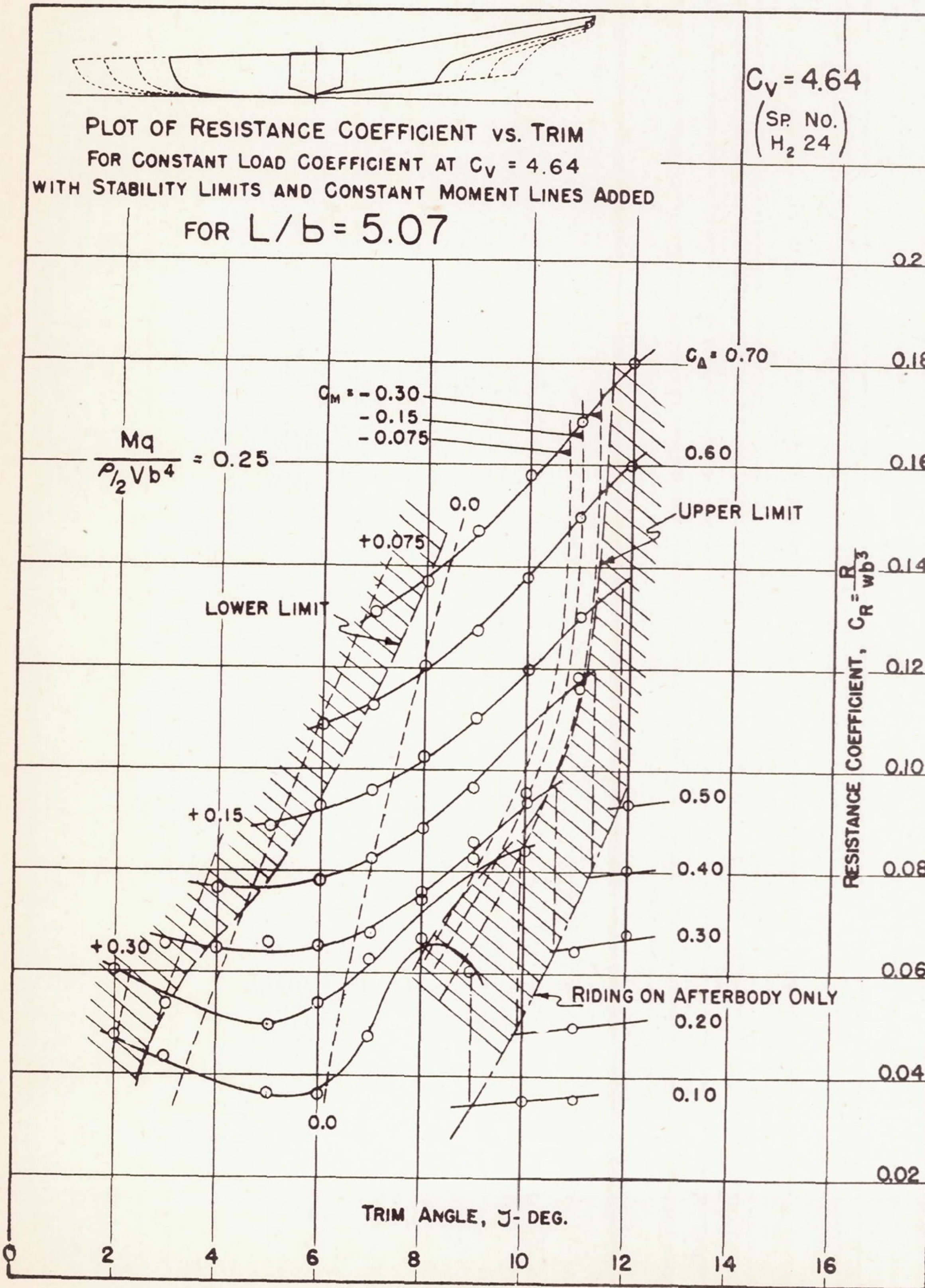

Figure 17.

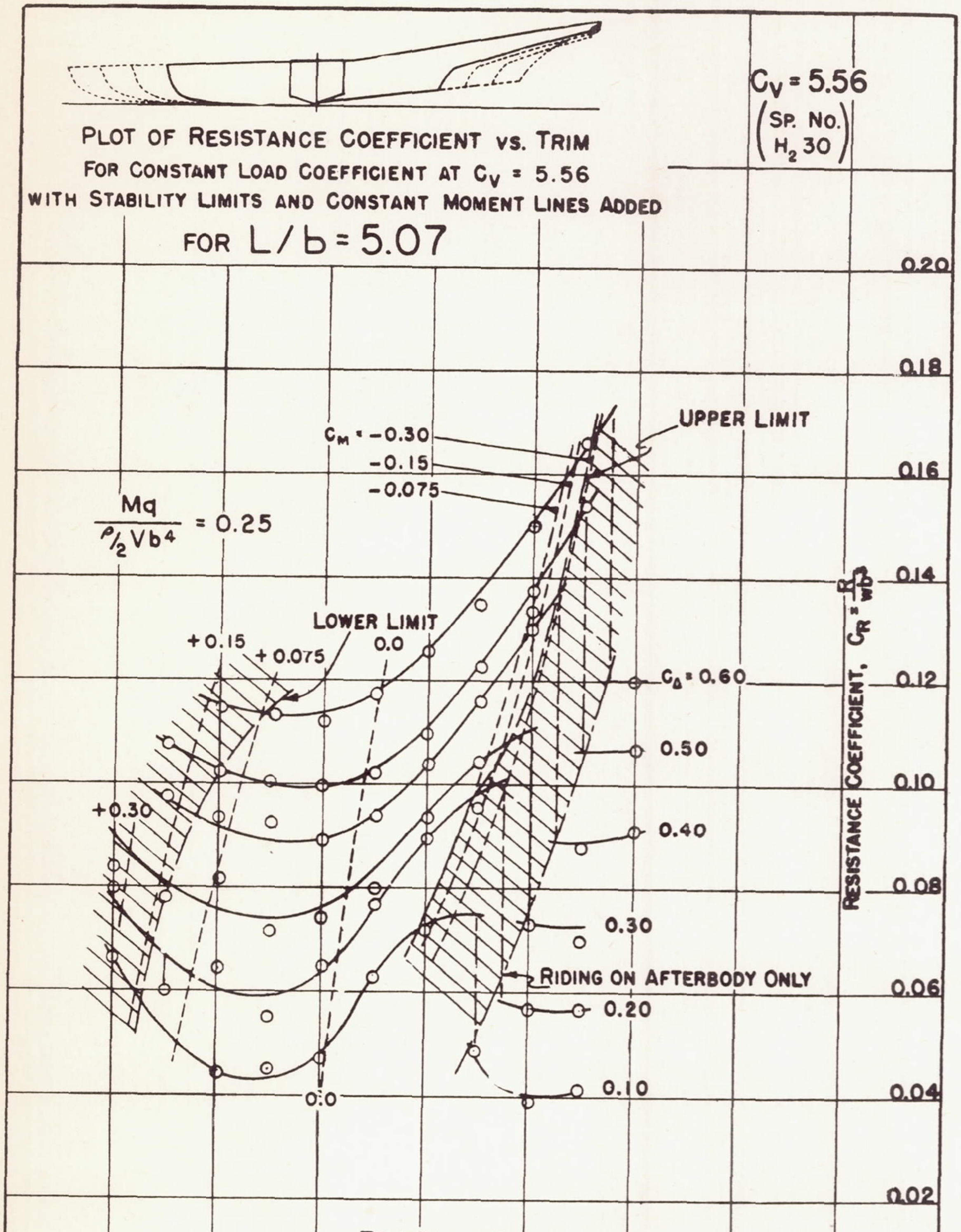
PLOT OF RESISTANCE COEFFICIENT vs. TRIM
FOR CONSTANT LOAD COEFFICIENT AT C_V = 5.56
WITH STABILITY LIMITS AND CONSTANT MOMENT LINES ADDED
FOR L/b = 5.07
C_V = 5.56
(SP. NO. H_2 30)
$\frac{Mq}{\rho/2\, V b^4}$ = 0.25
C_M = -0.30
-0.15
-0.075
UPPER LIMIT
LOWER LIMIT
+0.15
+0.075
0.0
+0.30
0.0
C_Δ = 0.60
0.50
0.40
0.30
RIDING ON AFTERBODY ONLY
0.20
0.10
RESISTANCE COEFFICIENT, $C_R = \frac{R}{wb^3}$
0.20
0.18
0.16
0.14
0.12
0.10
0.08
0.06
0.04
0.02
TRIM ANGLE, τ - DEG.
0
2
4
6
8
10
12
14
16

Figure 18.

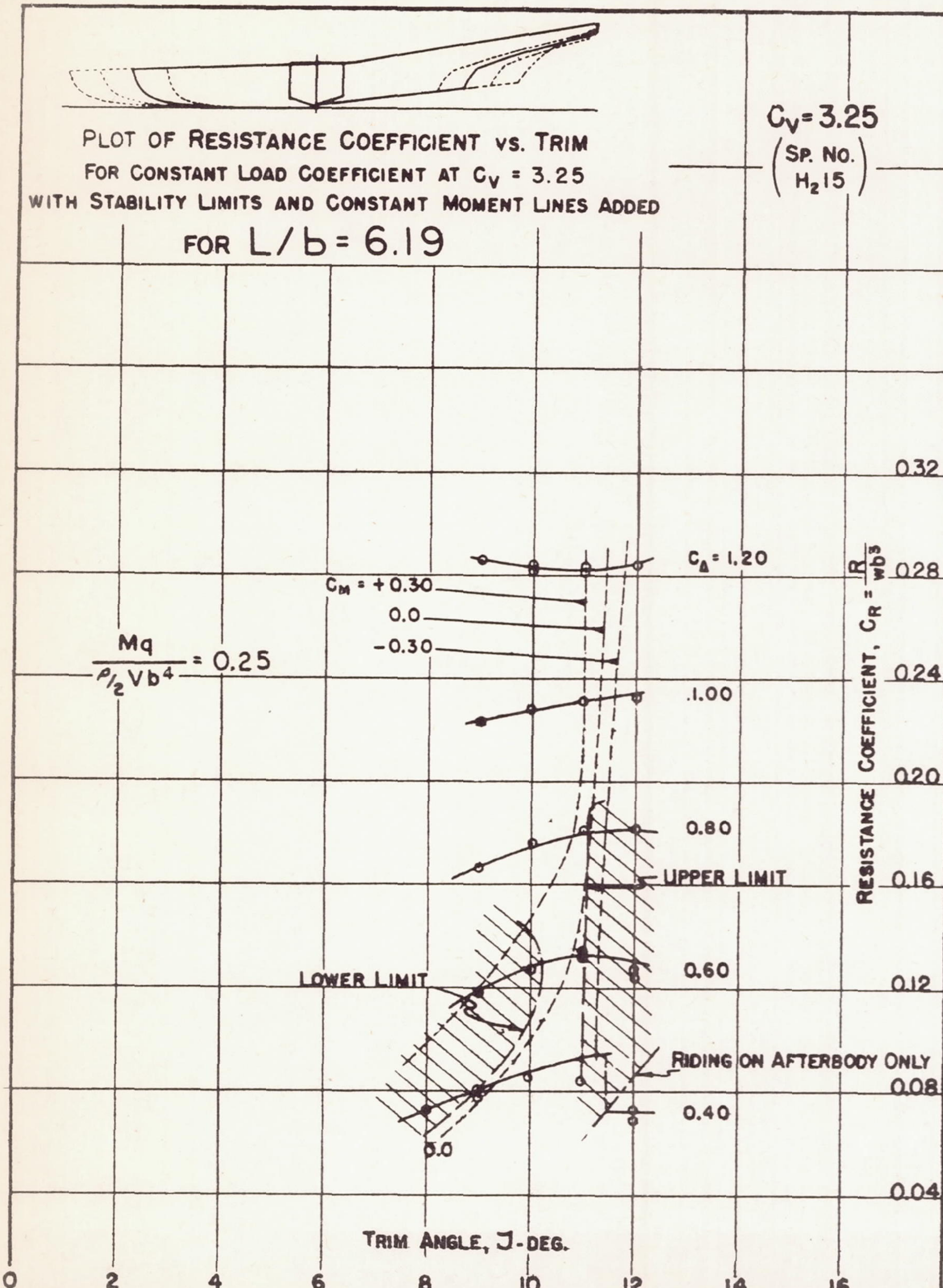
PLOT OF RESISTANCE COEFFICIENT VS. TRIM
FOR CONSTANT LOAD COEFFICIENT AT C_V = 3.25
WITH STABILITY LIMITS AND CONSTANT MOMENT LINES ADDED
FOR L/b = 6.19
C_V = 3.25
(SP. NO. $H_2$15)
$\frac{Mq}{\rho/2\, V b^4}$ = 0.25
C_Δ = 1.20
C_M = +0.30
0.0
-0.30
1.00
0.80
0.60
0.40
0.0
UPPER LIMIT
LOWER LIMIT
RIDING ON AFTERBODY ONLY
RESISTANCE COEFFICIENT, $C_R = \frac{R}{wb^3}$
0.32
0.28
0.24
0.20
0.16
0.12
0.08
0.04
TRIM ANGLE, τ-DEG.
0
2
4
6
8
10
12
14
16

Figure 19.

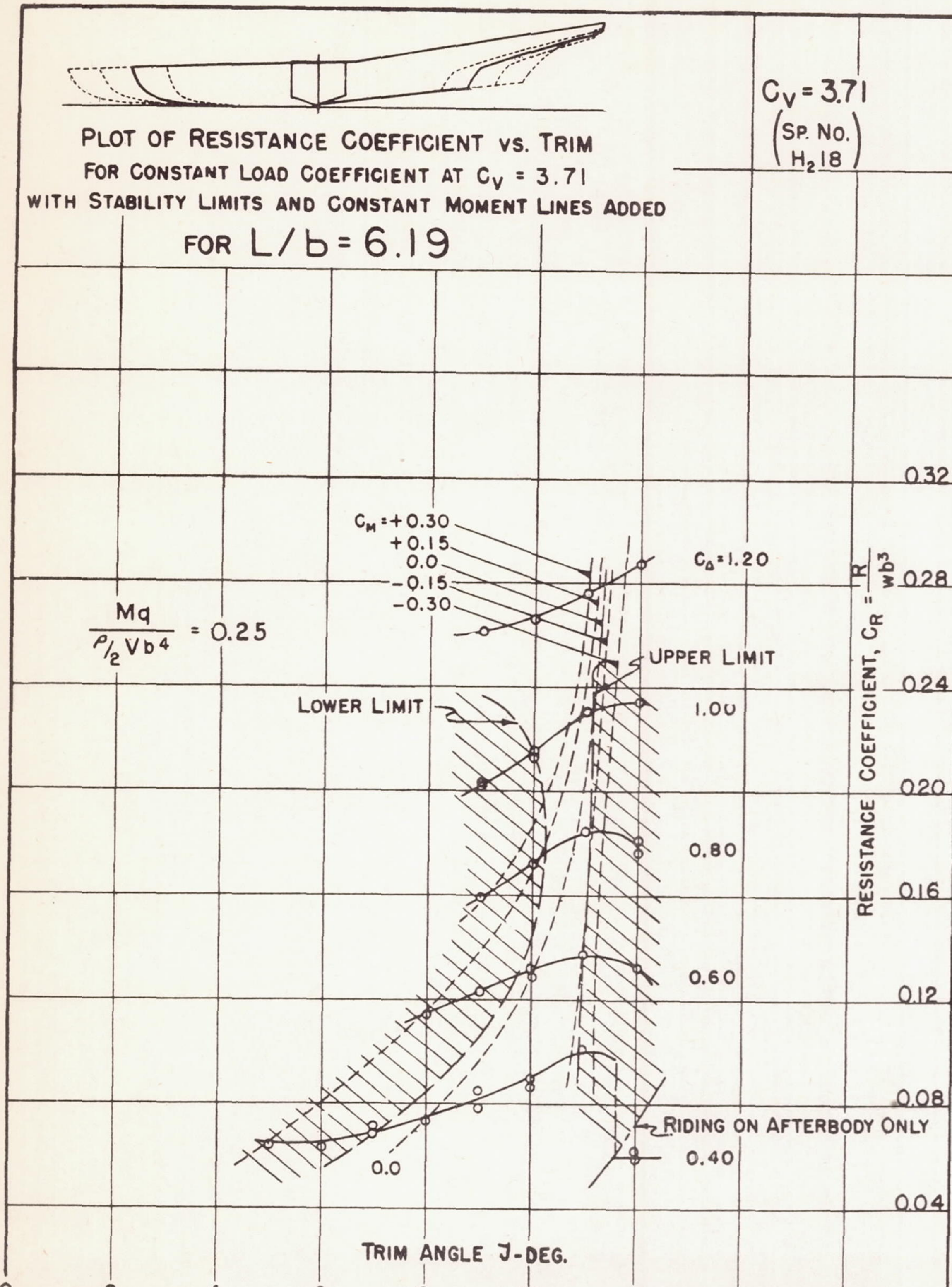
PLOT OF RESISTANCE COEFFICIENT vs. TRIM
FOR CONSTANT LOAD COEFFICIENT AT C_V = 3.71
WITH STABILITY LIMITS AND CONSTANT MOMENT LINES ADDED
FOR L/b = 6.19
C_V = 3.71
(SP. NO. H_2 18)
$\frac{Mq}{\rho/_2 V b^4}$ = 0.25
C_M = +0.30
+0.15
0.0
-0.15
-0.30
C_Δ = 1.20
UPPER LIMIT
LOWER LIMIT
1.00
0.80
0.60
0.0
RIDING ON AFTERBODY ONLY
0.40
RESISTANCE COEFFICIENT, $C_R = \frac{R}{wb^3}$
0.32
0.28
0.24
0.20
0.16
0.12
0.08
0.04
TRIM ANGLE J-DEG.
0
2
4
6
8
10
12
14
16

Figure 20.

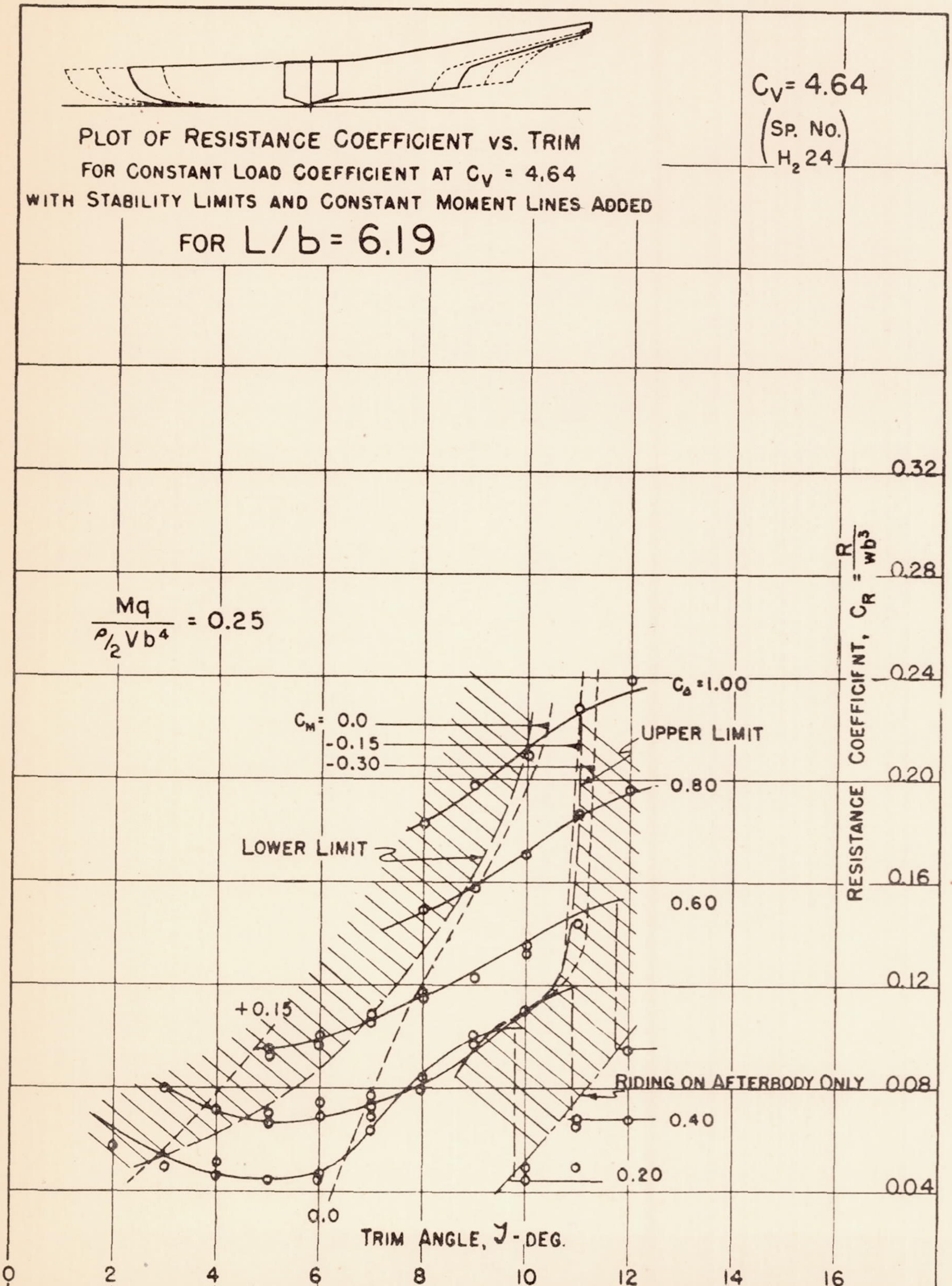

PLOT OF RESISTANCE COEFFICIENT VS. TRIM
FOR CONSTANT LOAD COEFFICIENT AT C_V = 4.64
WITH STABILITY LIMITS AND CONSTANT MOMENT LINES ADDED
FOR L/b = 6.19
C_V = 4.64
(SP. NO. $H_2$24)
$\frac{Mq}{\rho/2 V b^4}$ = 0.25
C_Δ = 1.00
0.80
0.60
0.40
0.20
C_M = 0.0
-0.15
-0.30
+0.15
0.0
UPPER LIMIT
LOWER LIMIT
RIDING ON AFTERBODY ONLY
TRIM ANGLE, τ - DEG.
RESISTANCE COEFFICIENT, $C_R = \frac{R}{wb^3}$
0 2 4 6 8 10 12 14 16
0.04 0.08 0.12 0.16 0.20 0.24 0.28 0.32

Figure 21.

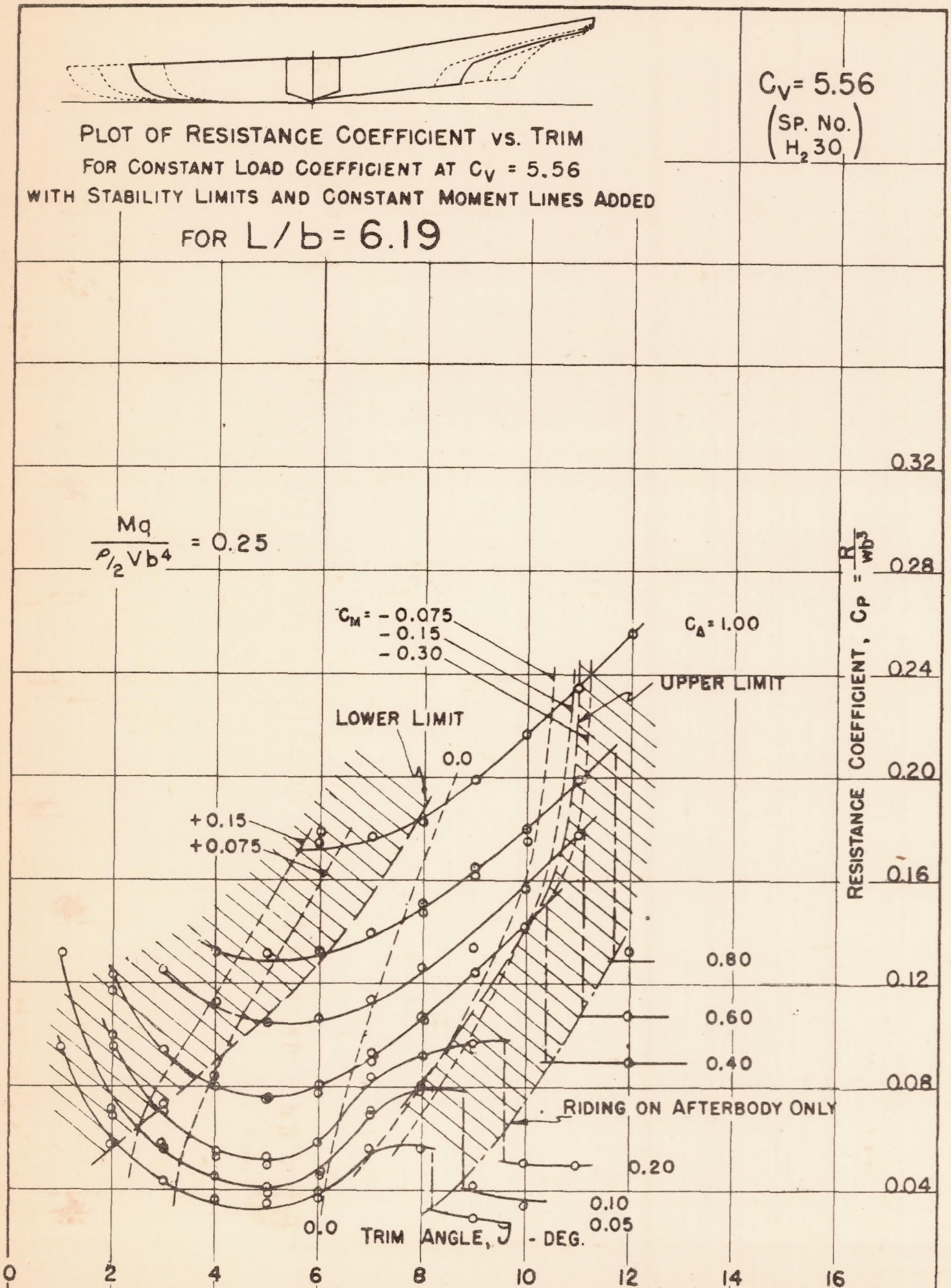
PLOT OF RESISTANCE COEFFICIENT vs. TRIM
FOR CONSTANT LOAD COEFFICIENT AT C_V = 5.56
WITH STABILITY LIMITS AND CONSTANT MOMENT LINES ADDED
FOR L/b = 6.19
C_V= 5.56
(SP. NO. $H_2$30)
$\frac{Mq}{\rho/2 V b^4}$ = 0.25
C_M = −0.075
−0.15
−0.30
C_Δ = 1.00
UPPER LIMIT
LOWER LIMIT
0.0
+0.15
+0.075
0.80
0.60
0.40
RIDING ON AFTERBODY ONLY
0.20
0.10
0.05
0.0
TRIM ANGLE, τ - DEG.
RESISTANCE COEFFICIENT, $C_R = \frac{R}{wb^3}$
0.32
0.28
0.24
0.20
0.16
0.12
0.08
0.04
0
2
4
6
8
10
12
14
16

Figure 22.

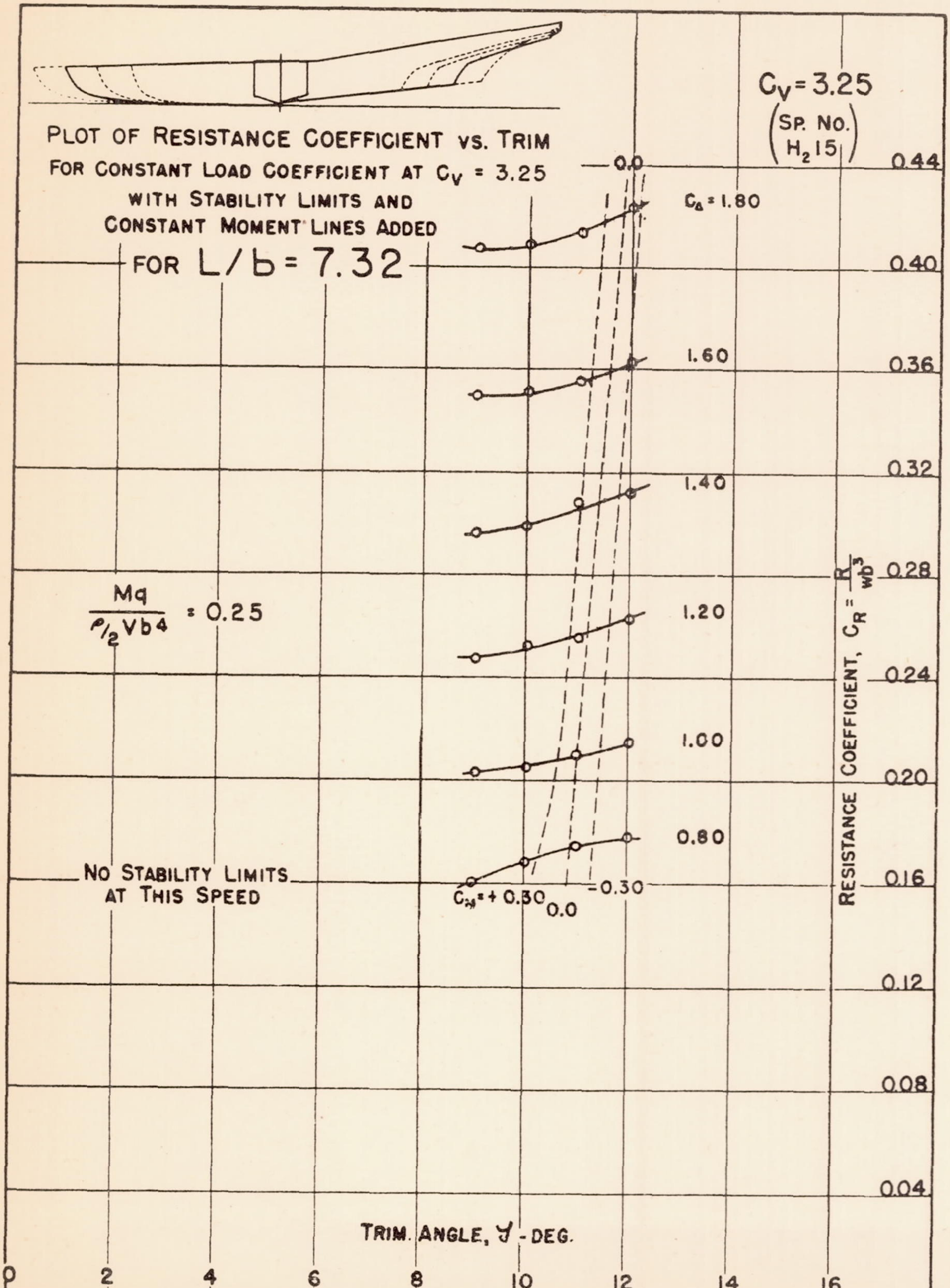
PLOT OF RESISTANCE COEFFICIENT vs. TRIM
FOR CONSTANT LOAD COEFFICIENT AT C_V = 3.25
WITH STABILITY LIMITS AND
CONSTANT MOMENT LINES ADDED
FOR L/b = 7.32
C_V = 3.25
(SP. NO. $H_2$15)
$\frac{Mq}{\rho/2\, V b^4}$ = 0.25
NO STABILITY LIMITS AT THIS SPEED
C_Δ = 1.80
1.60
1.40
1.20
1.00
0.80
0.0
C_M = + 0.30
0.0
-0.30
TRIM. ANGLE, τ - DEG.
RESISTANCE COEFFICIENT, $C_R = \frac{R}{wb^3}$
0
2
4
6
8
10
12
14
16
0.04
0.08
0.12
0.16
0.20
0.24
0.28
0.32
0.36
0.40
0.44

Figure 23.

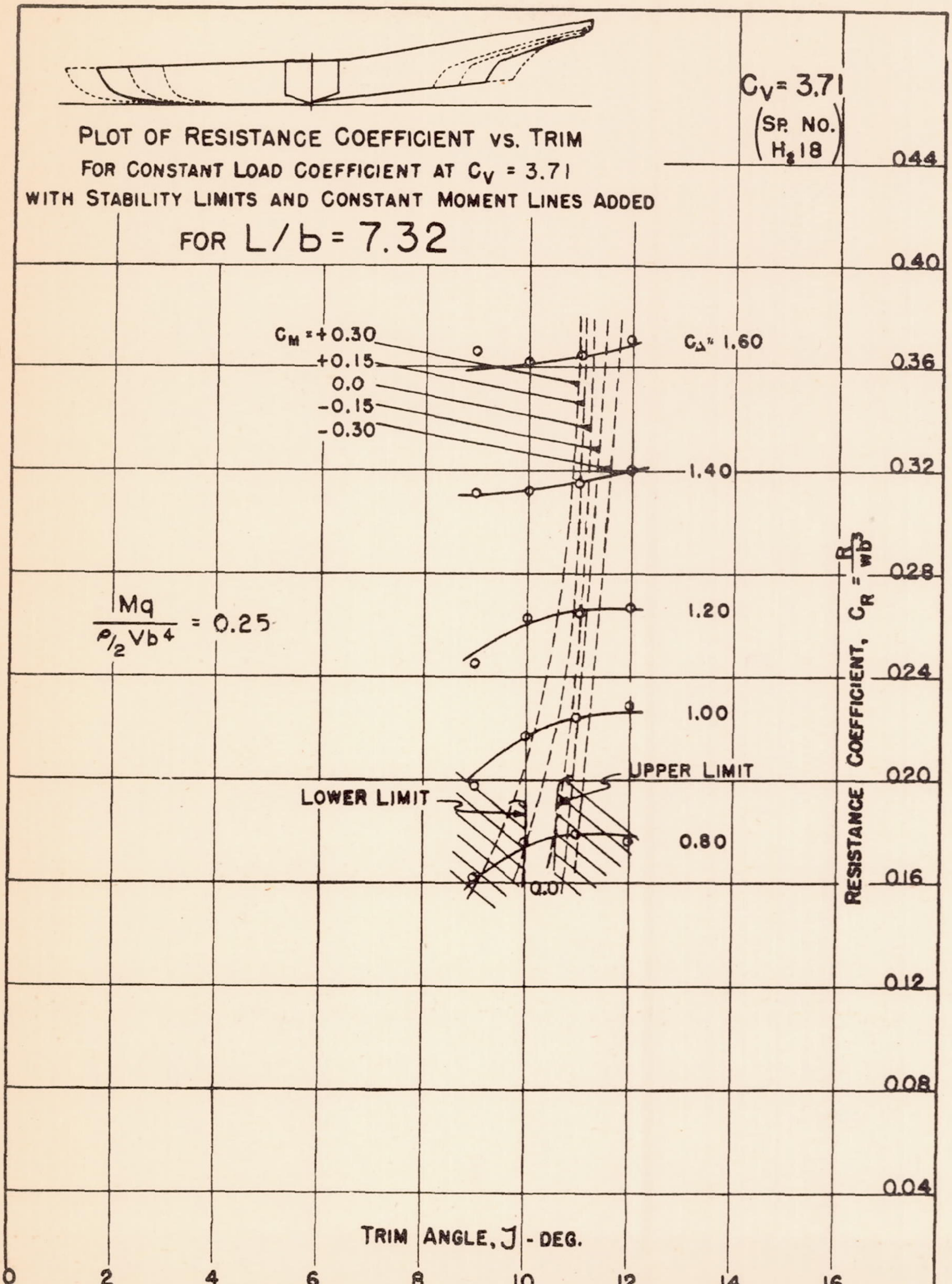
PLOT OF RESISTANCE COEFFICIENT VS. TRIM
FOR CONSTANT LOAD COEFFICIENT AT C_V = 3.71
WITH STABILITY LIMITS AND CONSTANT MOMENT LINES ADDED
FOR L/b = 7.32
C_V = 3.71
(SP. NO. $H_8$18)
C_M = +0.30
+0.15
0.0
-0.15
-0.30
C_Δ = 1.60
1.40
1.20
1.00
0.80
$\frac{Mq}{\rho/2 V b^4}$ = 0.25
UPPER LIMIT
LOWER LIMIT
0.01
TRIM ANGLE, τ - DEG.
RESISTANCE COEFFICIENT, $C_R = \frac{R}{wb^3}$
0.44
0.40
0.36
0.32
0.28
0.24
0.20
0.16
0.12
0.08
0.04
0
2
4
6
8
10
12
14
16

Figure 24.

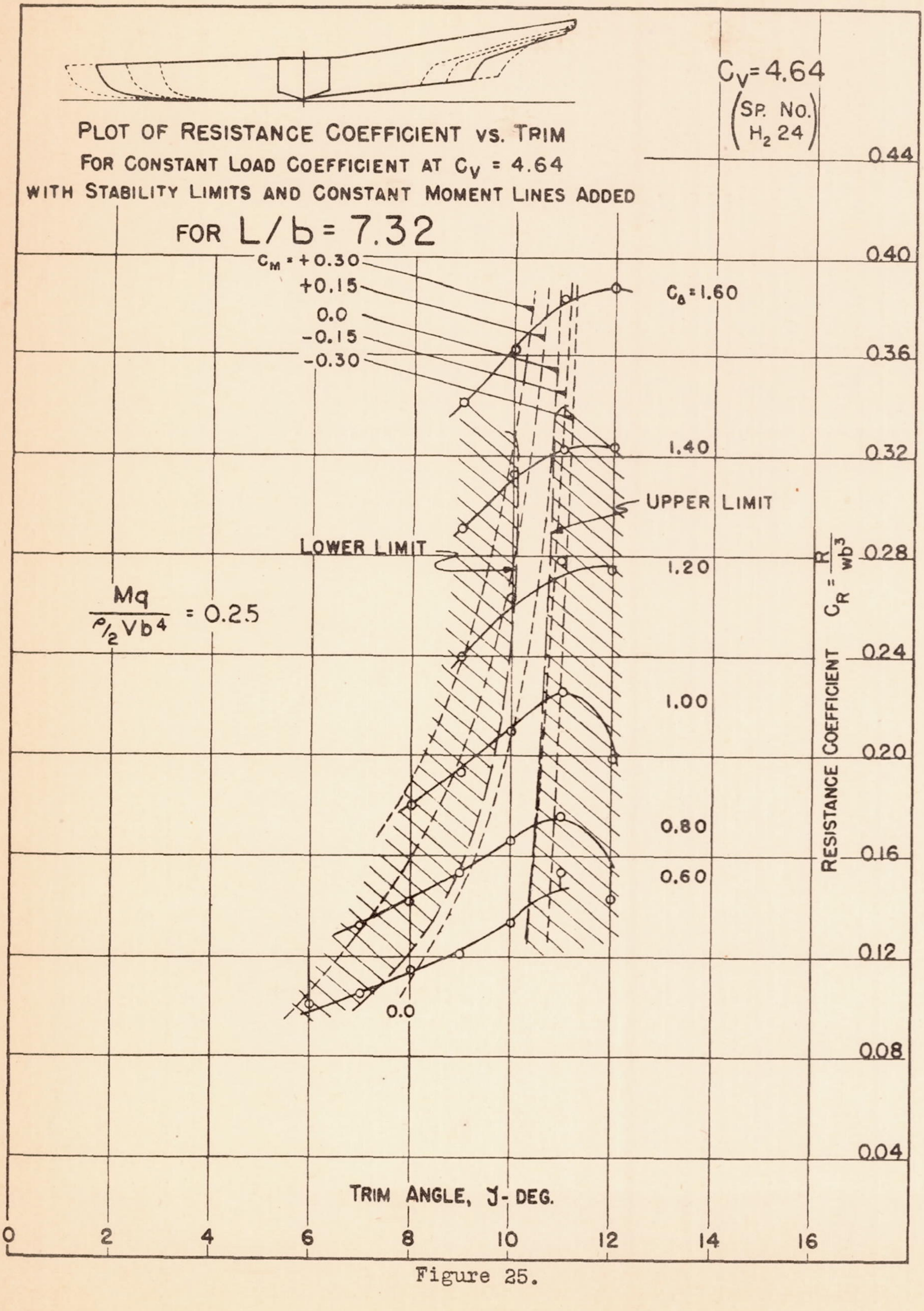
PLOT OF RESISTANCE COEFFICIENT VS. TRIM
FOR CONSTANT LOAD COEFFICIENT AT C_V = 4.64
WITH STABILITY LIMITS AND CONSTANT MOMENT LINES ADDED
FOR L/b = 7.32
C_V = 4.64
(SP. No. H_2 24)
C_M = +0.30
+0.15
0.0
-0.15
-0.30
C_Δ = 1.60
1.40
1.20
1.00
0.80
0.60
0.0
UPPER LIMIT
LOWER LIMIT
$\frac{Mq}{\rho/_2 V b^4}$ = 0.25
RESISTANCE COEFFICIENT $C_R = \frac{R}{wb^3}$
0.44
0.40
0.36
0.32
0.28
0.24
0.20
0.16
0.12
0.08
0.04
TRIM ANGLE, τ- DEG.
0
2
4
6
8
10
12
14
16

Figure 25.

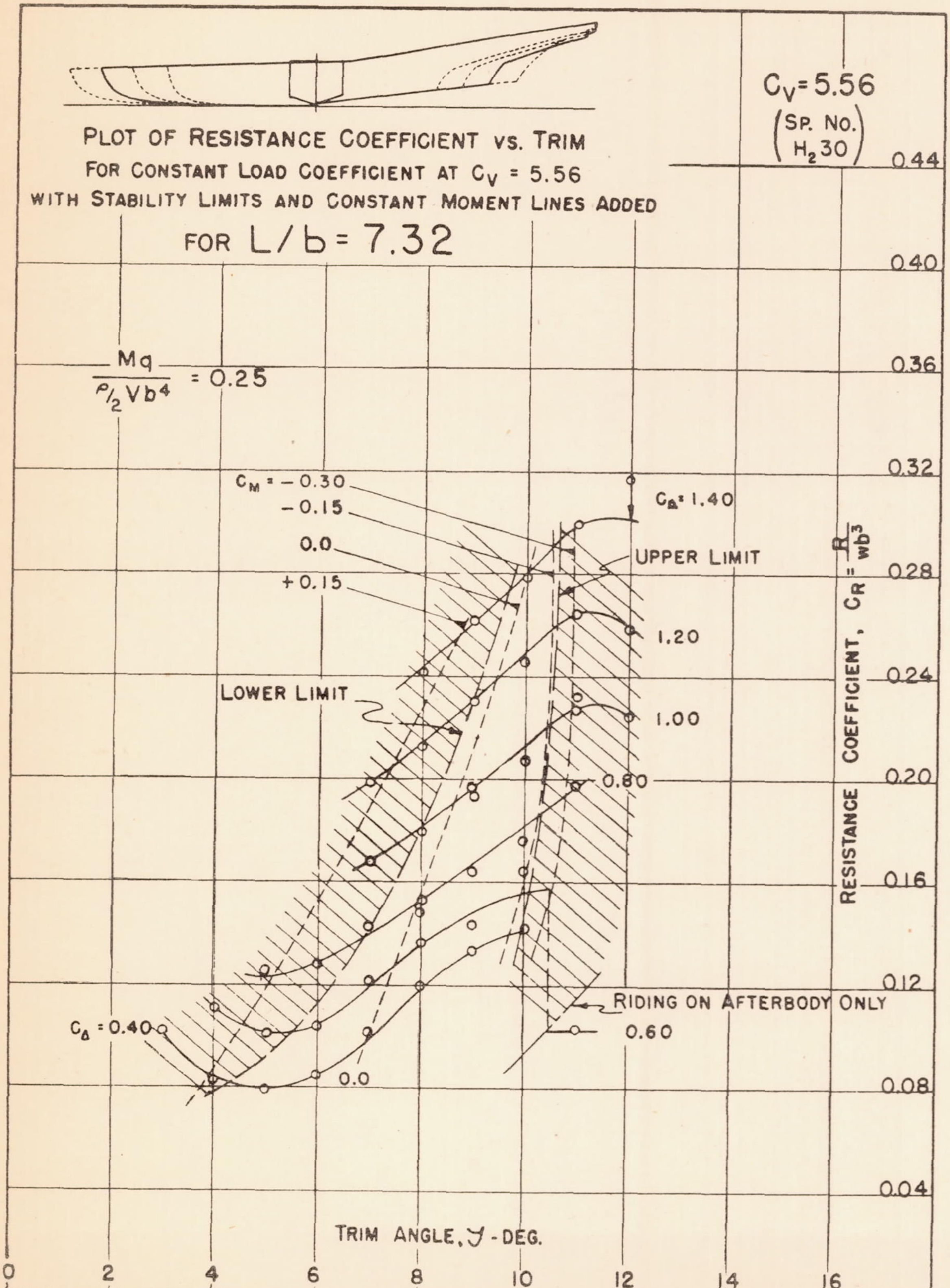
PLOT OF RESISTANCE COEFFICIENT vs. TRIM
FOR CONSTANT LOAD COEFFICIENT AT C_V = 5.56
WITH STABILITY LIMITS AND CONSTANT MOMENT LINES ADDED
FOR L/b = 7.32
C_V = 5.56
(SP. NO. $H_2$30)
$\frac{Mq}{\rho/2\, V b^4}$ = 0.25
C_M = −0.30
−0.15
0.0
+0.15
C_Δ = 1.40
UPPER LIMIT
1.20
LOWER LIMIT
1.00
0.80
RIDING ON AFTERBODY ONLY
0.60
C_Δ = 0.40
0.0
RESISTANCE COEFFICIENT, $C_R = \frac{R}{wb^3}$
TRIM ANGLE, τ - DEG.
0.44
0.40
0.36
0.32
0.28
0.24
0.20
0.16
0.12
0.08
0.04
0
2
4
6
8
10
12
14
16

Figure 26.

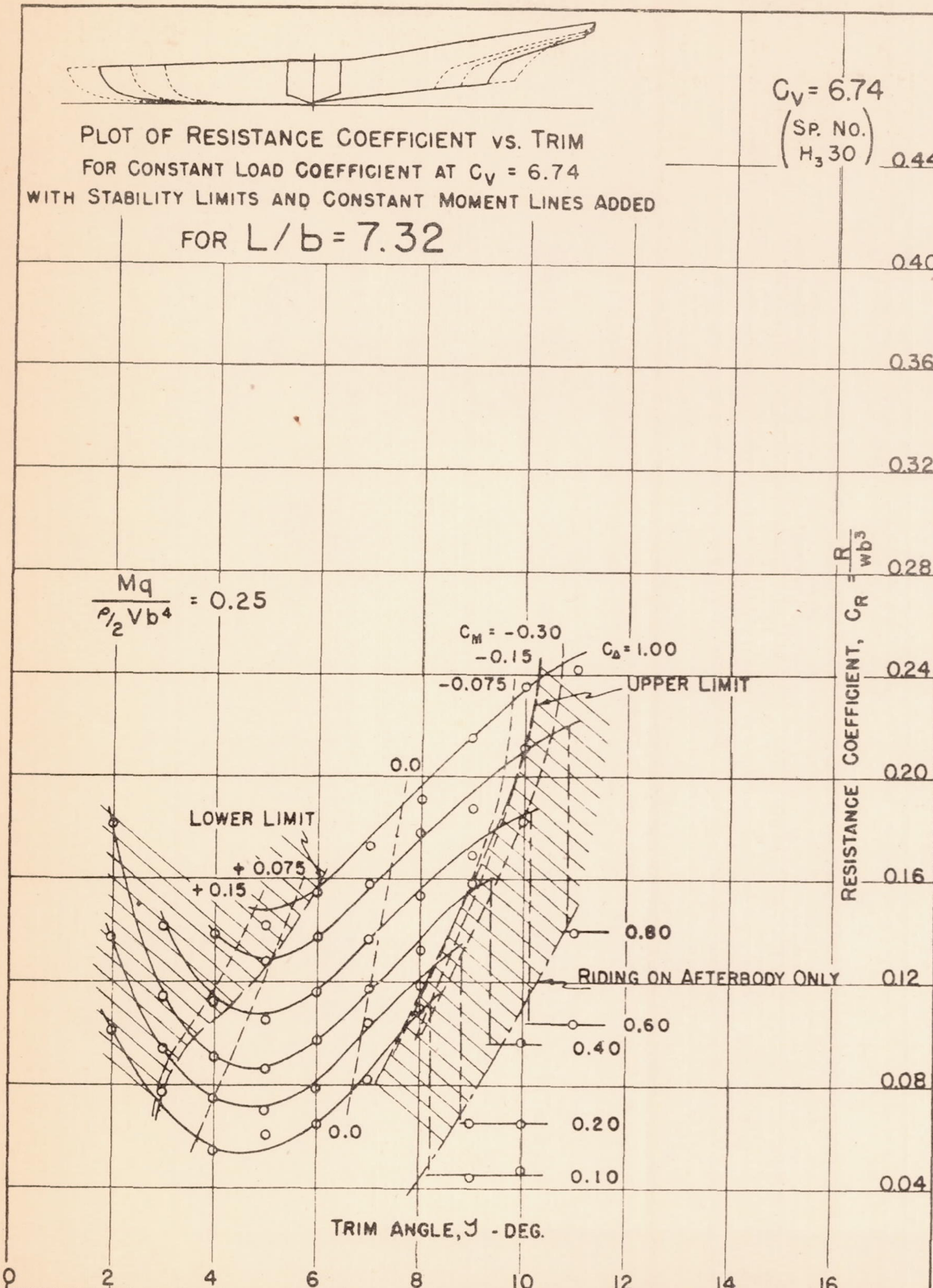

PLOT OF RESISTANCE COEFFICIENT vs. TRIM
FOR CONSTANT LOAD COEFFICIENT AT C_V = 6.74
WITH STABILITY LIMITS AND CONSTANT MOMENT LINES ADDED
FOR L/b = 7.32
C_V = 6.74
(SP. NO. $H_3$30)
$\frac{Mq}{\rho/2 V b^4}$ = 0.25
C_M = -0.30
-0.15
-0.075
C_Δ = 1.00
UPPER LIMIT
LOWER LIMIT
+0.075
+0.15
0.0
0.80
RIDING ON AFTERBODY ONLY
0.60
0.40
0.20
0.10
RESISTANCE COEFFICIENT, $C_R = \frac{R}{wb^3}$
TRIM ANGLE, τ - DEG.
0.44
0.40
0.36
0.32
0.28
0.24
0.20
0.16
0.12
0.08
0.04
0
2
4
6
8
10
12
14
16

Figure 27.

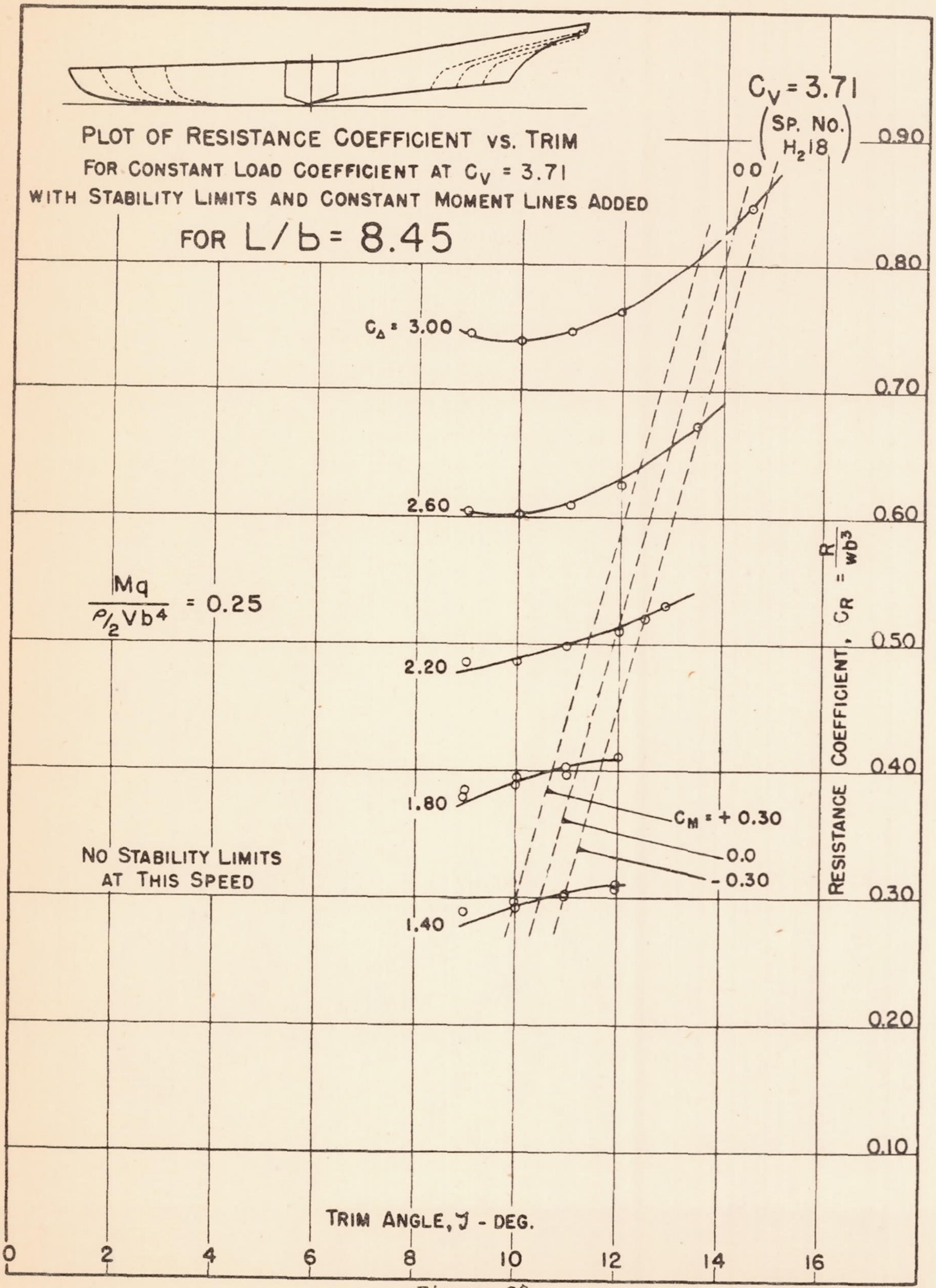
PLOT OF RESISTANCE COEFFICIENT VS. TRIM
FOR CONSTANT LOAD COEFFICIENT AT C_V = 3.71
WITH STABILITY LIMITS AND CONSTANT MOMENT LINES ADDED
FOR L/b = 8.45
C_V = 3.71
(SP. NO. $H_2$18)
C_Δ = 3.00
2.60
2.20
1.80
1.40
$\frac{Mq}{\rho/2 V b^4}$ = 0.25
C_M = + 0.30
0.0
- 0.30
NO STABILITY LIMITS AT THIS SPEED
RESISTANCE COEFFICIENT, $C_R = \frac{R}{wb^3}$
0.90
0.80
0.70
0.60
0.50
0.40
0.30
0.20
0.10
TRIM ANGLE, τ - DEG.
0
2
4
6
8
10
12
14
16

Figure 28.

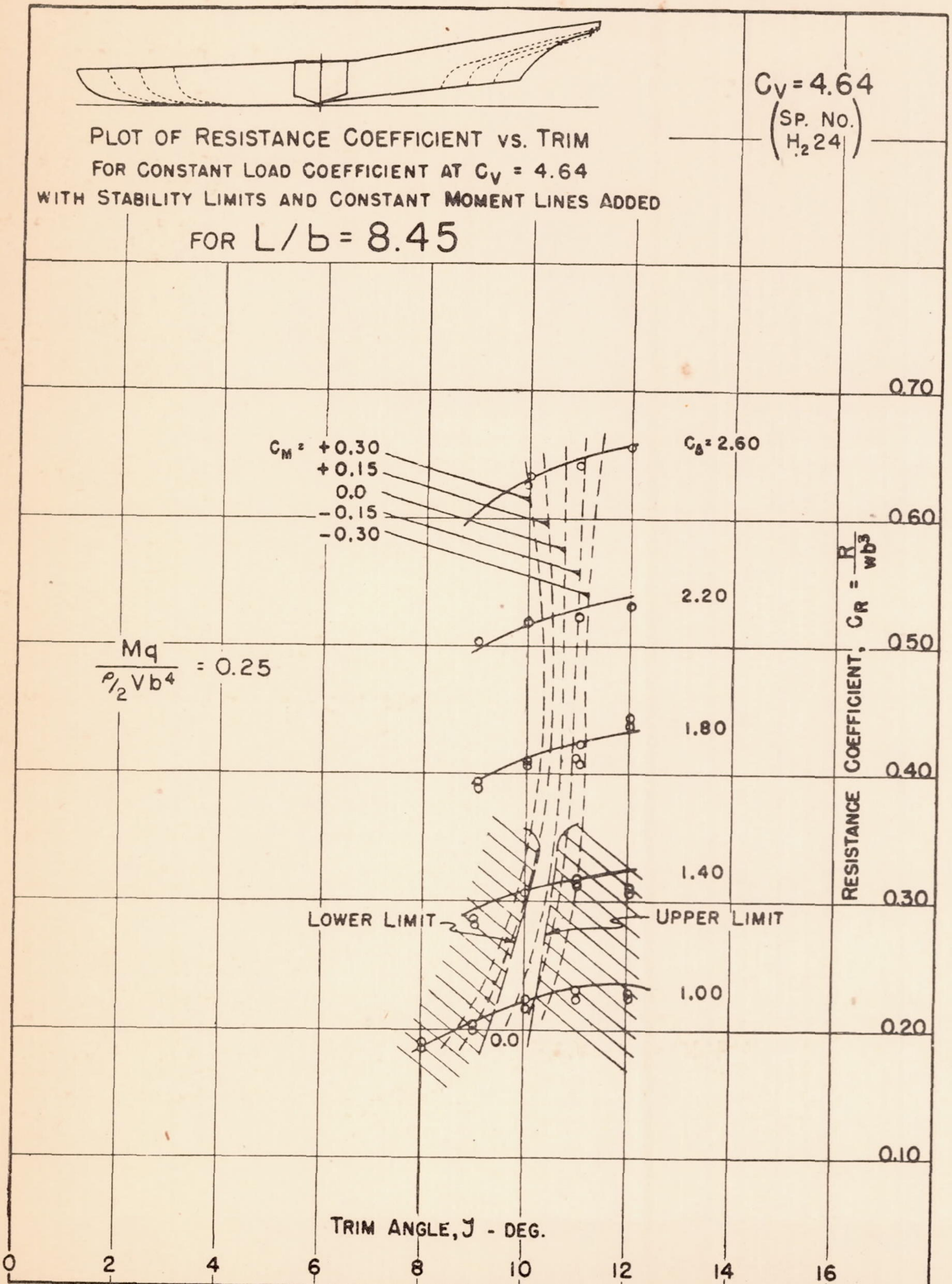
PLOT OF RESISTANCE COEFFICIENT vs. TRIM
FOR CONSTANT LOAD COEFFICIENT AT C_V = 4.64
WITH STABILITY LIMITS AND CONSTANT MOMENT LINES ADDED
FOR L/b = 8.45
C_V = 4.64
(SP. NO. $H_2$24)
C_M = +0.30
+0.15
0.0
-0.15
-0.30
C_Δ = 2.60
2.20
1.80
1.40
1.00
$\frac{Mq}{\rho/2\, V b^4}$ = 0.25
LOWER LIMIT
UPPER LIMIT
0.0
RESISTANCE COEFFICIENT, $C_R = \frac{R}{wb^3}$
0.70
0.60
0.50
0.40
0.30
0.20
0.10
TRIM ANGLE, τ - DEG.
0
2
4
6
8
10
12
14
16

Figure 29.

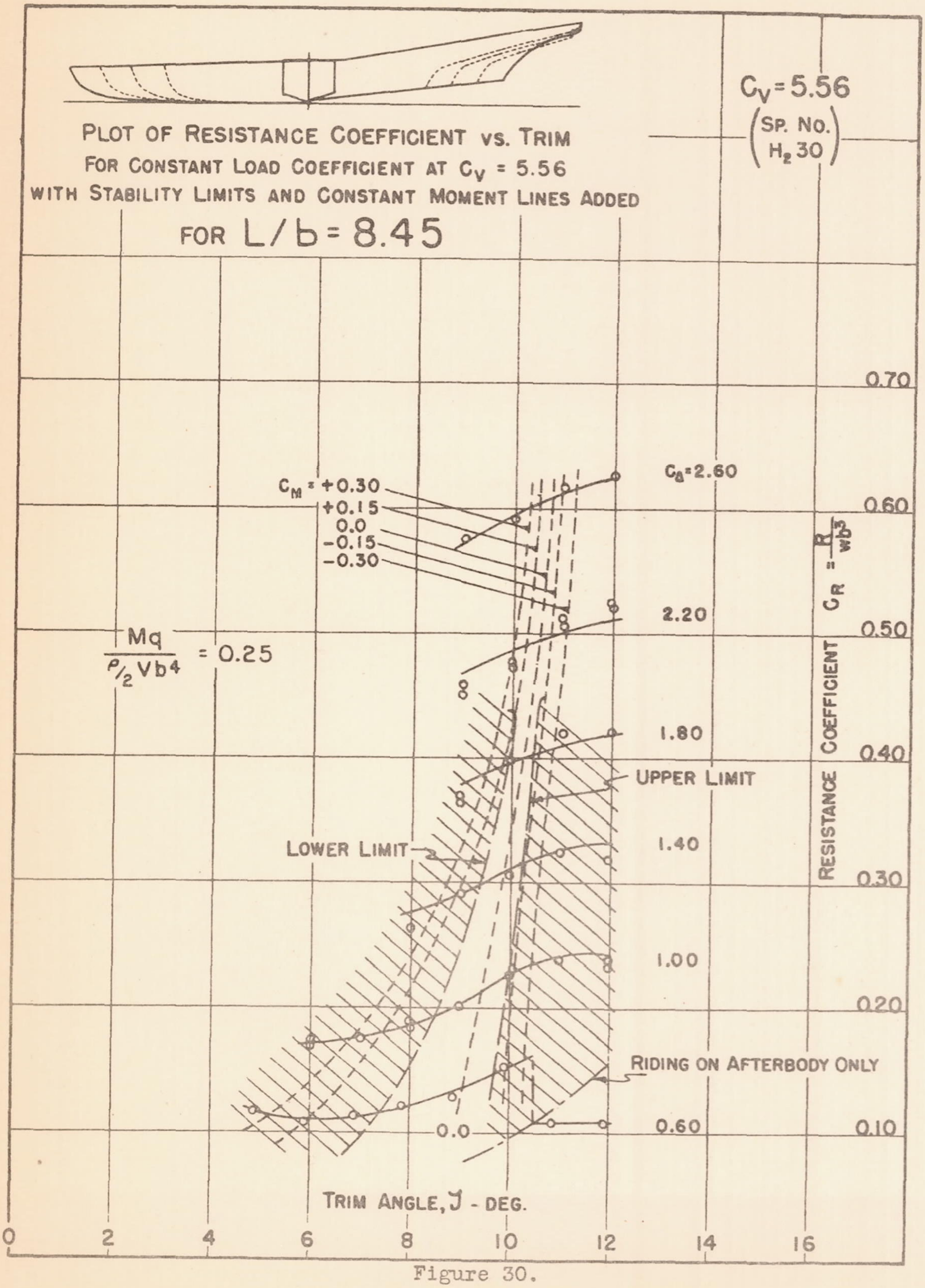
PLOT OF RESISTANCE COEFFICIENT vs. TRIM
FOR CONSTANT LOAD COEFFICIENT AT C_V = 5.56
WITH STABILITY LIMITS AND CONSTANT MOMENT LINES ADDED
FOR L/b = 8.45
C_V = 5.56
(SP. NO. H_2 30)
C_M = +0.30
+0.15
0.0
-0.15
-0.30
C_Δ = 2.60
2.20
1.80
1.40
1.00
0.60
0.0
$\frac{Mq}{\rho/2\, V b^4}$ = 0.25
UPPER LIMIT
LOWER LIMIT
RIDING ON AFTERBODY ONLY
RESISTANCE COEFFICIENT $C_R = \frac{R}{wb^3}$
0.70
0.60
0.50
0.40
0.30
0.20
0.10
TRIM ANGLE, τ - DEG.
0
2
4
6
8
10
12
14
16

Figure 30.

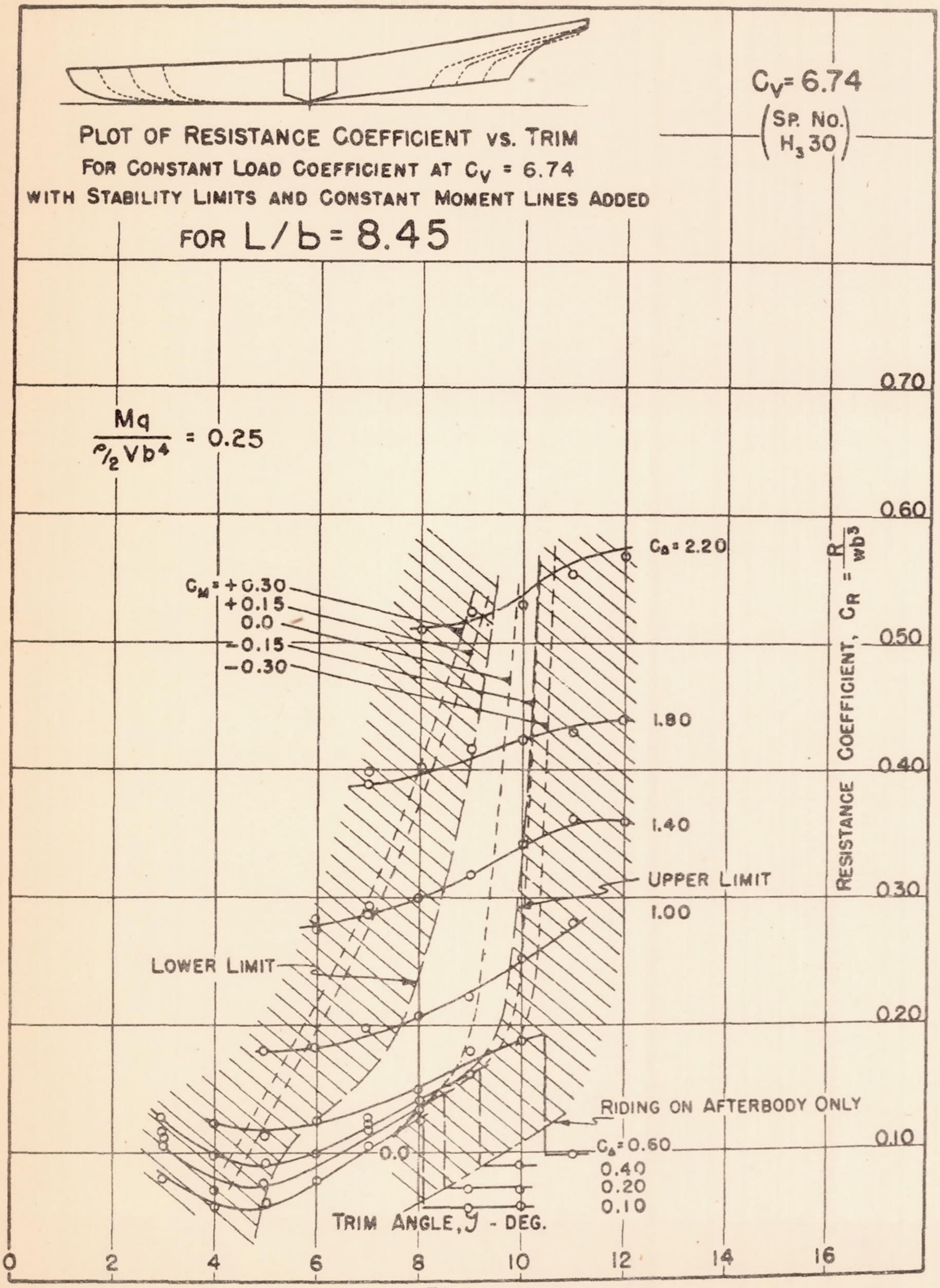
PLOT OF RESISTANCE COEFFICIENT vs. TRIM
FOR CONSTANT LOAD COEFFICIENT AT C_V = 6.74
WITH STABILITY LIMITS AND CONSTANT MOMENT LINES ADDED
FOR L/b = 8.45
C_V = 6.74
(SP. No. $H_3$30)
$\frac{Mq}{\rho/2\, V b^4}$ = 0.25
C_M = +0.30
+0.15
0.0
-0.15
-0.30
C_Δ = 2.20
1.80
1.40
UPPER LIMIT
1.00
LOWER LIMIT
RIDING ON AFTERBODY ONLY
C_Δ = 0.60
0.40
0.20
0.10
0.0
TRIM ANGLE, τ - DEG.
RESISTANCE COEFFICIENT, $C_R = \frac{R}{wb^3}$
0.70
0.60
0.50
0.40
0.30
0.20
0.10
0
2
4
6
8
10
12
14
16

Figure 31.

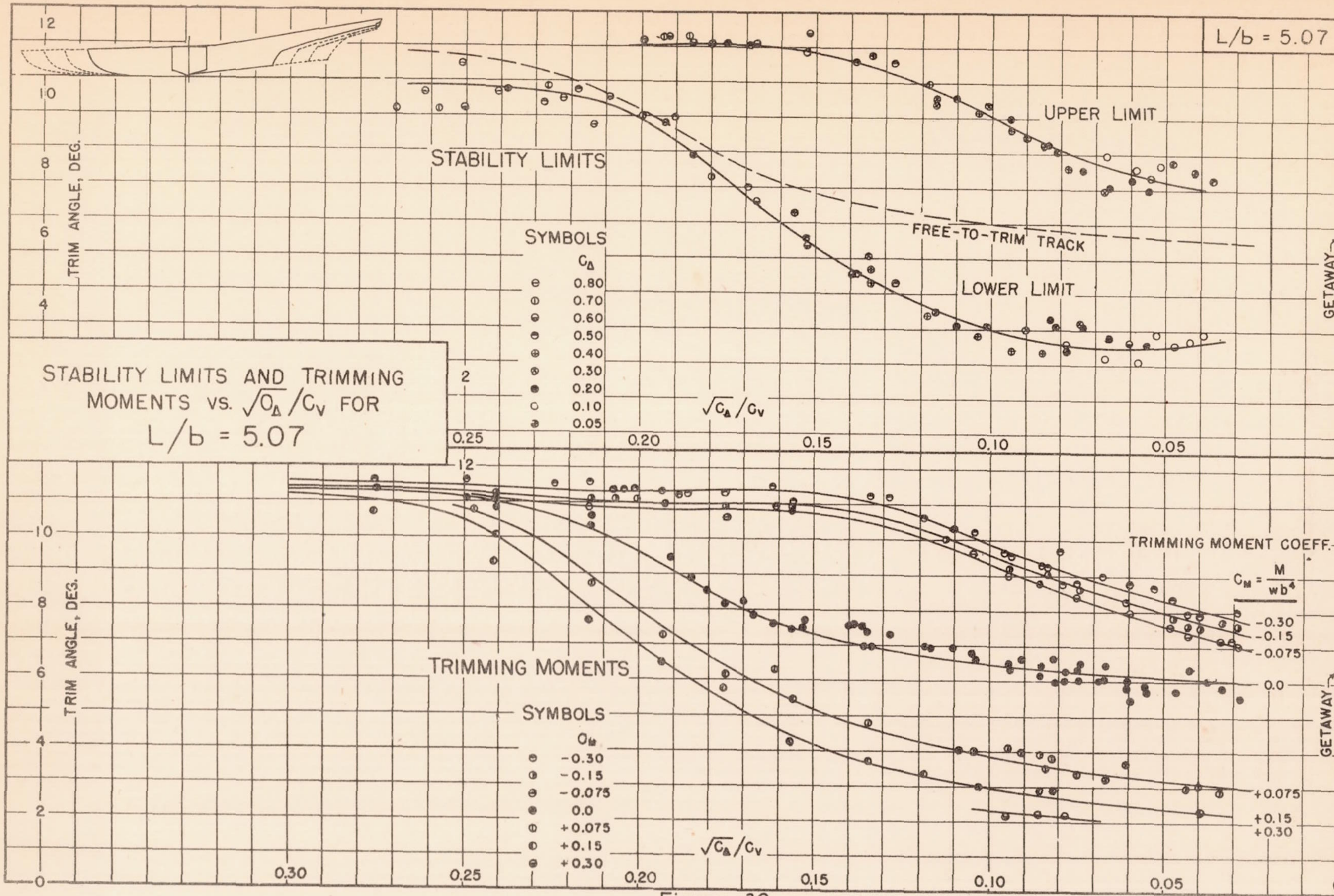

STABILITY LIMITS AND TRIMMING MOMENTS vs. $\sqrt{C_\Delta}/C_V$ FOR L/b = 5.07
L/b = 5.07
STABILITY LIMITS
UPPER LIMIT
LOWER LIMIT
FREE-TO-TRIM TRACK
GETAWAY
SYMBOLS
C_Δ
0.80
0.70
0.60
0.50
0.40
0.30
0.20
0.10
0.05
TRIM ANGLE, DEG.
$\sqrt{C_\Delta}/C_V$
TRIMMING MOMENTS
SYMBOLS
C_M
-0.30
-0.15
-0.075
0.0
+0.075
+0.15
+0.30
TRIMMING MOMENT COEFF.
$C_M = \frac{M}{wb^4}$
NACA ARR No. 4F15
(1 block = 10/40")
Fig. 32

Figure 32.

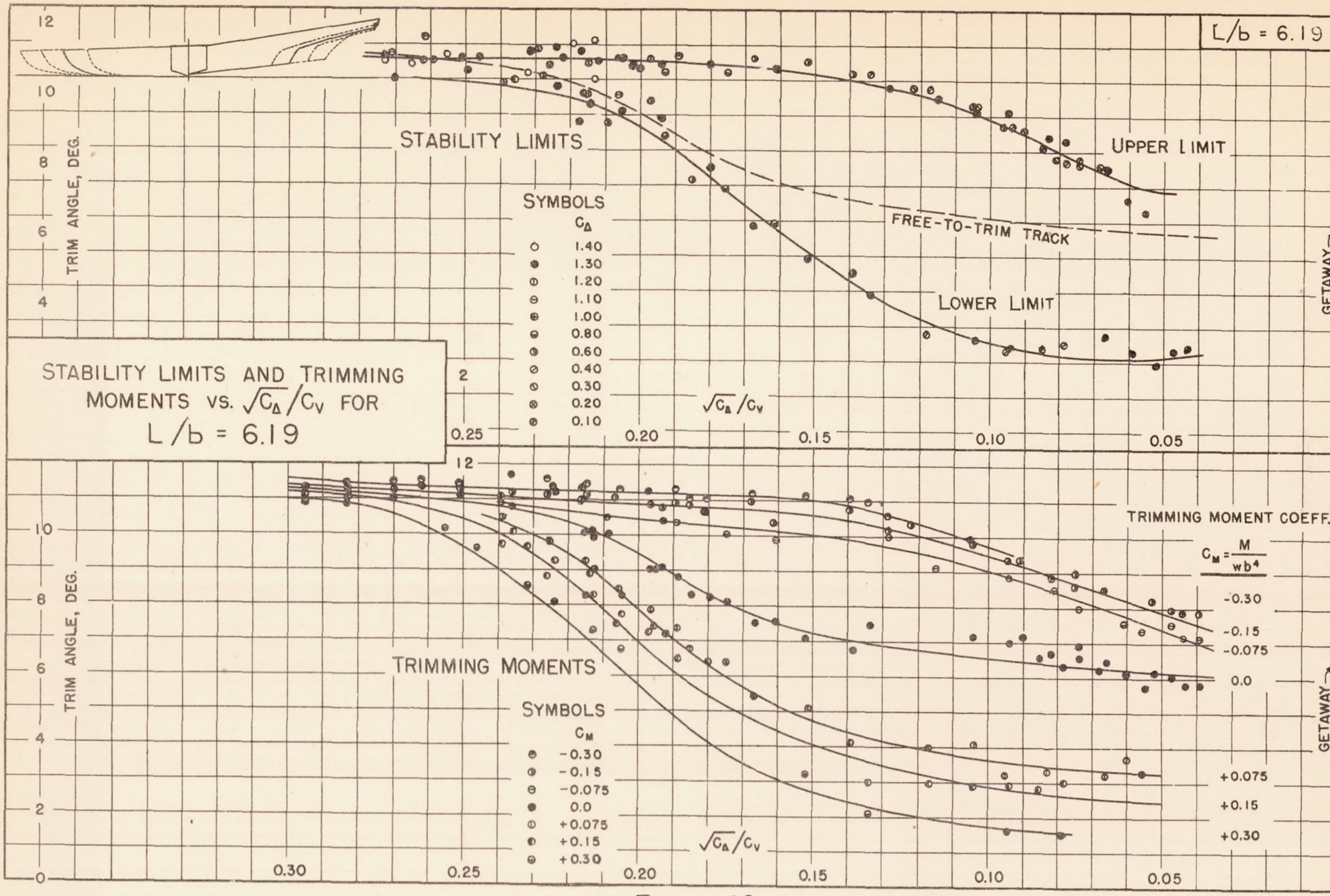
L/b = 6.19
STABILITY LIMITS AND TRIMMING MOMENTS VS. $\sqrt{C_\Delta}/C_V$ FOR L/b = 6.19
TRIM ANGLE, DEG.
STABILITY LIMITS
UPPER LIMIT
FREE-TO-TRIM TRACK
LOWER LIMIT
SYMBOLS
C_Δ
1.40
1.30
1.20
1.10
1.00
0.80
0.60
0.40
0.30
0.20
0.10
GETAWAY
$\sqrt{C_\Delta}/C_V$
TRIMMING MOMENTS
SYMBOLS
C_M
-0.30
-0.15
-0.075
0.0
+0.075
+0.15
+0.30
TRIMMING MOMENT COEFF.
$C_M = \frac{M}{wb^4}$
-0.30
-0.15
-0.075
0.0
+0.075
+0.15
+0.30
0.30
0.25
0.20
0.15
0.10
0.05

Figure 33.

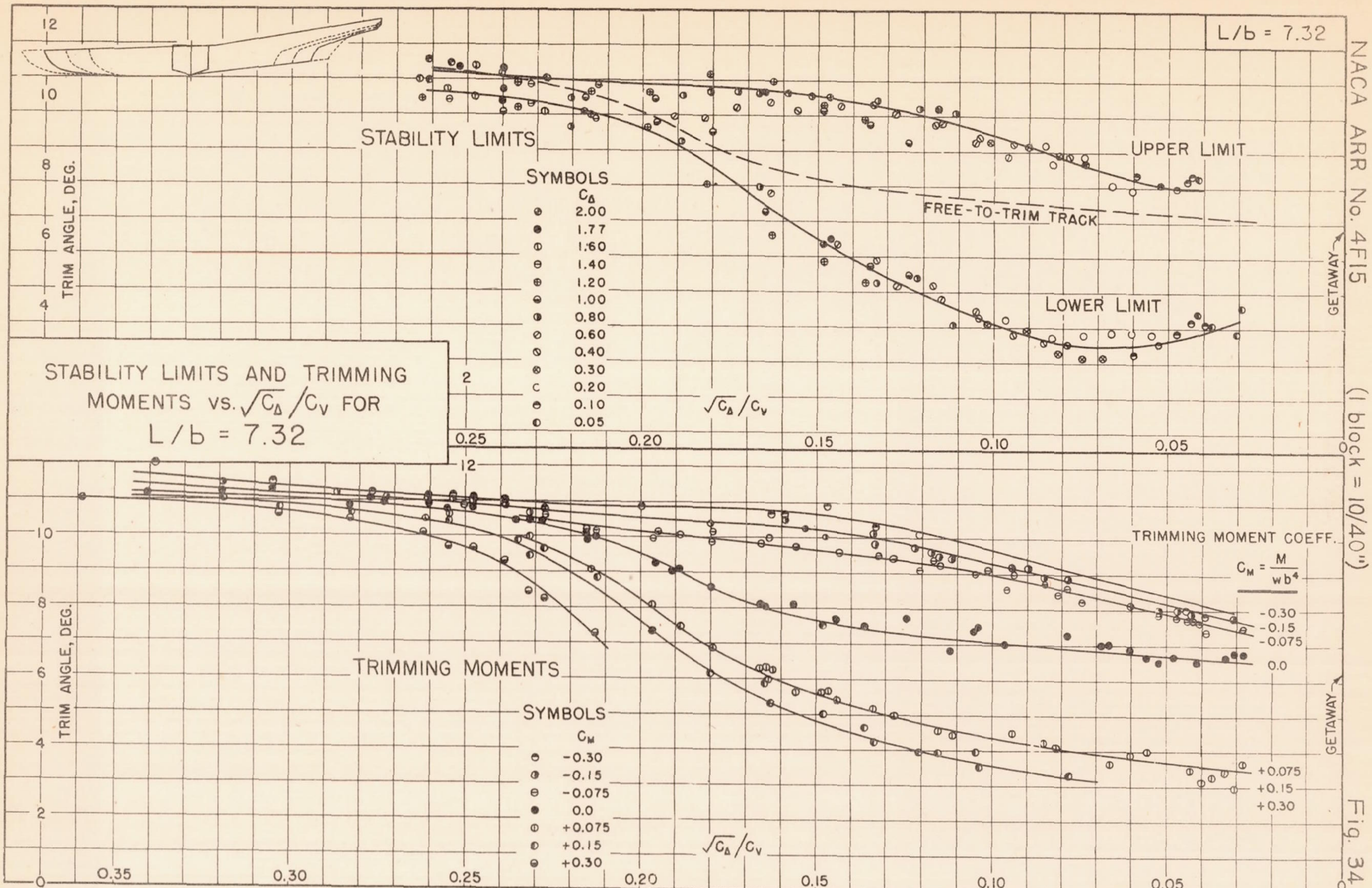
L/b = 7.32
STABILITY LIMITS
SYMBOLS
C_Δ
2.00
1.77
1.60
1.40
1.20
1.00
0.80
0.60
0.40
0.30
0.20
0.10
0.05
UPPER LIMIT
FREE-TO-TRIM TRACK
LOWER LIMIT
GETAWAY
TRIM ANGLE, DEG.
$\sqrt{C_\Delta}/C_V$
STABILITY LIMITS AND TRIMMING MOMENTS VS. $\sqrt{C_\Delta}/C_V$ FOR L/b = 7.32
TRIMMING MOMENTS
SYMBOLS
C_M
-0.30
-0.15
-0.075
0.0
+0.075
+0.15
+0.30
TRIMMING MOMENT COEFF.
$C_M = \frac{M}{wb^4}$
0.35
0.30
0.25
0.20
0.15
0.10
0.05
NACA ARR No. 4F15
(1 block = 10/40")
Fig. 34

Figure 34.

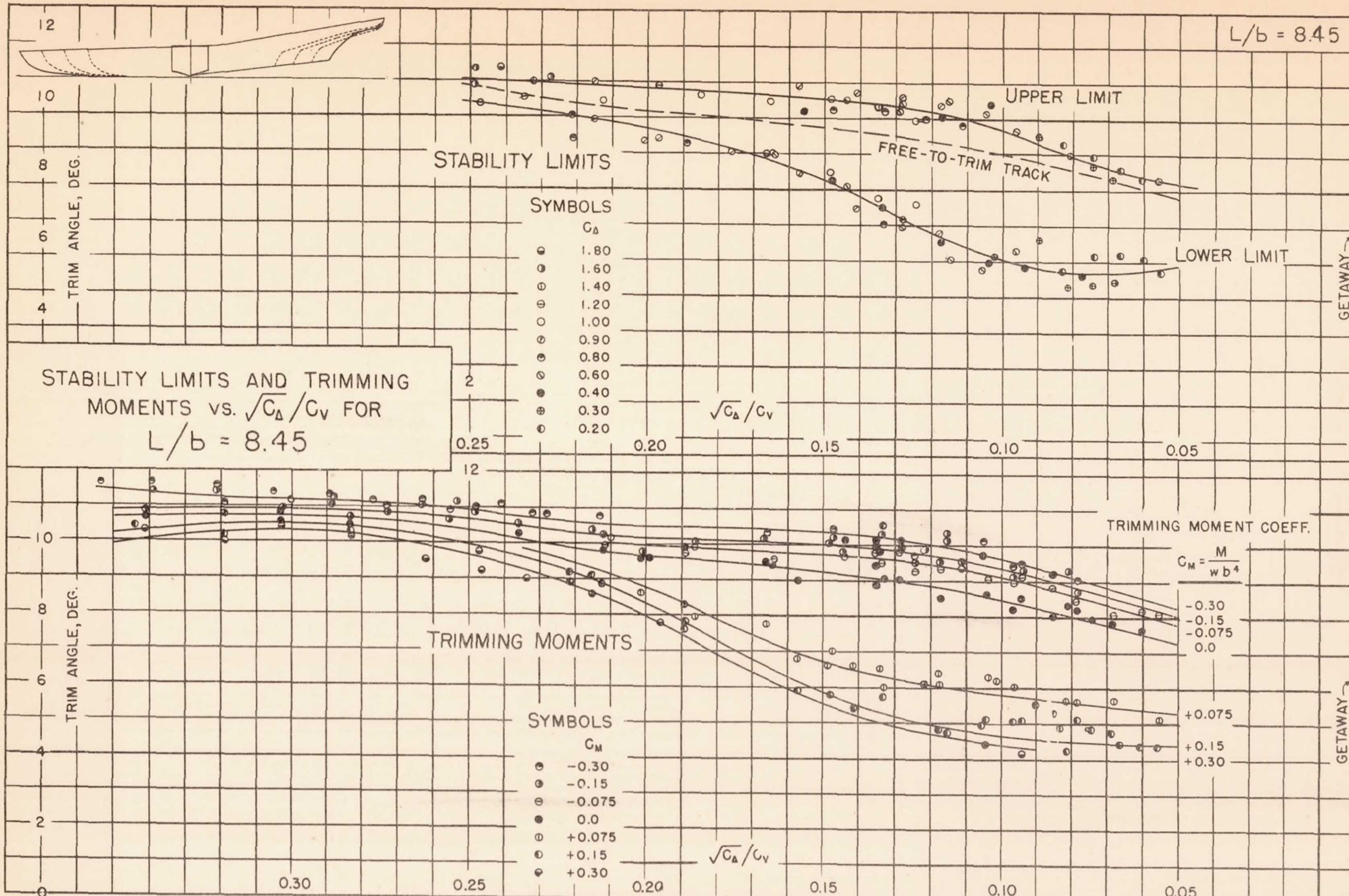

(1 block = 10/40")

Figure 35.

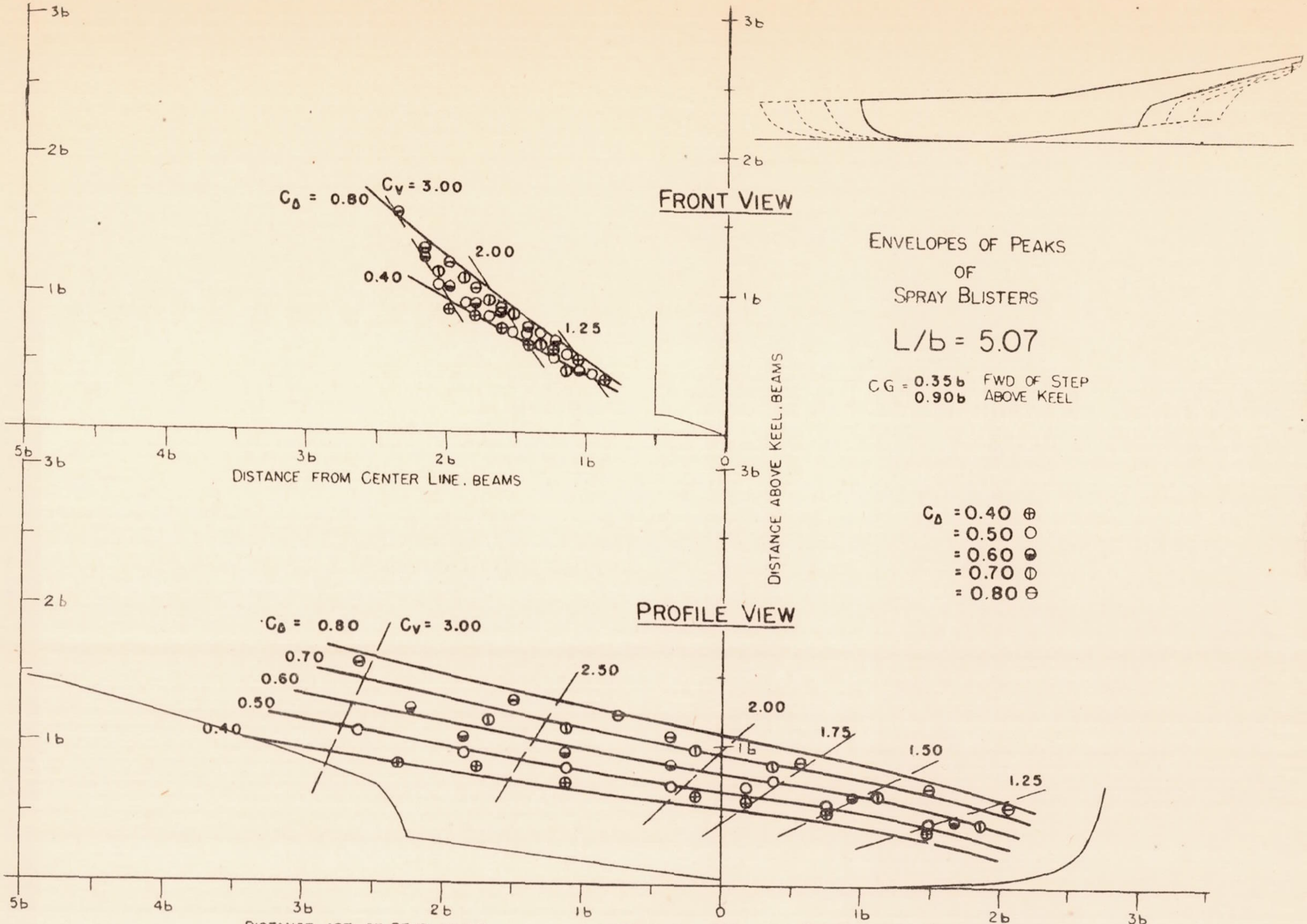
FRONT VIEW
PROFILE VIEW
ENVELOPES OF PEAKS
OF
SPRAY BLISTERS
L/b = 5.07
CG = 0.35b FWD OF STEP
0.90b ABOVE KEEL
C_Δ = 0.40 ⊕
= 0.50 ○
= 0.60
= 0.70
= 0.80 ⊖
C_Δ = 0.80
C_V = 3.00
2.00
0.40
1.25
0.70
0.60
0.50
2.50
1.75
1.50
DISTANCE FROM CENTER LINE, BEAMS
DISTANCE ABOVE KEEL, BEAMS
DISTANCE AFT OF STEP, BEAMS
DISTANCE FWD OF STEP, BEAMS
5b
4b
3b
2b
1b
0

Figure 36.

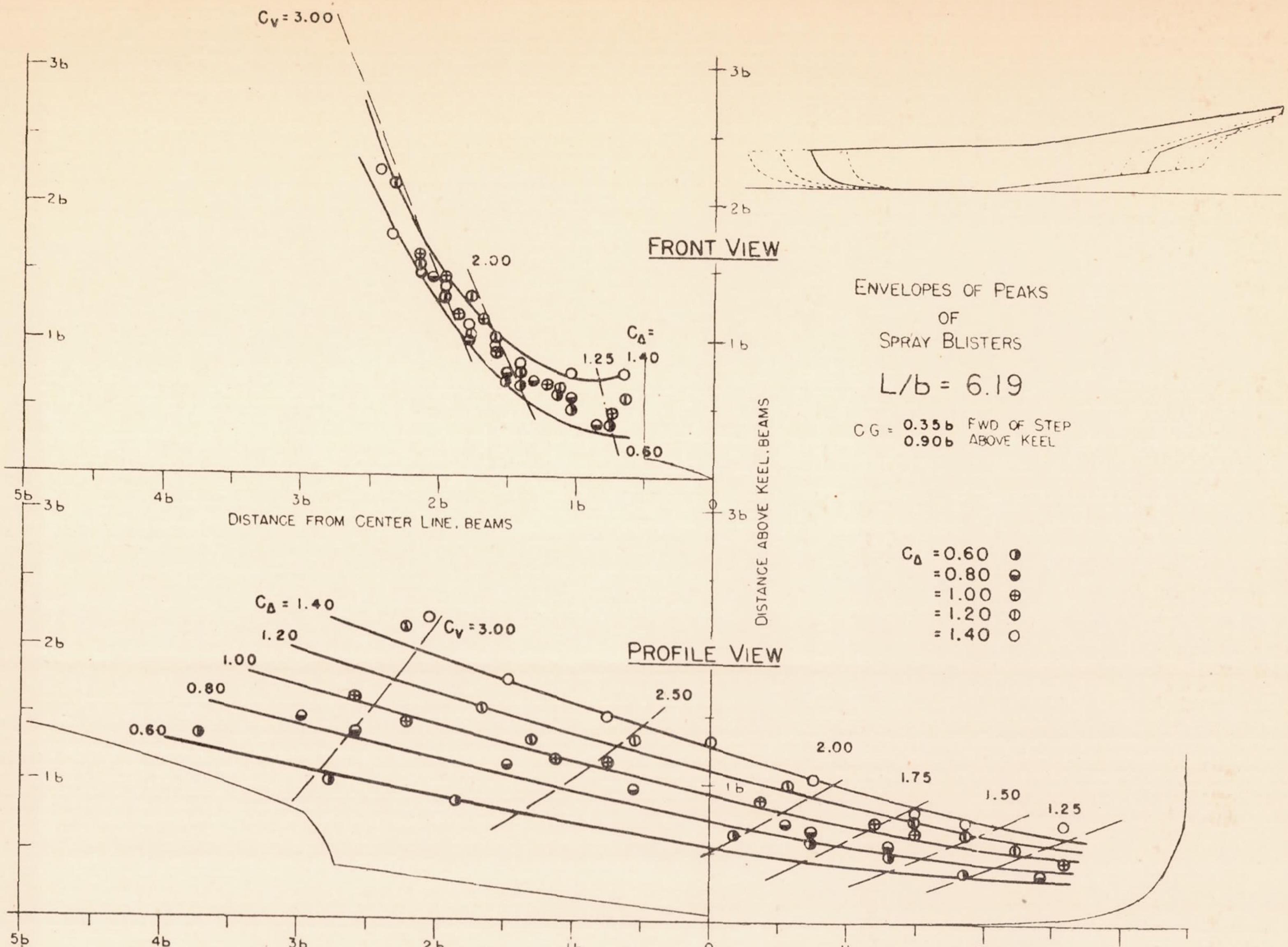
FRONT VIEW
PROFILE VIEW
ENVELOPES OF PEAKS
OF
SPRAY BLISTERS
L/b = 6.19
CG = 0.35b FWD OF STEP
0.90b ABOVE KEEL
C_Δ = 0.60
= 0.80
= 1.00
= 1.20
= 1.40
C_V = 3.00
2.50
2.00
1.75
1.50
1.25
C_Δ = 1.40
1.20
1.00
0.80
0.60
DISTANCE FROM CENTER LINE, BEAMS
DISTANCE ABOVE KEEL, BEAMS
DISTANCE AFT OF STEP, BEAMS
DISTANCE FWD OF STEP, BEAMS

Figure 37.

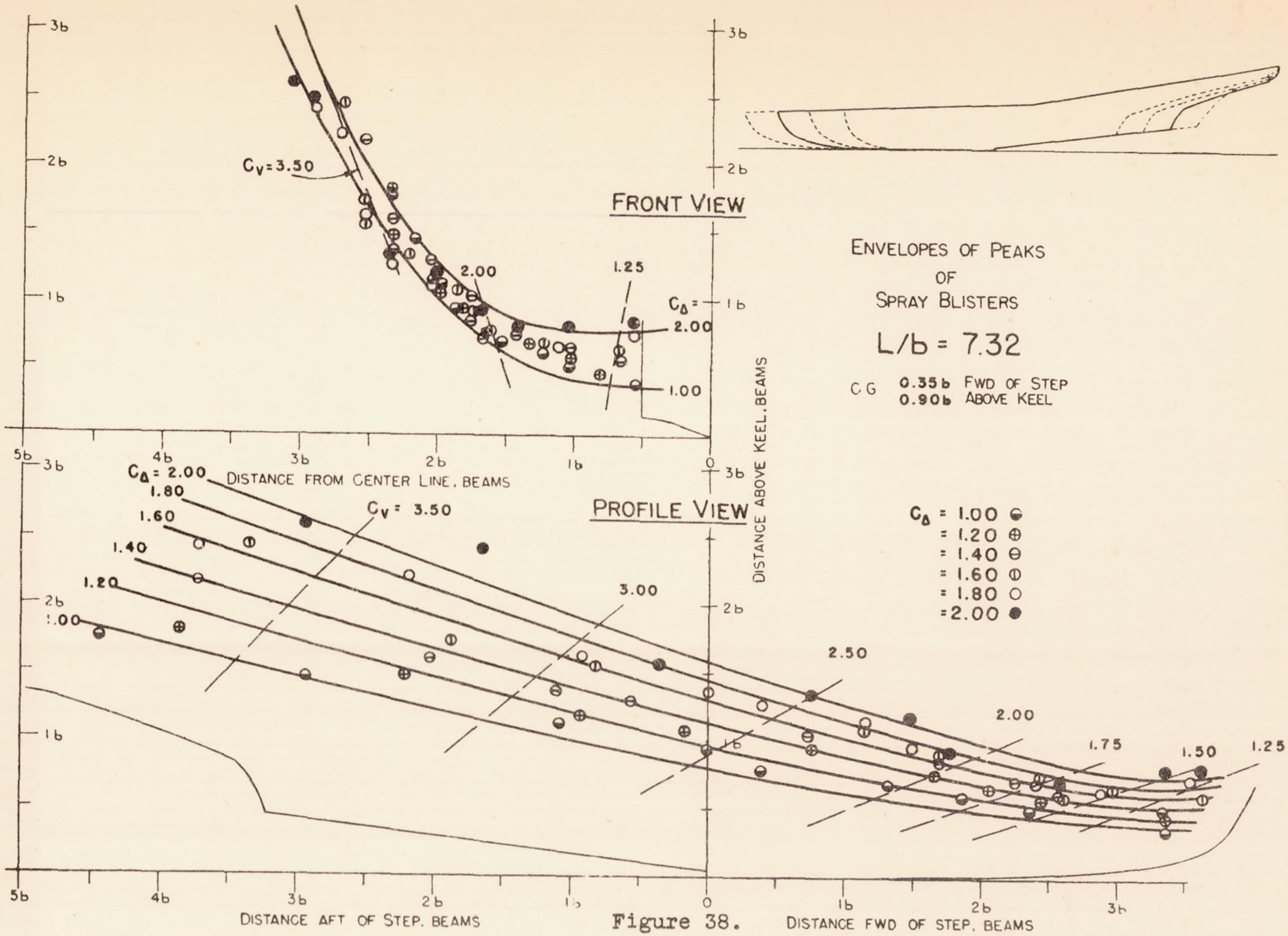
FRONT VIEW
PROFILE VIEW
ENVELOPES OF PEAKS
OF
SPRAY BLISTERS
L/b = 7.32
CG 0.35b FWD OF STEP
0.90b ABOVE KEEL
C_V = 3.50
2.00
1.25
C_Δ = 2.00
1.00
C_Δ = 2.00
1.80
1.60
1.40
1.20
1.00
3.00
2.50
2.00
1.75
1.50
1.25
C_Δ = 1.00
= 1.20
= 1.40
= 1.60
= 1.80
= 2.00
DISTANCE FROM CENTER LINE, BEAMS
DISTANCE ABOVE KEEL, BEAMS
DISTANCE AFT OF STEP, BEAMS
DISTANCE FWD OF STEP, BEAMS
5b
4b
3b
2b
1b
0

Figure 38.

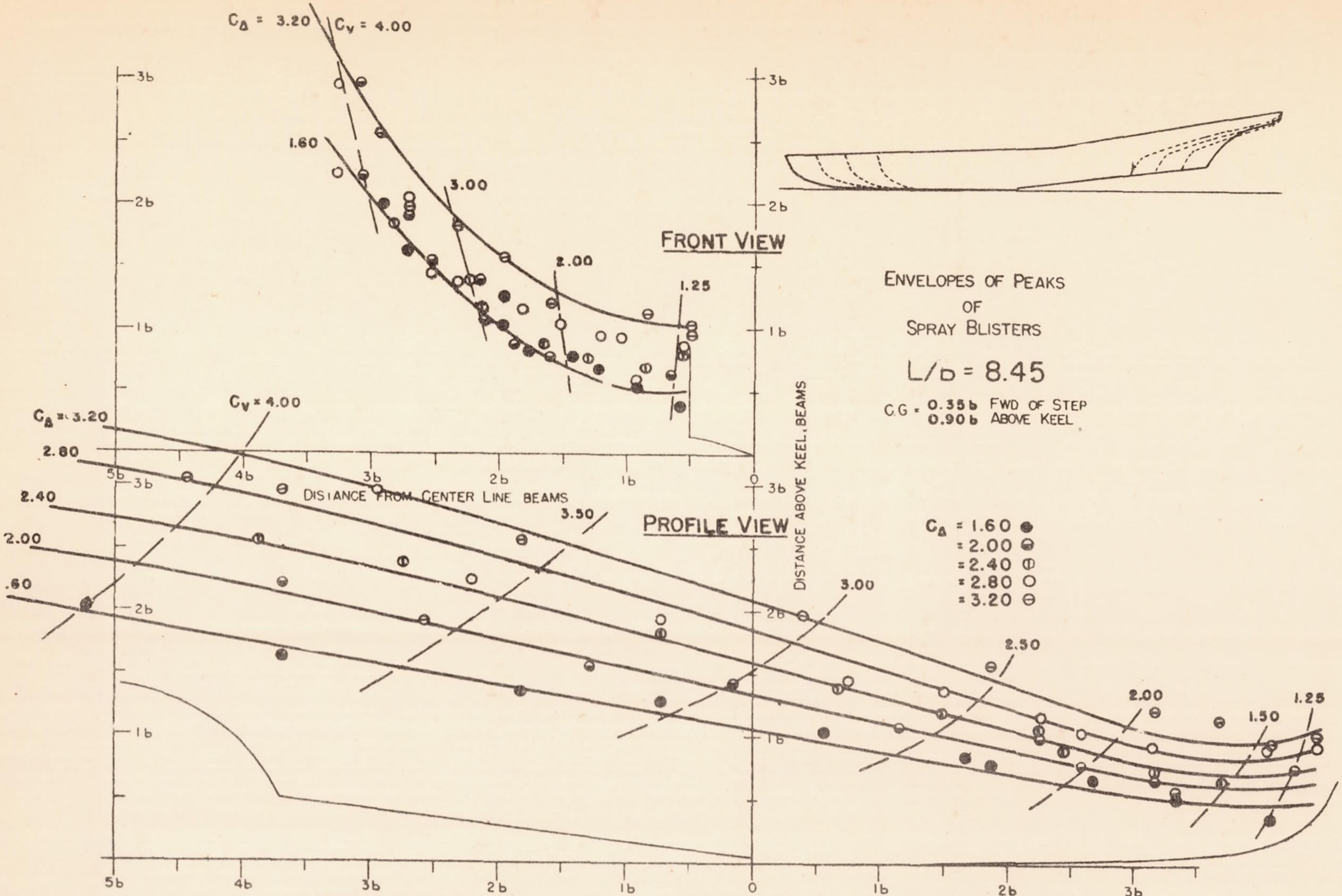

FRONT VIEW
PROFILE VIEW
ENVELOPES OF PEAKS OF SPRAY BLISTERS
L/D = 8.45
C.G. = 0.35 b FWD OF STEP
0.90 b ABOVE KEEL
C_Δ = 3.20
C_V = 4.00
C_Δ = 1.60
= 2.00
= 2.40
= 2.80
= 3.20
3.50
3.00
2.50
2.00
1.50
1.25
1.60
2.80
2.40
.60
DISTANCE FROM CENTER LINE BEAMS
DISTANCE ABOVE KEEL, BEAMS
DISTANCE AFT OF STEP, BEAMS
DISTANCE FWD OF STEP, BEAMS
5b
4b
3b
2b
1b
0

Figure 39.

Effect of Changes of Load and Length-Beam Ratio on Bow Spray in Waves of H=0.3 beam and L=6.0 beam

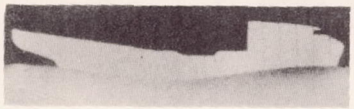

$C_V = 1.05$

$C_\Delta = 0.60$ 0.80 1.00

L/b = 5.07
MODEL 339-22

L/b = 6.19
MODEL 339-1

L/b = 7.32
MODEL 339-23

L/b = 8.45
MODEL 339-46

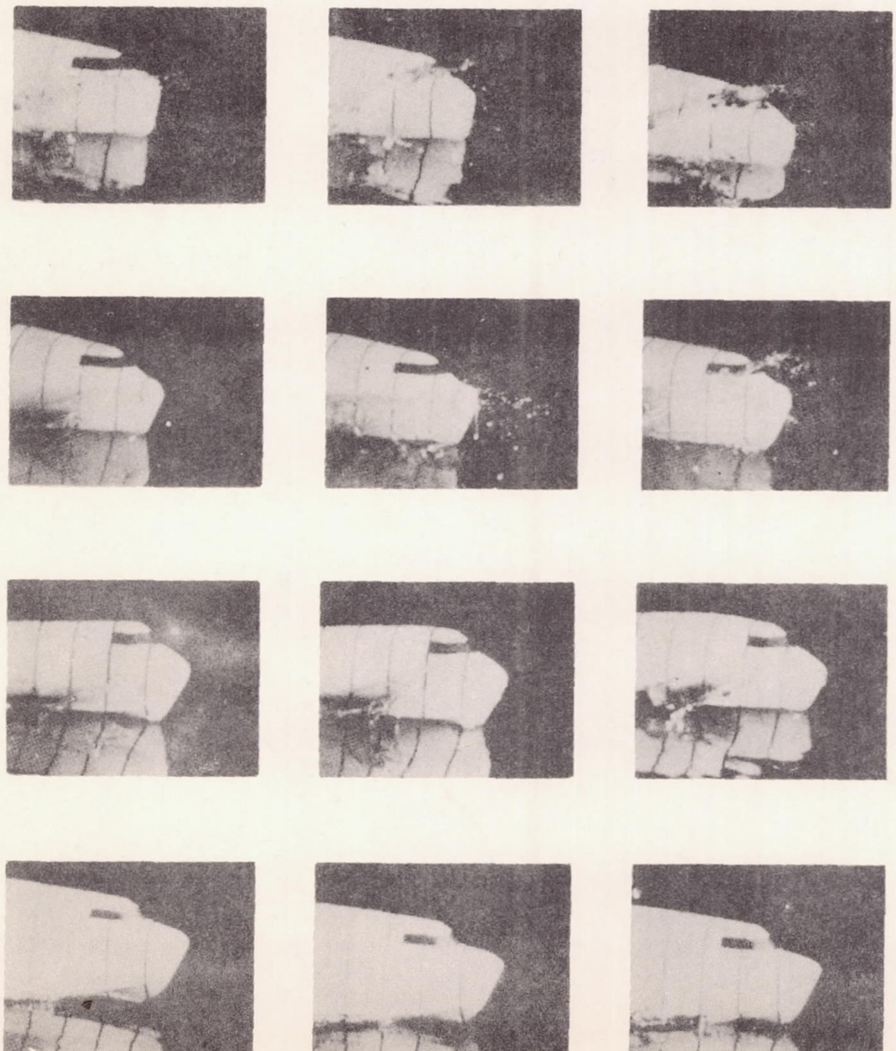

Figure 40

W-105

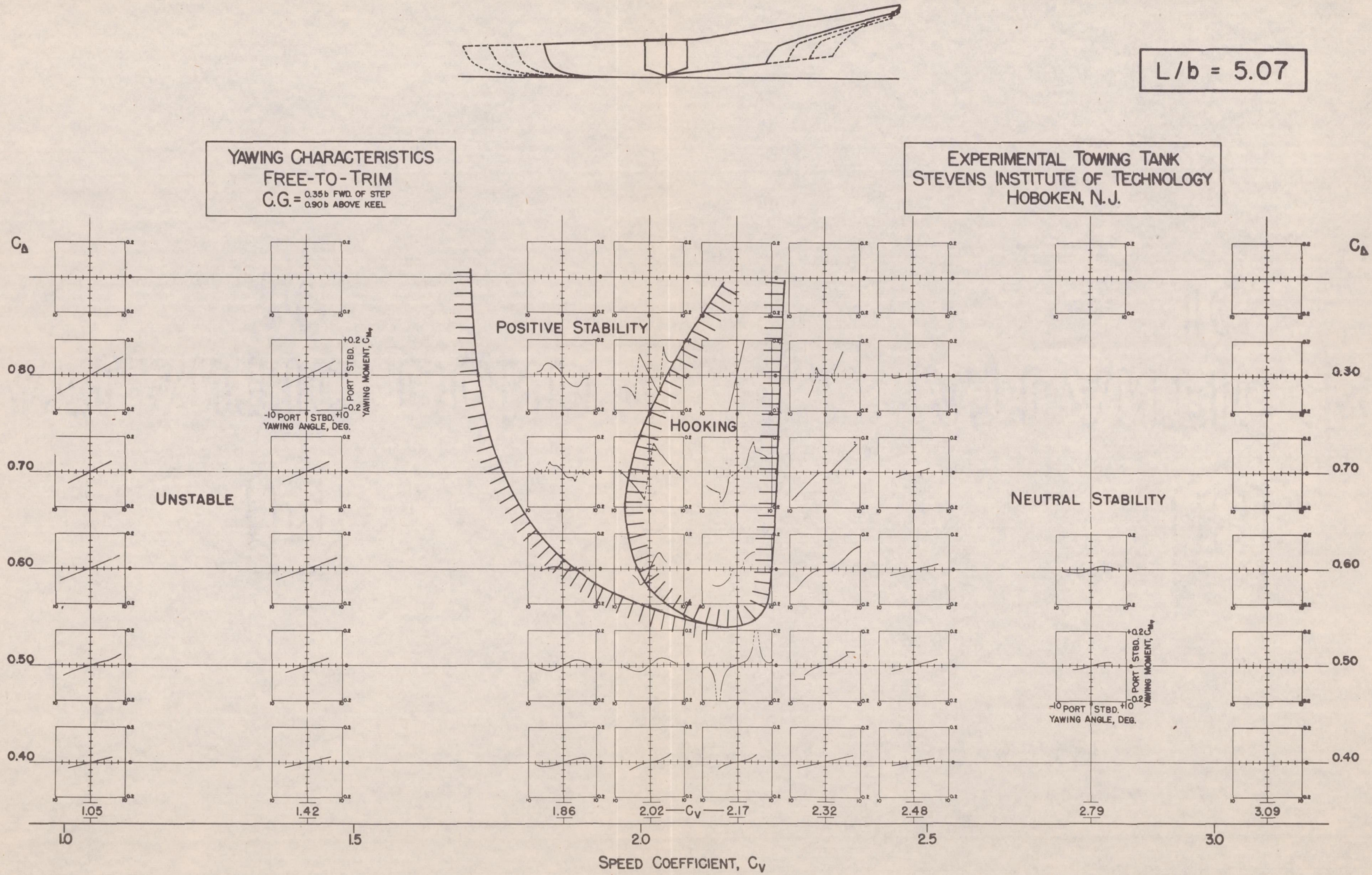

Figure 41

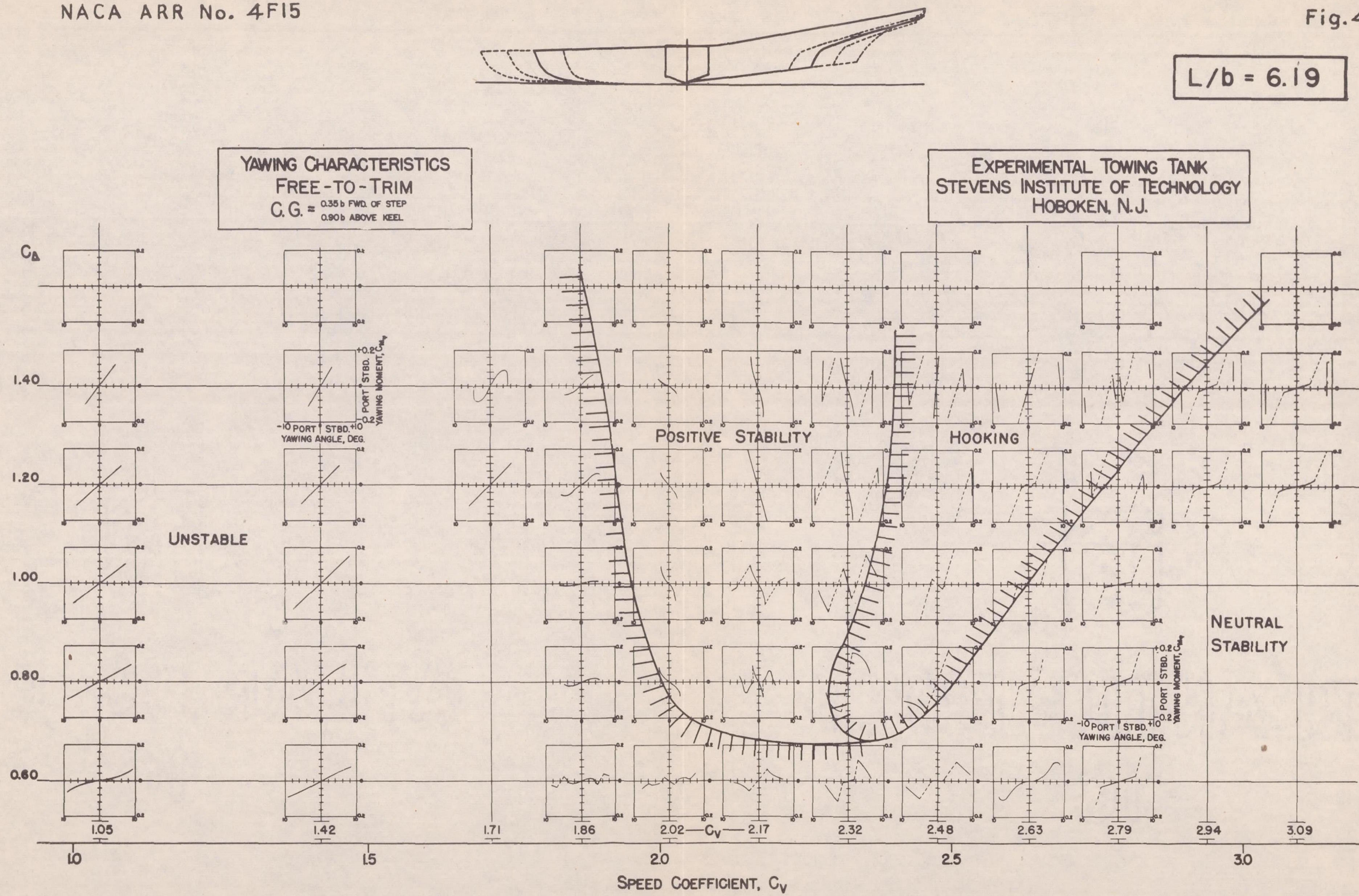
L/b = 6.19
YAWING CHARACTERISTICS
FREE-TO-TRIM
C.G. = 0.35b FWD. OF STEP 0.90b ABOVE KEEL
EXPERIMENTAL TOWING TANK
STEVENS INSTITUTE OF TECHNOLOGY
HOBOKEN, N.J.
C_Δ
1.40
1.20
1.00
0.80
0.60
UNSTABLE
POSITIVE STABILITY
HOOKING
NEUTRAL STABILITY
-10 PORT STBD. +10
YAWING ANGLE, DEG.
+0.2 STBD. PORT -0.2
YAWING MOMENT, C_{M_ψ}
1.05
1.42
1.71
1.86
2.02 — C_V — 2.17
2.32
2.48
2.63
2.79
2.94
3.09
1.0
1.5
2.0
2.5
3.0
SPEED COEFFICIENT, C_V

Figure 42

L/b = 7.32

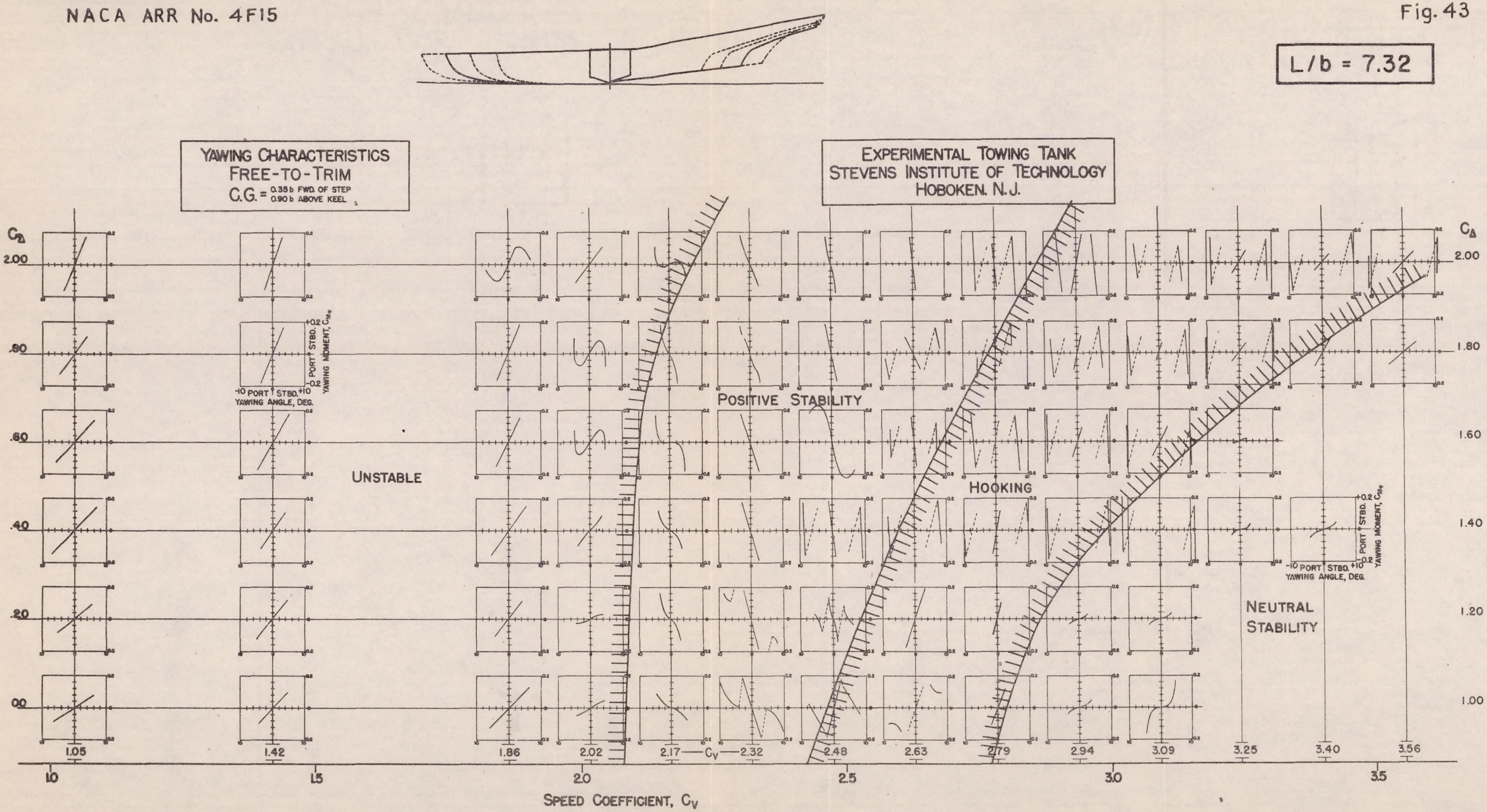

Figure 43

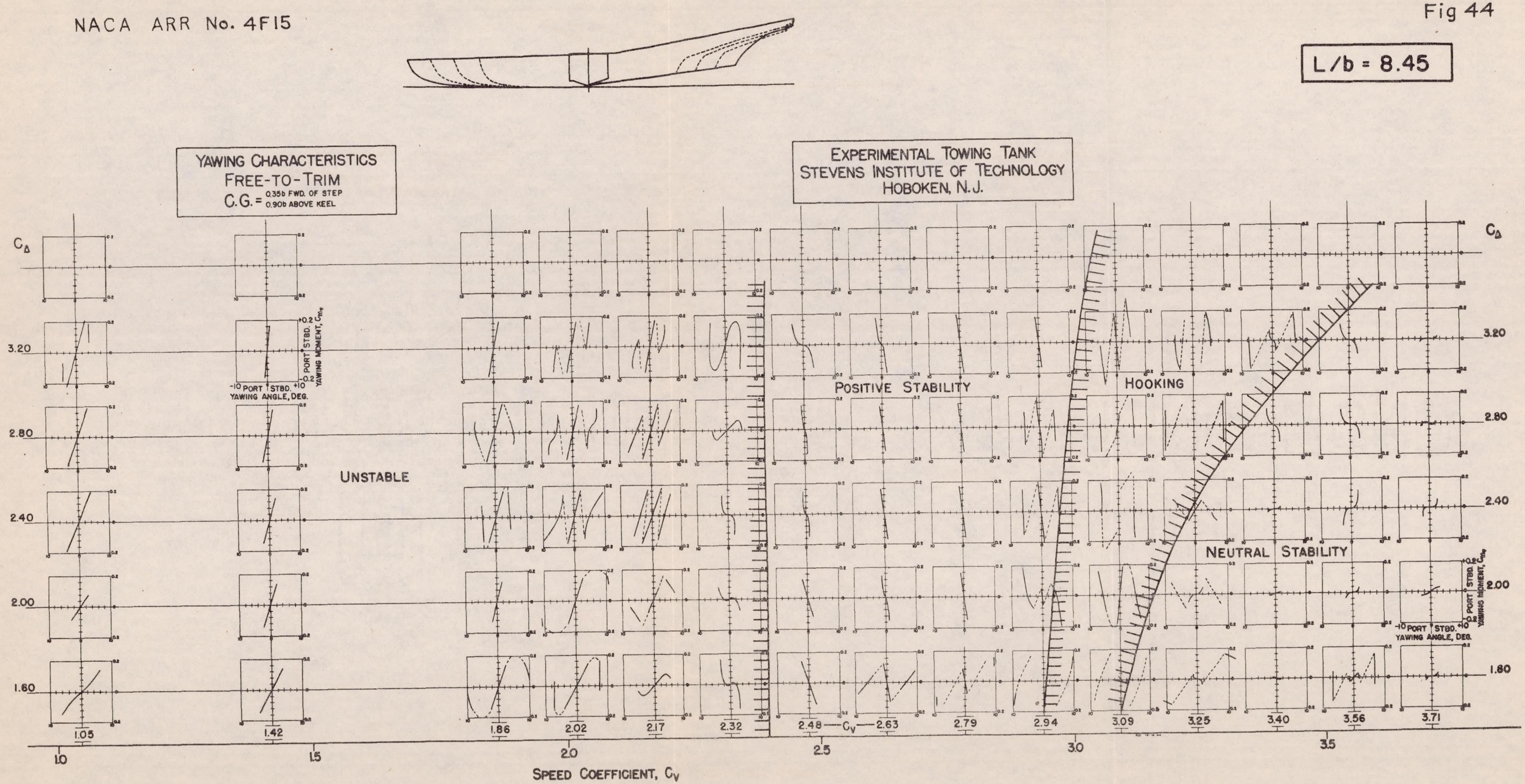
L/b = 8.45
YAWING CHARACTERISTICS
FREE-TO-TRIM
C.G. = 0.35b FWD. OF STEP
0.90b ABOVE KEEL
EXPERIMENTAL TOWING TANK
STEVENS INSTITUTE OF TECHNOLOGY
HOBOKEN, N.J.
UNSTABLE
POSITIVE STABILITY
HOOKING
NEUTRAL STABILITY
-10 PORT STBD. +10
YAWING ANGLE, DEG.
+0.2 PORT STBD. -0.2 YAWING MOMENT, C_{m_ψ}
C_Δ
3.20
2.80
2.40
2.00
1.60
1.80
1.05
1.42
1.86
2.02
2.17
2.32
2.48 — C_V — 2.63
2.79
2.94
3.09
3.25
3.40
3.56
3.71
1.0
1.5
2.0
2.5
3.0
3.5
SPEED COEFFICIENT, C_V

Figure 44

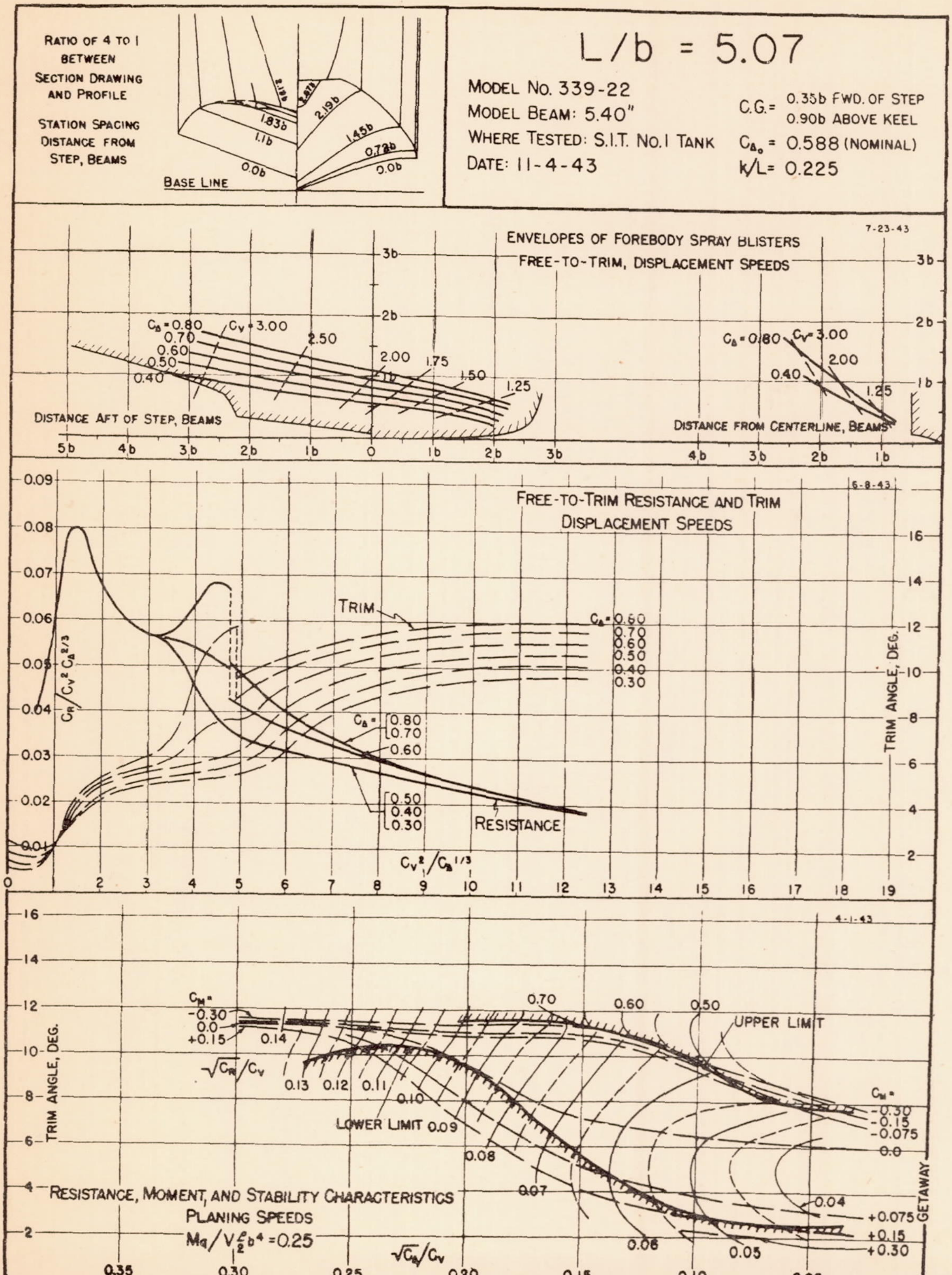
RATIO OF 4 TO 1 BETWEEN SECTION DRAWING AND PROFILE
STATION SPACING DISTANCE FROM STEP, BEAMS
BASE LINE
L/b = 5.07
MODEL No. 339-22
MODEL BEAM: 5.40"
WHERE TESTED: S.I.T. No. 1 TANK
DATE: 11-4-43
C.G. = 0.35b FWD. OF STEP 0.90b ABOVE KEEL
C_{Δ_0} = 0.588 (NOMINAL)
k/L = 0.225
ENVELOPES OF FOREBODY SPRAY BLISTERS
FREE-TO-TRIM, DISPLACEMENT SPEEDS
DISTANCE AFT OF STEP, BEAMS
DISTANCE FROM CENTERLINE, BEAMS
FREE-TO-TRIM RESISTANCE AND TRIM
DISPLACEMENT SPEEDS
TRIM
RESISTANCE
TRIM ANGLE, DEG.
$C_R / C_V^2 C_\Delta^{2/3}$
$C_V^2 / C_\Delta^{1/3}$
UPPER LIMIT
LOWER LIMIT
GETAWAY
RESISTANCE, MOMENT, AND STABILITY CHARACTERISTICS
PLANING SPEEDS
$M_q / V \frac{\rho}{2} b^4 = 0.25$
$\sqrt{C_R}/C_V$
$\sqrt{C_\Delta}/C_V$

Figure 45.

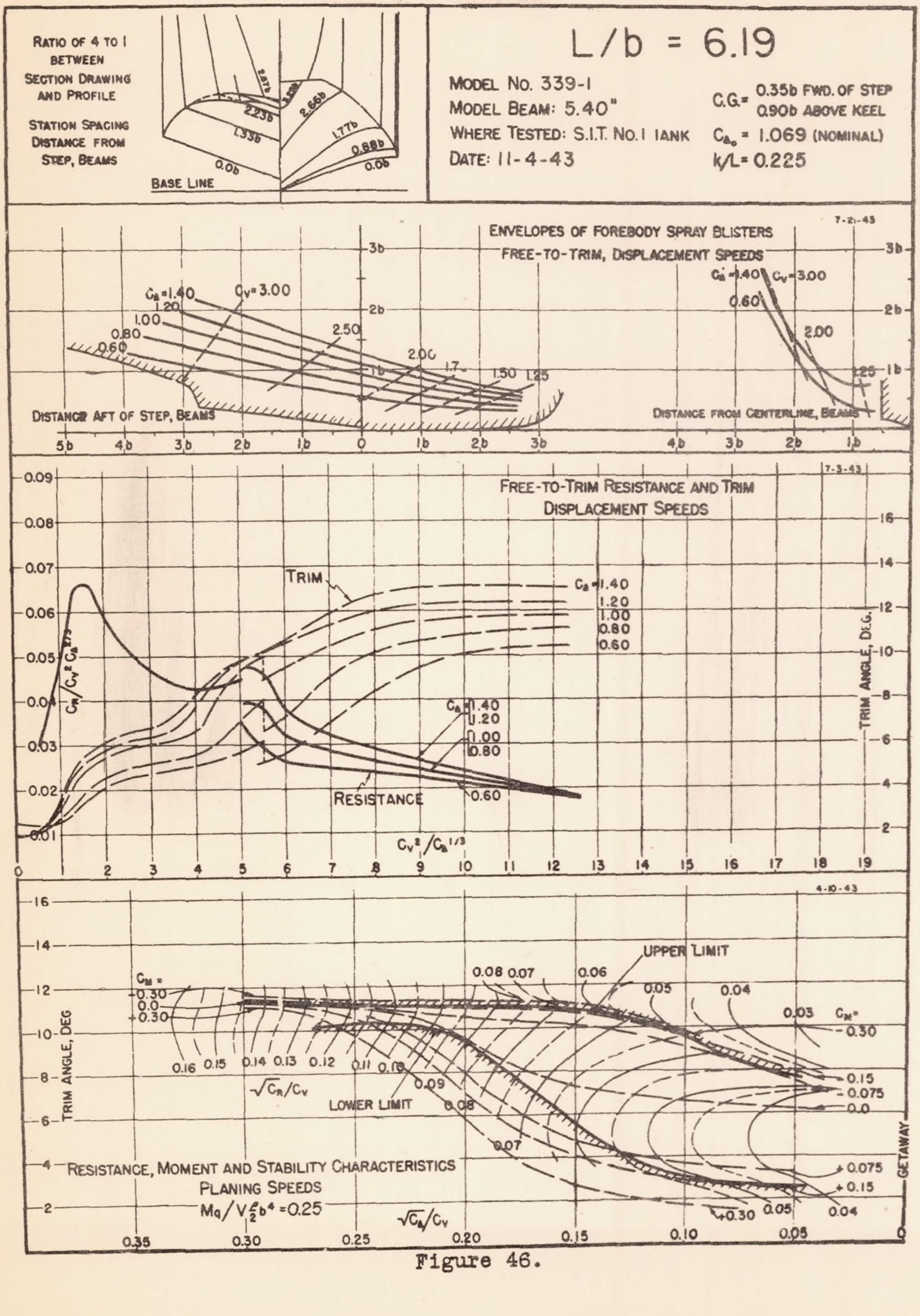
RATIO OF 4 TO 1 BETWEEN SECTION DRAWING AND PROFILE
STATION SPACING DISTANCE FROM STEP, BEAMS
BASE LINE
L/b = 6.19
MODEL NO. 339-1
MODEL BEAM: 5.40"
WHERE TESTED: S.I.T. NO. 1 TANK
DATE: 11-4-43
C.G. = 0.35b FWD. OF STEP 0.90b ABOVE KEEL
C_{Δ_0} = 1.069 (NOMINAL)
k/L = 0.225
ENVELOPES OF FOREBODY SPRAY BLISTERS
FREE-TO-TRIM, DISPLACEMENT SPEEDS
DISTANCE AFT OF STEP, BEAMS
DISTANCE FROM CENTERLINE, BEAMS
FREE-TO-TRIM RESISTANCE AND TRIM
DISPLACEMENT SPEEDS
TRIM
RESISTANCE
$C_R/C_V^2 C_\Delta^{2/3}$
$C_V^2/C_\Delta^{1/3}$
TRIM ANGLE, DEG.
UPPER LIMIT
LOWER LIMIT
$\sqrt{C_R}/C_V$
$\sqrt{C_\Delta}/C_V$
GETAWAY
RESISTANCE, MOMENT AND STABILITY CHARACTERISTICS
PLANING SPEEDS
$M_q/V\frac{\rho}{2}b^4 = 0.25$

Figure 46.

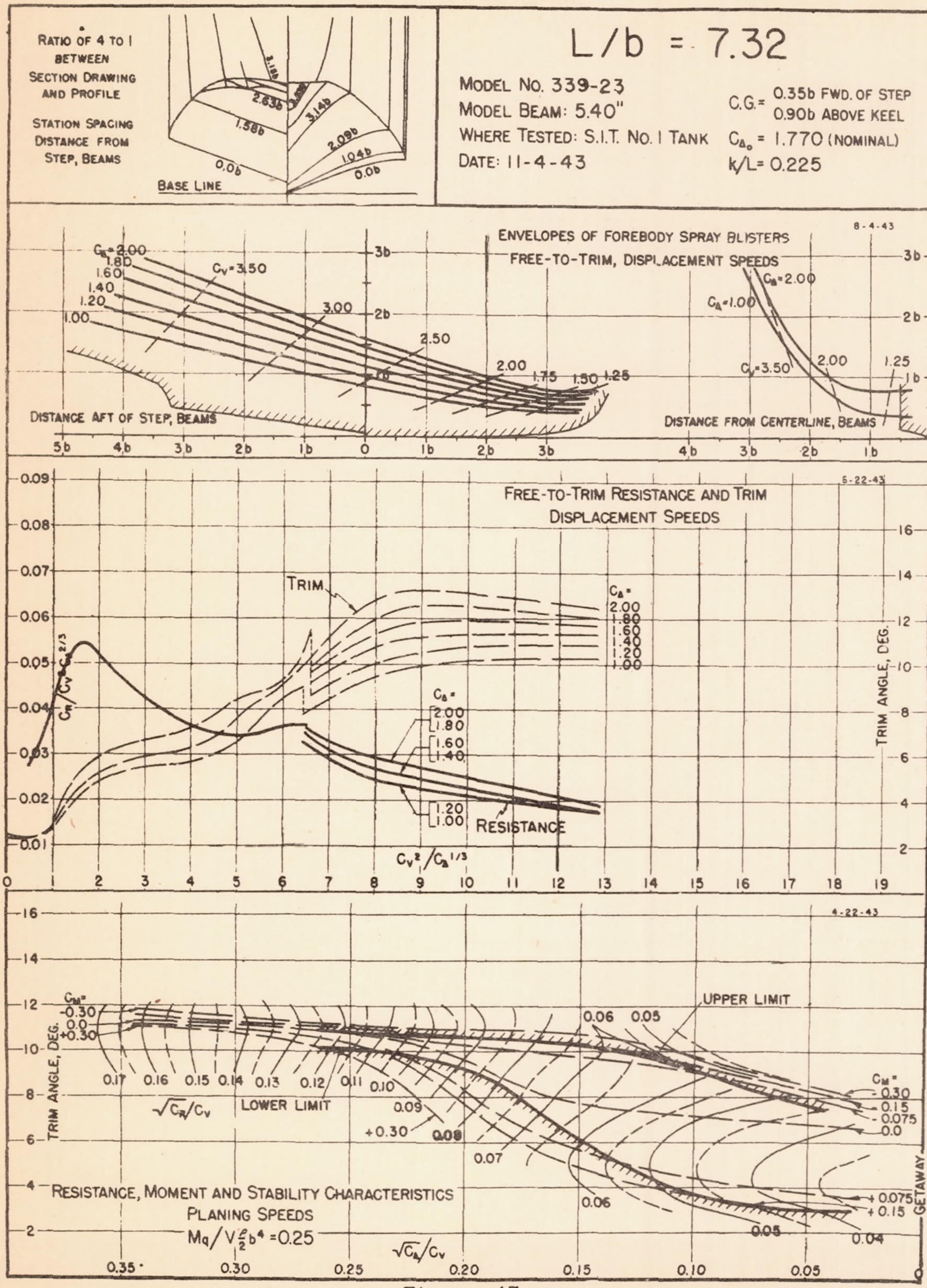
RATIO OF 4 TO 1 BETWEEN SECTION DRAWING AND PROFILE
STATION SPACING DISTANCE FROM STEP, BEAMS
BASE LINE
L/b = 7.32
MODEL NO. 339-23
MODEL BEAM: 5.40"
WHERE TESTED: S.I.T. NO. I TANK
DATE: 11-4-43
C.G. = 0.35b FWD. OF STEP 0.90b ABOVE KEEL
C_{Δ_0} = 1.770 (NOMINAL)
k/L = 0.225
ENVELOPES OF FOREBODY SPRAY BLISTERS
FREE-TO-TRIM, DISPLACEMENT SPEEDS
DISTANCE AFT OF STEP, BEAMS
DISTANCE FROM CENTERLINE, BEAMS
FREE-TO-TRIM RESISTANCE AND TRIM
DISPLACEMENT SPEEDS
TRIM
RESISTANCE
TRIM ANGLE, DEG.
UPPER LIMIT
LOWER LIMIT
GETAWAY
RESISTANCE, MOMENT AND STABILITY CHARACTERISTICS
PLANING SPEEDS
$M_q/V\frac{\rho}{2}b^4 = 0.25$

Figure 47.

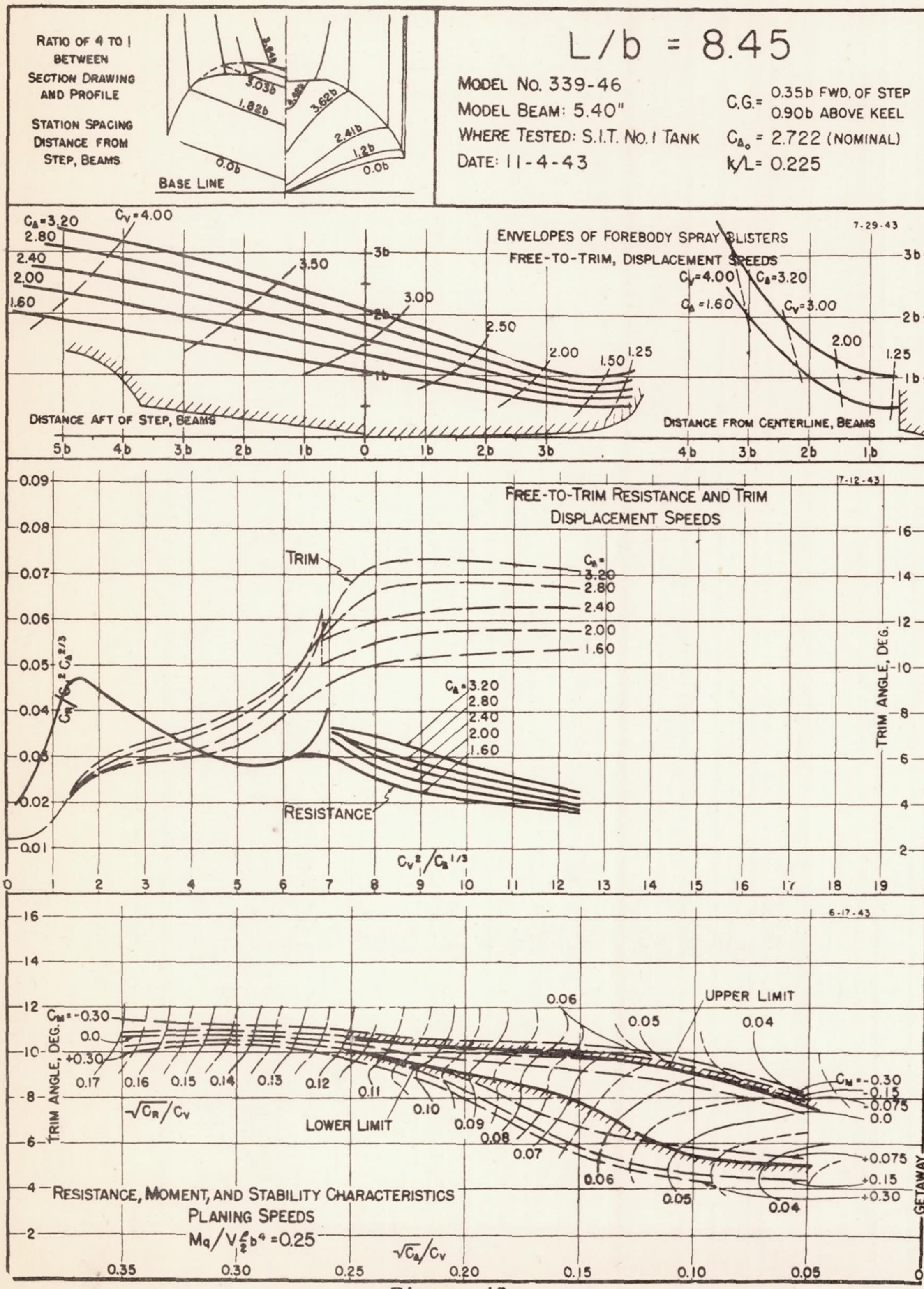
RATIO OF 4 TO 1 BETWEEN SECTION DRAWING AND PROFILE
STATION SPACING DISTANCE FROM STEP, BEAMS
BASE LINE
L/b = 8.45
MODEL NO. 339-46
MODEL BEAM: 5.40"
WHERE TESTED: S.I.T. NO. I TANK
DATE: 11-4-43
C.G. = 0.35b FWD. OF STEP 0.90b ABOVE KEEL
C_{Δ_0} = 2.722 (NOMINAL)
k/L = 0.225
ENVELOPES OF FOREBODY SPRAY BLISTERS
FREE-TO-TRIM, DISPLACEMENT SPEEDS
DISTANCE AFT OF STEP, BEAMS
DISTANCE FROM CENTERLINE, BEAMS
FREE-TO-TRIM RESISTANCE AND TRIM
DISPLACEMENT SPEEDS
TRIM
RESISTANCE
$C_R/C_V^2 C_\Delta^{2/3}$
$C_V^2/C_\Delta^{1/3}$
TRIM ANGLE, DEG.
UPPER LIMIT
LOWER LIMIT
$\sqrt{C_R}/C_V$
$\sqrt{C_\Delta}/C_V$
GETAWAY
RESISTANCE, MOMENT, AND STABILITY CHARACTERISTICS
PLANING SPEEDS
$M_q/V\frac{\rho}{2}b^4$ = 0.25

Figure 48.